

12-2010

ELUCIDATING THE ROLE OF CD44 EXPRESSION ON MESENCHYMAL STEM CELLS WITHIN THE TUMOR MICROENVIRONMENT

Erika L. Spaeth

Follow this and additional works at: https://digitalcommons.library.tmc.edu/utgsbs_dissertations



Part of the [Medical Sciences Commons](#)

Recommended Citation

Spaeth, Erika L., "ELUCIDATING THE ROLE OF CD44 EXPRESSION ON MESENCHYMAL STEM CELLS WITHIN THE TUMOR MICROENVIRONMENT" (2010). *The University of Texas MD Anderson Cancer Center UTHealth Graduate School of Biomedical Sciences Dissertations and Theses (Open Access)*. 100.
https://digitalcommons.library.tmc.edu/utgsbs_dissertations/100

This Dissertation (PhD) is brought to you for free and open access by the The University of Texas MD Anderson Cancer Center UTHealth Graduate School of Biomedical Sciences at DigitalCommons@TMC. It has been accepted for inclusion in The University of Texas MD Anderson Cancer Center UTHealth Graduate School of Biomedical Sciences Dissertations and Theses (Open Access) by an authorized administrator of DigitalCommons@TMC. For more information, please contact digitalcommons@library.tmc.edu.

ELUCIDATING THE ROLE OF CD44 EXPRESSION ON MESENCHYMAL STEM
CELLS WITHIN THE TUMOR MICROENVIRONMENT

By

Erika Leigh Spaeth, B.S.

APPROVED:

Frank Marini, Ph.D.
Supervisory Chair

Brian Davis, Ph.D.

Ann Klopp, M.D., Ph.D.

Frederick Lang, M.D.

Sendurai Mani, Ph.D.

APPROVED:

Dean, The University of Texas
Graduate School of Biomedical Sciences at Houston

ELUCIDATING THE ROLE OF CD44 EXPRESSION ON MESENCHYMAL STEM
CELLS WITHIN THE TUMOR MICROENVIRONMENT

A
DISSERTATION

Presented to the Faculty of
The University of Texas Health Science Center at Houston
and
The University of Texas M. D. Anderson Cancer Center
Graduate School of Biomedical Sciences
in Partial Fulfillment
of the Requirements
for the Degree of
DOCTOR OF PHILOSOPHY
by
Erika Leigh Spaeth, B.S. Houston, Texas
December, 2010

Dedication

To my mother who taught me to be passionate about every endeavor.

To my father who taught me to be patient and hard-working.

To my brother who embodies ambition and who continues to laugh with me through
life.

Thank you for your love, support and encouragement.

Acknowledgements

If there is one thing that I have learned from graduate school it is the more knowledge one gains the more unanswered questions one has. And thus Wernher von Braun had it right when saying “Research is what I'm doing when I don't know what I'm doing.”

I would like to first and foremost thank my mentor, Frank Marini, who gave me the support to think independently, the freedom to make mistakes and the guidance to keep me on track. I would also like to thank Jennifer Dembinski for early contributions to my work. A million thanks to Adam Labaff for his endless scientific support. Who secretly taught me how to do a western blot so I did not feel foolish in lab and who is my primary adversary in scientific debate. Thanks to Shannon Kidd who inspired, and motivated me through my research even during stressful times, to Shanna Wilson for rescuing my sanity and to Jason Williams who has a never-ending supply of sarcasm. And to Dr. Michael Andreeff who was always very supportive of my research and my other lab mates without whom lab-life would have been much less enjoyable: Rodrigo Jacamo who always, with a sense of humor, had antidotes to every molecular technique; Hongbo Lu who listened, joked and laughed with me; Olga Frolova who always told me to be young and live a life outside of lab; Lokesh Battula who taught me how to first characterize MSC by Flow; Chen Ye who was my good friend and mouse-killer; Michelle Zhou who was so kind and always had a smile on her face; Duncan Mac who could solve any problem I had; Twee Tsao who would stop what she was doing at any moment to help me; Teresa McQueen who endlessly helped me with housekeeping issues; Sesha Duvvuri who always had something up his sleeve; April Zeng who was always around late at night to talk to.

I also have to thank the Flow Cytometry and Imaging Core Facility for all the help: Wendy Schober helped me with many complicated fluorochrome problems and always squeezed me in at the last minute. Amy was always friendly and ready to help solve a problem. Jared Burks spent a lot of time helping me learn how to

manipulate a microscope and was always available for a chat, image and non-image related.

Thanks to my committee members for taking time out of their busy schedules to see through the progression of my project. To Dr. Davis and Dr. Lang who stuck with me from the first advisory meeting, Dr. Mani who offered a lot of good experimental design suggestions, and Dr. Klopp who has always been available for discussion scientific or simple table-talk.

I would also like to thank the GSBS administration. Dr. Goka thanks for always having an open door and Dr. Knutson for having good, sound advice. Thanks to Lilly for making visits to the front office not always about the candy bowl and Bunny for helping in those many administrative crunch times.

And to Albert Einstein who was so right when he said, "Science is a wonderful thing if one does not have to earn one's living at it."

ELUCIDATING THE ROLE OF CD44 EXPRESSION ON MESENCHYMAL STEM CELLS WITHIN THE TUMOR MICROENVIRONMENT

Publication No._____

Erika Leigh Spaeth, B.S.

Supervisory Professor: Frank C. Marini III, Ph.D.

The tumor microenvironment is comprised of a vast array of heterogeneous cells including both normal and neoplastic cells. The tumor stroma recruitment process has been exploited for an effective gene delivery technique using bone marrow derived MSC. Targeted migration of the MSC toward the tumor microenvironment, while successful, is not yet fully understood. This study was designed to assess the role of CD44 in the migration of MSC toward the tumor microenvironment and to determine the implications of CD44-deficient MSC within the tumor stroma. Inhibition of MSC migration was evaluated through a variety of methods *in vitro* and *in vivo* including CD44 receptor knockdown, CD44 antagonists, CD44 neutralizing antibodies and small molecule inhibitor of matrix metalloproteinases. Blocking CD44 signaling through MMP inhibition was characterized by lack of intracellular domain cleavage and lead to the decrease in Twist gene expression. A functional relationship between CD44 and Twist expression was confirmed by chromatin immunoprecipitation.

Next, a series of murine tumor models were used to examine the role of CD44 deficient stroma within the tumor microenvironment. Labeled transgenic CD44 knockout (KO) MSC or wild type (WT) C57/b6 MSC were used to analyze the stromal incorporation within murine breast carcinomas (EO771 and 4T1). Subsequent tumors were analyzed for vessel formation (CD31), and the presence of tumor associated fibroblast (TAF) markers, α -smooth muscle actin (α -SMA), fibroblast activation protein (FAP), and fibroblast specific protein (FSP). The tumors with CD44KO MSC cells had less vessel formation than the tumors with WT MSC. The lack of fibroblastic TAF population as defined by FAP/FSP expression by the

CD44KO MSC admixed tumors suggest that the bone marrow derived population of MSC were unable to contribute to the fibroblastic stromal population. Subsequently, a bone marrow transplantation experiment confirmed the endogenous migratory deficiencies of the CD44KO bone marrow derived stromal cells toward the tumor microenvironment *in vivo*. WT mice with CD44KO bone marrow had less CD44KO-derived tumor stroma compared to mice with WT bone marrow. These results indicate that CD44 is crucial to stromal cell migration and incorporation to the tumor microenvironment as TAF.

Table of Contents

Dedication.....	iii
Acknowledgements.....	iv
Abstract.....	vi
List of Table/Figures.....	xiii
Abbreviations.....	xv
1. Introduction	
1.1 Cancer biology.....	1
1.2 Tumor microenvironment.....	1
1.3 Origin of tumor stroma components.....	2
1.3.1 Immunomodulatory components.....	3
1.3.2 Structurally supportive components.....	4
1.3.3 Vascular supportive components.....	6
1.4 Mesenchymal stem cell.....	7
1.4.1 Characterization.....	7
1.4.2 Naïve origin and function.....	8
1.4.3 Tumor tropism.....	8
1.4.4 Function in pathogenic states.....	9
1.5 Tumor inflammatory profiles.....	12
1.6 Glycoprotein CD44.....	12
1.6.1 CD44 Ligands.....	13

1.7 Migration.....	13
1.7.1 Chemokines, motogenic growth factors and peptides.....	14
1.7.2 Cell signaling pathways.....	15
1.8 MSC and anti-tumor gene therapy.....	16
1.9 Objectives and hypothesis.....	17
2.0 Materials and Methods	
2.1 Cell culture.....	19
2.2 Isolation and propagation of MSC.....	19
2.2.1 Human MSC.....	19
2.2.2 Murine MSC.....	20
2.3 Differentiation assays.....	20
2.3.1 Osteoblast differentiation.....	20
2.3.2 Adipocyte differentiation.....	21
2.3.3 Chondrocyte differentiation.....	21
2.3.4 CFU-F assay.....	22
2.4 Flow cytometry.....	22
2.5 Fluorescence activated cell sorting.....	23
2.6 Migration assay.....	23
2.6.1 Transwell assay.....	23
2.6.2 Scratch assay.....	23
2.7 Tube formation assay.....	24

2.8 Western blot.....	24
2.9 Chromatin Immunoprecipitation.....	25
2.10 Immunocytochemistry.....	25
2.11 Immunohistochemistry.....	25
2.12 Immunofluorescence.....	26
2.13 Molecular analysis.....	27
2.13.1 PCR.....	27
2.13.2 real time RT-PCR.....	27
2.14 Transfections.....	30
2.14.1 siRNA.....	30
2.14.2 Luciferase reporter assay.....	30
2.15 Viral Transduction.....	30
2.15.1 Adenoviral vectors.....	30
2.15.2 Lentiviral vectors.....	31
2.16 Animals.....	32
2.16.1 Exogenous MSC migration study.....	32
2.16.2 Tumor growth study.....	33
2.16.3 Bone marrow transplantation study.....	33
2.17 Bioluminescent imaging.....	33
2.18 Statistical analysis.....	34

3.0 Results

3.1 Characterization of MSC.....	35
3.2 Defining characteristics of tumor tropic MSC.....	42
3.2.1 Chemokine and cytokine expression profiles.....	42
3.2.2 <i>In vitro</i> migration of MSC.....	47
3.2.3 Blocking CD44 inhibits tumor tropic migration of MSC.....	52
3.2.4 Inhibition of tumor tropic MSC migration <i>in vivo</i>	56
3.2.5 CD44 signaling in MSC migration.....	59
3.2.6 CD44 activation by TCM induces Twist expression.....	64
3.3 Incorporation of MSC within the tumor microenvironment.....	70
3.3.1 Tumor conditioned MSC differentiate into activated fibroblasts.....	70
3.3.2 MSC as TAF contribute to tumor growth.....	77
3.4 CD44 deficient MSC become inadequate TAF.....	81
3.4.1 sh44 MSC are deficient as a supportive stromal cell.....	81
3.4.2 Characterization of CD44 deficient murine MSC.....	85
3.4.3 Delayed tumor progression in CD44KO mice.....	88
3.4.4 Tumor microenvironment impact of CD44KO MSC.....	91
3.4.5 CD44-deficient stroma tumor growth deficiency.....	95
3.4.6 Tumor recruitment of CD44KO bone marrow derived stroma.....	98
3.4.7 CD44KO stromal participation in the tumor microenvironment.....	104

4.0 Discussion

4.1 Role of CD44 in MSC tumor tropism.....	117
4.2 MSC contribution to the tumor microenvironment through TAF.....	119
4.3 Obstructed trans-differentiation of CD44 deficient MSC into TAF....	121
5.0 References.....	127
6.0 Vita.....	154

List of Table/Figures

Table 1. Primers.....	29
Figure 1. The tumor microenvironment.....	11
Figure 2. MSC characterization by flow cytometry.....	37
Figure 3. Human MSC trilineage differentiation potential.....	39
Figure 4. Murine MSC trilineage differentiation potential.....	41
Figure 5. Chemokine and cytokine expression by tumor stimulated MSC...	44
Figure 6. Expression of CD44 ligand in tumor cell lines and tissues.....	46
Figure 7. Migration of hMSC to tumor conditioned media.....	49
Figure 8. CD44 expression on human MSC.....	51
Figure 9. Migration inhibition of MSC toward Skov-3 conditioned medium..	54
Figure 10. <i>In vivo</i> tumor-tropic migration of MSC is inhibited by s44.....	58
Figure 11. MSC expressed CD44 localized to the nucleus following stimulation with SCM.....	61
Figure 12. MMP activation in tumor conditioned MSC drives migration partially through CD44.....	62
Figure 13. Inhibition of CD44 on MSC leads to decreased Twist expression.....	67
Figure 14. Tumor conditioned MSC induce CD44 binding to Twist promoter by ChIP.....	69
Figure 15. MSC can differentiate into TAF.....	72

Figure 16. Expression of TAF markers in MSC-admixed Skov-3 tumors	
<i>in vivo</i>	74
Figure 17. Growth advantage of tumors admixed with MSC.....	79
Figure 18. Deficient stromal supportive features of shCD44MSC.....	84
Figure 19. Characterization of murine CD44KO MSC.....	87
Figure 20. Tumor growth in CD44KO mice compared to WT mice.....	90
Figure 21. CD44KO MSC/4T1 admixed tumors have less tumor	
associated fibroblast presence and less vascularization <i>in vivo</i>	93
Figure 22. Differences in tumor size between CD44KO MSC/4T1 admixed	
and control tumors.....	97
Figure 23. Bone marrow transplantation into GFP recipient mice.....	100
Figure 24. H&E stained organs and tumor sections of BMT mice.....	102
Figure 25. Example analysis of marker co-expression by InForm	
Software.....	108
Figure 26. Fluorescent images of EO771 tumors in mice with	
CD44KO BMT or Red BMT.....	110
Figure 27. Statistical summary of tumor stroma origin.....	115

Abbreviations

α -MEM alpha-minimum essential medium

α -SMA α -smooth muscle actin

Ad adenoviral vector

ATCC American Type Culture Collection

β -gal beta galactosidase

BLI bioluminescent image

BM bone marrow

BMT bone marrow transplantation

CAF cancer associated fibroblast

CCD charge-coupled device

CCL chemokine ligand (C-C motif)

CD44KO transgenic mouse with endogenous loss of CD44 transcription

CD44KO BMT mouse GFP mouse with CD44KO derived bone marrow

CFU-F colony forming unit- fibroblast

CXCL chemokine ligand (C-X-C motif)

DMEM Dulbecco's modified eagle medium

ECM extracellular matrix

EGF epidermal growth factor

EMT epithelial to mesenchymal transition

EPC endothelial progenitor cells

FAP fibroblast activation protein

FBS fetal bovine serum

ffLuc firefly luciferase

FGF fibroblast growth factor

FSP fibroblast specific protein

GFP green fluorescent protein

HGF hepatocyte growth factor

HLA human leukocyte antigen

hMSC human mesenchymal stem cell

HSC hematopoietic stem cell

HUVEC human umbilical vein endothelial cell
IF immunofluorescence
IGF-1 insulin like growth factor 1
IHC immunohistochemistry
IL6 interleukin 6
IP intraperitoneal
IV intravenous
LacZ gene encoding for β -galactosidase
LT-MSC long term (21-31day) tumor conditioned MSC
MMP matrix metalloproteinase
mMSC murine mesenchymal stem cell
MOI multiplicity of infection
MSC mesenchymal stem cell
NS not statistically significant ($p>0.05$)
oHA hylauronan oligomer antagonist
OPN osteopontin
PBS phosphate buffered saline
PDGF platelet derived growth factor
PDGF β platelet derived growth factor receptor beta
Red BMT mouse GFP mouse with tdTomato derived bone marrow
RFP red fluorescent protein
rLuc renilla luciferase
ROI region of interest
RPMI Roswell Park Institute medium
s44 soluble CD44 receptor antagonist
SC subcutaneous
Sca-1 stem cell antigen-1
SCM Skov-3 conditioned media
SDF-1 stromal derived factor 1
SL1 stromelysin-1 (MMP3)
SF serum free

shCD44MSC MSC modified to express shRNA against CD44
shNeg MSC MSC modified to express negative control shRNA
TAF tumor associated fibroblast
TCM tumor conditioned media
tdTomato fluorophore derivative of RFP
TGF- β transforming growth factor β
Tn-c Tenascin C
TNF α tumor necrosis factor α
TSP-1 Thrombospondin 1
VEGF vascular endothelial growth factor

1. Introduction

1.1 Cancer Biology

In the United States, cancer accounts for almost 1 of every 4 deaths. (1) In women, over a quarter of newly diagnosed cancer patients will have breast cancer. Furthermore, there is a strong correlation between primary breast cancer survivors and the risk of subsequent cancers including ovarian cancer. While ovarian cancer affects a smaller proportion of women, it has a high mortality rate compared to other cancers inflicting women's reproductive organs. In these studies, we utilize both breast and ovarian cancer models to elucidate the interaction between the cancer and surrounding normal tissues in which the cancer subsists. By bettering our understanding of the tumor's microenvironment, we will enhance our ability to provide anticancer treatments.

Cancer is defined by a series of "hallmarks;" as described by Hanahan and Weinberg in 2000 these include the acquisition of self-sufficient growth, insensitivity to anti-growth signals, ability to invade and metastasize, replicate indefinitely, maintain angiogenesis and evade apoptosis. (2) These traits are vital to the growth and progression of cancer cells, and have been used as the basis for several anti-cancer therapies targeting proliferation, anti-apoptosis and angiogenesis. However, because the cancer cell does not sustain itself in isolation from normal cells in the body, interactions between normal and neoplastic cells within the tumor's microenvironment is likely involved in the progression and growth of the tumor and furthermore involved in the evasion of anti-tumor therapies.

1.2 Tumor microenvironment

The theory of microenvironment interactions with tumor cells extends from the late 1800s when Stephen Paget proposed the 'seed and soil' hypothesis suggesting that the cancer cells (seeds) need the appropriate environment (soil) for survival. Investigators now acknowledge that the idea of metastatic tumor cells is not a random, passive process, but that tumor cells engage with a microenvironment that

fits the needed homeostatic balance. When the criteria are filled, the cancer cell finds a home in a pro-growth, pro-angiogenic, pro-survival environment that is perhaps at first permissive to tumor growth but over time may become supportive to tumor growth. Allowing the outgrowth of the tumor is a feature of the cancer microenvironment when not only the cancer cells themselves express the 7 recognized “hallmarks of cancer,” but the “tumor activated” microenvironment becomes tumor permissive.

The tumor microenvironment is composed of several cell types including fibroblast, endothelial, myofibroblast and immune cells. The tumor stroma provides architectural and structural support as well as paracrine and juxtacrine growth factors that support proliferation, angiogenesis and invasion and enhance neovascularization (3, 4). Tumor stromal fibroblast studies suggest these non-neoplastic cells may not be normal, but may be “activated” by the tumor within which they reside (5, 6). Identifying the tumor associated stromal populations—their origin and their mechanism of interaction with and within the tumor may provide an attractive anti-cancer therapy targeted against tumor specific stroma.

1.3 Origin of tumor stroma components

Tumor stroma can be recruited from the local, surrounding tissue or from distant tissues through the circulation. The “local” tissue is a naturally convenient location of stromal recruitment for a developing tumor. While anatomical location is variable between tumor types, many tissues are rich in fibroblasts, pericytes and vascular cells that may contribute to the microenvironment of a growing tumor. In an elegant transplant model by Udagawa *et al.*, tumors were engrafted into mice receiving a GFP+ bone marrow transplant or adjacent to a GFP+ skin transplant. The tumors adjacent to the GFP+ skin transplant had organized GFP+ vasculature as opposed to hematopoietic derived GFP+ cells that were spatially unorganized and unstructured (7).

Udagawa *et al.* did describe distant (bone marrow derived) recruitment of stromal components into the tumor microenvironment, however incorporation was sparse. As a tumor grows, the angiogenic demand increases leading to increased vascularization that supplies blood, nutrients, oxygen and hematopoietic cells to the tumor. The hematopoietic stem cell population resides in the bone marrow and repopulates the blood lineages—several of which have been found in the tumor stroma including macrophages and lymphocytes. The other main bone marrow resident stem cell population includes the mesenchymal stem cell that repopulates the connective tissue populations. IV injected bone marrow derived populations are able to circulate and migrate to the tumor microenvironment (8, 9). Several studies have examined the incorporation of the bone marrow to the tumor microenvironments through transgenic models, or labeled bone marrow transplant studies. Bone marrow derived cells have been found in gliomas (10), sarcomas (11) and we have identified bone marrow derived populations in syngeneic breast cancer models (unpublished data). Contradictory studies show the bone marrow derived populations are incapable of participating in tumor endothelium (12). Further evidence suggests that the bone marrow derived cells are indeed capable of not only supporting tumor growth, but if mutated, are capable of forming tumors (13, 14).

Recruited from local neighboring tissue or distant tissue through the vascular or lymphatic circulation, these stromal components are heterogeneous and will be further divided into categories found within the tumor microenvironment including those modulating the immune, vascular and structural characteristics of the tumor and its microenvironment.

1.3.1 Immunomodulatory components

The chemotactic profile of the tumor is crucial to the induction of immune cell migration into the tumor microenvironment. Several chemokines are suggested to be involved in both the leukocyte infiltration and in immune surveillance—evading detection by immune cells (15). The tumor stroma is an active participant in the

immune evasion technique employed by the tumor—fibroblast precursors such as MSC have been shown to modulate dendritic cells, natural killer cells and T cells to a more “tolerant” phenotype, thereby protecting the tumor (16). Observing leukocytes in tumor stroma in 1863, Rudolf Virchow suggested a link between inflammation and cancer; his successors have since implicated leukocytes to play a role in the promotion of tumor growth, angiogenesis and metastases (17, 18). Immune cells including T lymphocytes and T helper cells have been isolated from the breast cancer patient tumor microenvironment (19).

One such immune cell found in the tumor microenvironment is the macrophage. The macrophage within the tumor microenvironment is shown to be a pro tumorigenic component inducing angiogenesis and proliferation through paracrine factor production. Furthermore, the macrophages immune-surveillance functions are compromised by the tumor microenvironment, thus creating a tumor associated macrophage (TAM) that supports tumor growth (20, 21). Reducing the inflammation in the tumor microenvironment leads to decreased TAM infiltration that leads to decreased tumor progression (21).

1.3.2 Structurally supportive components

The fibroblast expresses extracellular matrix (ECM) including collagen and laminin and provides a structural bed on which tissues and organs are situated. The function of the normal fibroblast is to repair wounded/inflamed tissues (22). However, fibroblasts, along with other components of the tumor microenvironment, have been implicated in the progression of tumorigenesis (23-26). The “activated” fibroblast has been described by a number of surface markers (25) that include:

- 1-** fibroblast and myofibroblast markers including fibroblast activation protein (FAP), fibroblast specific protein (FSP) and alpha smooth muscle actin (α -SMA)
- 2-** proteins associated with aggressive and invasive tumor phenotypes including secreted matrix remodeling proteinases such as the matrix metalloproteinase family

3- pro-growth paracrine factors including those that promote both proliferation and vascularization including VEGF, PDGF and EGF

These markers have been associated with pathogenic fibroblasts as opposed to the naïve fibroblast counterpart (6, 27); however, it appears that there may be several non-overlapping markers associated with the “activated” fibroblast populations (28). Activated fibroblasts can be defined as a heterogeneous population on many levels, intra-tumorally within a single tumor and inter-tumorally between several tumor subgroups. It is suspected that the tumor enlists participation of neighboring stromal components and thus this population is defined by but not limited to the markers described in the following sections.

The expression of the cell surface bound protease, FAP, is up regulated in activated fibroblasts involved in tissue remodeling of pathogenic conditions including wound healing of chronic inflammation and tumor development (29-31). The expression of FAP has been identified on tumor stroma in several carcinomas including thyroid (32) and colon (33) and has been used as an anti-tumor-stroma target in a breast tumor microenvironment model (34).

Similar to FAP expression patterns on activated fibroblasts, FSP, also called S100A4, is associated with aggressive and metastatic tumor phenotypes (35, 36). FSP is a member of the S100 super family which is involved in calcium signal transduction and cytoskeletal membrane interactions; it also functions in a paracrine factor by promoting angiogenesis in its secreted form (37).

Yet another marker of activated fibroblasts is the intracellular contractile protein, α -SMA. While this protein is expressed at basal levels on fibroblasts, and on myofibroblasts, the expression is up regulated under pathological states including active wound healing. Under normal wound healing environments, following wound contraction, as seen by an increase in α -SMA expression, the myofibroblasts undergo apoptosis. However, under TGF- β stimulation, the myofibroblast is resistant to apoptosis (38) thereby causing constitutive inflammatory paracrine

factor secretion and persistent fibrosis. Furthermore, as TGF- β is a growth factor secreted within the tumor microenvironment, it is reasonable to expect a correlation between TGF- β , myofibroblast α -SMA expression and increased malignant transformation (39).

1.3.3 Vascular supportive components

Neovascularization is a significant component in the growth and proliferation of a tumor. Beyond a diameter of 1mm, a tumor must create its own blood supply for nutrient exchange through angiogenesis (40). Both the tumor cells and the stromal cells are capable of secreting pro-angiogenic factors like VEGF, which is a current clinical target for many cancers (41, 42). Tumors rapidly vascularize in order to maintain their nutrient and oxygen supply through angiogenic sprouting. Bone marrow derived endothelial progenitor cells (EPC) have been shown to contribute to the angiogenic switch in tumor growth and metastases (43, 44). The numbers of EPC within a tumor as well as the number of circulating endothelial cells have been shown to correlate with tumor stage (45).

Tumor induced neovascularization is a deregulated process in which the vessel formation consists of endothelial cells, tumor cells and aberrant pericytes, such as activated fibroblasts. The lack of proper vessel structure results in leaky and inefficient vessels (46). Furthermore, permeable vessels can cause tumor interstitial hypertension that can inhibit the delivery of anti-tumor agents such as chemotherapy. Interestingly, inhibition of PDGFR β within the tumor microenvironment has been shown to relieve this interstitial pressure and thus allow the delivery of the chemotherapy (47). In a more recent study, combination therapy with PDGF and VEGF antibody treatment has been shown to have additive effects on tumor growth inhibition; furthermore, when used alone, anti-VEGF therapy is believed to up regulate the PDGF secretion by the supportive stromal populations to maintain angiogenic support (48).

A myofibroblast, briefly described above as a tumor supportive fibroblast cell, has often been confused with a vascular supportive cell known as the pericyte. Furthermore, it also has very similar properties and is very likely one in the same as the mesenchymal stem cell (49). The pericyte is a cell that helps to support the vasculature by forming close contacts and with and surrounding the endothelial cells comprising blood vessels. Pericytes can be defined by many of the same markers as the myofibroblast including α -SMA. Interestingly, the pericyte expression markers change when exposed to a TGF- β gradient; at low levels of TGF- β , the pericyte expressed desmin and NG-2 as opposed to high levels of TGF- β that induce the expression of α -SMA (50).

1.4 Mesenchymal stem cell

The fibroblast precursor is an adult stem cell known as the mesenchymal stem/stromal cell (MSC) that retains the potential to differentiate into osteoblasts, chondrocytes and adipocytes as well as many other tissues including neurons, muscle, endothelium, and more (51). It is one of the stem cell populations of the bone marrow, but can also be found as a resident stem cell population in most tissues.

1.4.1 Characterization

MSC are easily isolated from tissues. In general, they are obtained from the mononuclear fraction of a bone marrow aspirate and are selected for based on their plastic adherence in tissue culture. A group of markers cell surface markers have been used to characterize the cells, although there is no standard group of phenotypic markers to completely encompass the MSC (52). We characterize our human MSC by the positive expression of CD90, CD105, CD44, CD73, CD166 and CD140b and the negative expression of the hematopoietic markers CD45 and CD34, the endothelial marker CD31 and the macrophage marker CD11b. Murine MSC can be obtained similarly to human MSC and can be prospectively isolated on the positive expression of Sca1, CD105, CD106, CD44, and negative expression of CD117 (c-kit), CD45 and Cd11b. For both human and murine MSC, no

standardized set of markers has yet to be agreed upon. However, the markers listed above are the most generally agreed upon markers in the literature. Furthermore, the expressions of specific surface marker combinations appear microenvironment-dependent, suggesting a strong tissue-specific-influence on the MSC phenotype.

1.4.2 Naïve origin and function

The MSC is a progenitor cell capable of generating several different connective tissue cell lineages including bone, cartilage, muscle, fat and tendon. The primary function of the cell is to repair injured tissues. Upon injury, the tissue elicits a chemotactic inflammatory response to attract immune cells of various leukocyte lineages and the MSC—a fibroblastic stromal repair cell that contributes to the formation of granulation tissue through promoting angiogenic invasion to replenish the oxygen and nutrient supply, and the fibroblasts and contractile cells (myofibroblast) that help to close the wound (53).

Initially, the MSC was characterized as a bone marrow derived cell, consisting of a mere 0.01% of the bone marrow cell population (54). More recently, the MSC has been isolated from several other organs including adipose, umbilical cord, lung, heart, brain and muscle tissue (55-59). Given that MSC have been found in several tissues throughout the body suggests they play a significant role in maintaining the population of cells that facilitates wound healing even as a minor cell population. However, when confronted with an inflammatory incident, chronic or acute, MSC will accumulate at the site of injury and provide growth factors, angiogenic factors and structural support that include tissue reorganization and cell differentiation (3, 60). Evidence of MSC accumulation in inflamed/injured environments have been shown in models of myocardial infarction, ischemic brain tissue, injured lung tissue, allograft rejection and SC incisions (61-66).

1.4.3 Tumor tropism

Just as injured tissue, the tumor elicits an inflammatory response that mimics that of a wound. As stated by Dvorak and colleagues in the early 80s, tumors are “wounds

that never heal” (67). Consequently, MSC respond to the tumor microenvironment much in the same way they do a wound.

The migratory process that enables an MSC to migrate towards an inflamed microenvironment such as the tumor is a lesser known process. Similar to the more established leukocyte migration process, the MSC express many of the same chemokine and cytokine receptors known to be involved in leukocyte migration. Recent identification of chemotactic inducers, have implicated several chemokines, SDF-1(68), CXCL8 (69), MCP-1 (70), IL-1 β , and TNF- α (71) growth factors including PDGF-A/B (72), IGF-1 (73) and TGF- β 1 (71), components of the extracellular matrix including fibronectin, vitronectin, and collagen I (74), and peptides such as LL-37 (Cathelicidin hCAP18) (75). Furthermore, chemokine receptors expressed by MSC that have been implicated in the role of MSC migration include CCR2 in its role in amplifying MSC tropism to breast tumors receiving low dose irradiation (76), CXCR2 and CXCR4 in glioma tumor models expressing IL-8 and SDF-1, respectively (77, 78) In response to the chemotactic gradient from the tumor, the MSC will promote a migratory response through the modulation of extracellular proteases including the family of matrix metalloproteinases MMP-1, MMP-2, MMP-13, TIMP-1 and TIMP-2 (79).

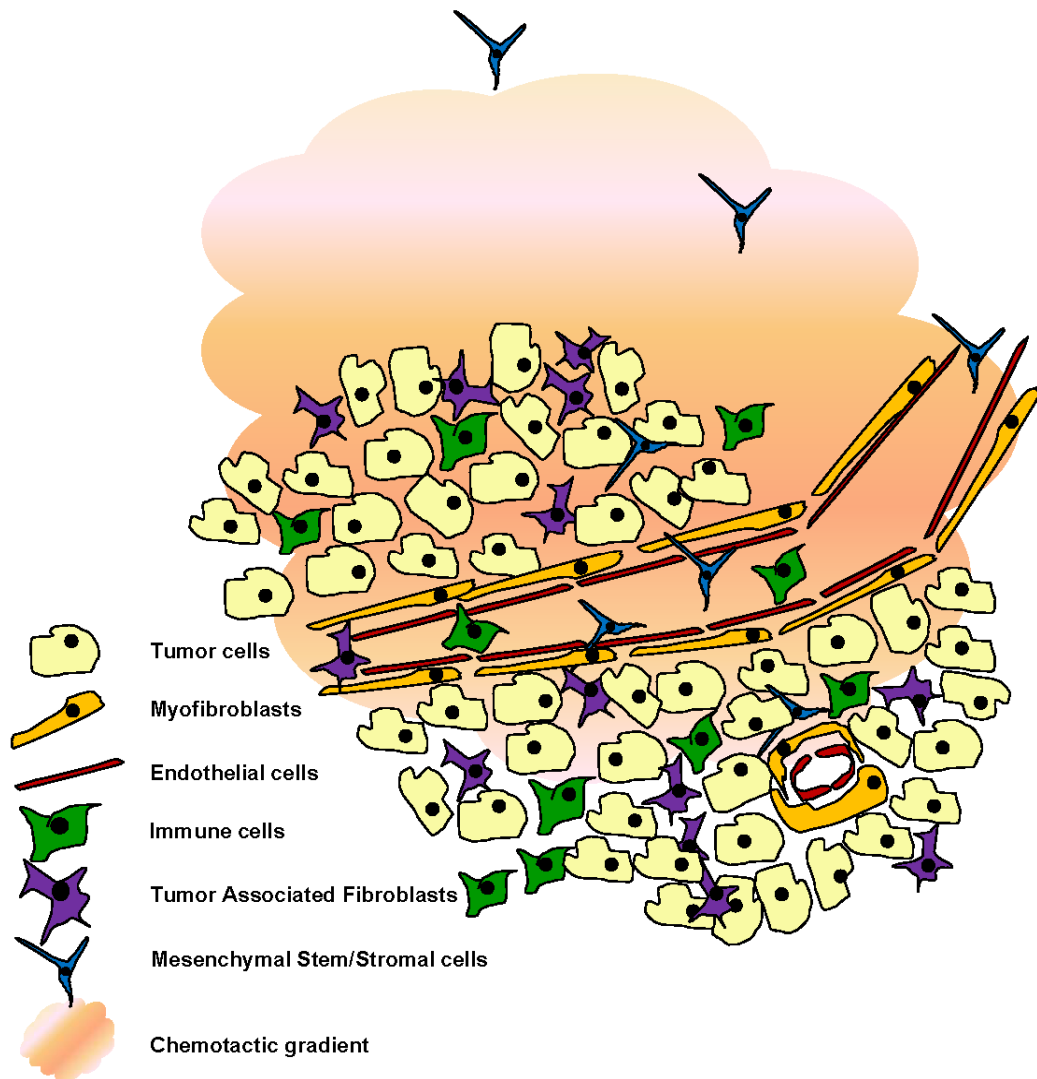
1.4.4 Function in pathogenic states

While the MSC facilitate the healing process of a wound, they also “facilitate the healing” of a tumor which involves a repertoire of pro-growth, pro-angiogenic, and structurally supportive functions. (Figure 1) Unfortunately, the hijacked function of the MSC serves a pro-tumorigenic role in cancers. Investigators have shown the MSC in the tumor microenvironment participating in the proliferation, vascularization, and the metastatic/invasive state of the tumor cells (8).

As discussed by Kidd and colleagues in a 2008 review (3): there remains a debate between investigators regarding the potential of MSC to inhibit (80-83) or enhance (8, 84-87) tumor progression. The animal models currently used to assess the MSC

potential may not accurately portray physiological conditions. Ultimately, the pathogenic potential of MSC is likely dependent on the immediate microenvironment and each tumor microenvironment is unique.

Figure 1. The tumor microenvironment. A heterogeneous composition of tumor cell, immune cells, fibroblasts and endothelial cells that act in concert with one another maintaining a supportive, pro-proliferative, pro-angiogenic, immunoevasive environment. The chemotactic signature from a tumor microenvironment summons the participation of additional cells like MSC for growth, support and sustenance.



1.5 Tumor inflammatory profiles

Tumors elicit an inflammatory response analogous to that of a wounded environment; this response includes peripheral cell migration, tissue remodeling, cell proliferation and angiogenesis (67, 88). The tumor cell interaction with the surrounding stroma provides a more drastic inflammatory signature that has been implicated in the derivation and acquisition of additional stromal components from both local and distant sources as well as a means for increased tumor metastases/invasion potential. Investigators have identified factors including chemokines such as CCL2, CCL3 and CCL5 (8, 89) that increase the migration potential of both the contributing stroma and the tumor cells. Furthermore, it is evident that amplification of inflammatory signals augments the stromal component infiltration as seen by radiation (76), hypoxia (90) or Triterpenoid CDDO-Me (91) treatment.

In addition to chemokines, glycosaminoglycans such as hyaluronan and glycoproteins like osteopontin are associated with chronic inflammation and are often present within the tumor microenvironment. Tumor associated fibroblasts from hyaluronan overproducing mammary tumors have been isolated and transplanted with tumor cells to show an increase in lymphangiogenesis in particularly in the tumor-stromal interface in association with VEGF up regulation (92).

The chemotactic profile employed by the tumor will promote the incorporation of local and distant cells that may be tumor suppressive or tumor promotive in nature (3). The presence of these immune cells, fibroblasts and endothelial precursors in the tumor microenvironment will further modify the chemotactic profile.

1.6 Glycoprotein CD44

CD44 is a class I transmembrane glycoprotein that has been shown to mediate cell growth, survival, differentiation and migration (93). CD44 is a highly conserved gene that has 12 alternatively spliced exons (94) that make up more than 100 splice forms of the protein. The splice variability occurs in the extracellular portion of

CD44. In addition to the splice variants, the post-translational modifications (e.g. glycosylation) account for the discrepancies in CD44 expression between cell types and local environments. The cytoplasmic tail of CD44 is known to interact with components of the cytoskeleton including ankyrin and the ERM (ezrin, radixin and moesin) proteins which are thought to regulate cell migration and shape (95-97). The cytoplasmic tail also has an intracellular cleavage domain that has been shown to translocate to the nucleus. Through association with Stat3 and p300 the CD44-ICD has been shown to bind to promoter elements and influence transcriptional regulation of target genes including Cyclin D1 (98). Furthermore, CD44 expression has become well known as one of the markers of a “tumor initiating cell” particularly in breast cancer, and is associated with drug resistance, apoptosis evasion and cell survival (99-102).

1.6.1 CD44 ligands

Extracellular matrix proteins such as laminin, collagen, fibronectin, and hyaluronan (HA) are able to bind to CD44 through docking sites in the extracellular region, although the HA-binding domain is the only site that has been extensively mapped (93). As the most well known CD44 ligand, HA functions as a mediator of the inflammatory response and subsequent wound repair. In cancer, expression of HA synthase has been associated with a pro-metastatic phenotype.

Osteopontin (OPN) is another known ligand of CD44 that has been implicated in chronic inflammation. It is a secreted phosphoprotein produced by immune cells and injured cells and is known to induce the motility of macrophages, neutrophils, MSC, osteoclasts and tumor cells through association with CD44 and integrins (95,103-106).

1.7 Migration

In a review on stem cell trafficking, Laird et al. discriminate the act of migration described as an active phase of recruitment that is preceded by a passive phase of circulation defined as homing (107). The migratory stimulation factors secreted by

the tumor and its microenvironment selects for a population of circulating, or “homing,” MSC. Given the large variability in the MSC population at the phenotypic level, it is not surprising to discover that MSC are transient in nature and differ in phenotype depending on the surrounding stimulus provided.

MSC are known to migrate towards sites of inflammation including wounds and tumor microenvironments (66). Exogenously injected MSC have now been extensively exploited as delivery vehicle for anti-cancer agents to tumors including ovarian, glioma, lung, breast and Burkitt's lymphoma tumor models (9, 91, 108-111).

1.7.1 Chemokines, motogenic growth factors and peptides

In response to insult, inflamed environments secrete a variety of chemokines, cytokines, growth and angiogenic factors and shed a large number of extracellular matrix proteins. Tumor cells and the cells in the surrounding local tissue secrete many chemokines and cytokines that mimic a wound response. Consequently, the tumor microenvironment is under constant inflammation and is analogous to a wound that does not heal (67). Chemokine profile from the tumor can be amplified by adding insult such as radiation treatment which enhances the migration of MSC to the environment (76).

CCL25 has been shown to induce the migration potential of MSC (112). SDF-1 is produced by MSC under tumor stimulation and has been shown to modulate migration through focal adhesion kinase and activation of Stat3 (68). In turn, Stat3 has a large number of downstream transcriptional targets implicated in regulation of invasion (113). MCP-1 (CCL2) has been implicated in several tumor models to modulate MSC migration (76, 78, 114).

Growth factors have also been implicated in the migration of MSC. PDGF-b has been shown to play a role in the migration of MSC towards malignant gliomas (115). EGF has been implicated in the migration of keratinocytes (116) and breast cancer cells (117).

In a tumor microenvironment, tissue remodeling is constantly taking place. Throughout this process, a large amount of cellular debris is accumulated, this debris is often cleaved extracellular matrixes and other peptides, proteoglycans and glycoconjugates. These elements can induce an inflammatory response, but they are also capable of binding and presenting chemokines and growth factors. Such elements include the CD44 ligands, osteopontin (118) and hyaluronic acid (119). A peptide fragment of the anti-microbial protein, LL-37, is over-expressed in ovarian, breast and lung cancers and has been shown to facilitate MSC migration towards tumor cells (120).

1.7.2 Cell signaling pathways

Cellular migration is an intricate mechanistic process much like a Rube Goldberg machine. Multiple receptors can be stimulated/activated to induce the same physiological outcome—cellular migration. The chemotactic factors eluded to in the previous section have corresponding receptors on the cell surface of MSC. There are several different receptors implicated in the migration of MSC from G-coupled protein receptors to tyrosine kinase receptors to integrins. By blocking endogenous HA from binding to and activating CD44, the activation of several receptor tyrosine kinases can be inhibited including ERBB2, EGFR, IGF1R β , c-MET, and PDGFR β (121, 122).

Migration is a polarized process sustained by a series of signals to the leading and lagging edges of the cytoskeleton. CD44 has been implicated in the signaling pathways of migration as an intermediary in the activation of non receptor tyrosine kinases (e.g. Src family) (123).

In a recent paper, one of the CD44 variants is shown to stabilize androgen receptor activation through complex interaction with cMet upon HGF and hyaluronan activation of cMet and CD44, respectively (124). Furthermore, using a renal cell carcinoma line model, CD44 was shown to activate Stat3, complex with the

acetyltransferase, p300 and by ChIP sequencing was shown to bind 19 different promoter elements including Cyclin D1 (98). Furthermore, Lee *et al* confirmed that CD44 was able to mediate expression of other Stat3 responsive gene targets including VEGF and MMP2 (98). Moreover, the Stat3 transcription factor is associated with migration/invasive phenotype of tumor cells through the transcriptional activation of genes such as Twist (113, 116, 125-127).

Twist has been described as a “master regulator” in embryonic development as it plays a crucial role in the epithelial to mesenchymal transition of mesoderm formation (128) and neural crest development (129). More recently, Twist has been implicated in tumor EMT and is associated with cell invasiveness. (130)

1.8 MSC and anti-tumor gene therapy

Targeted gene therapy/drug delivery is an appealing treatment tool because of the potential avoidance of toxic side-effects to normal tissues. With a targeted delivery system, many factors that impede drug efficacy including the pharmacokinetics and pharmacodynamics can be improved. Localizing the site of drug activity to the targeted tumor using a delivery vehicle can enhance the anti-tumor effect as well as the non-specific toxicity to normal tissues.

While other cell types have been reported to display tumor tropism (10, 20, 45), MSC are arguably better suited as a targeted gene therapy delivery tool. First, MSC are as easily accessible from bone marrow and liposuction aspirates. They readily propagate *in vitro*. Furthermore, *ex vivo* expanded MSC retain their tumor homing potential. Finally, MSC can be easily gene modified because they possess the metabolic activity and molecular machinery for sufficient production of therapeutic gene products (9, 131).

Studeny *et al* first reported the efficacy of the MSC as a delivery vehicle in the delivery of interferon beta in the treatment of melanoma (9). Since this initial report, several investigators have showed the targeted migration and engraftment of MSC to the tumor model and furthermore reported an efficacious anti-tumor effect using

biological proteins including interferon alpha (132), IL7 (133), IL12 (134) and TRAIL (135). MSC have also been used to deliver molecular antagonists against hepatocyte growth factor (109), urokinase-type plasminogen (136), and truncated soluble vascular endothelial growth factor decoy receptor (110, 137). Furthermore, MSC expressing pro-drug converting enzymes (cytosine deaminase and HSV-thymidine kinase) have also been delivered to the tumor microenvironment to enhance the anti-tumor therapy (138-140).

MSC have already shown great potential as a tumor-targeted delivery vehicle, but therapeutic efficacy may be enhanced by genetic manipulations of MSC to further improve target potential. This has been achieved in a myocardial infarction model where MSC modified to over express the surface receptor CXCR4 were better able to target and home to the infarcted region (141). The potential to modify MSC for enhanced tumor-tropic migration rate is a foreseeable stride in the effort to achieve an unparalleled anti-tumor delivery vector.

1.9 Objectives and Hypothesis

Despite the migratory propensity of the MSC for site of inflammation like the tumor microenvironment, the potential of an exogenously injected population of MSC to reach the tumor target is less than 15%. The efficacy of MSC as a delivery vehicle could be greatly improved if the mechanism of migration were elucidated, and could subsequently be exploited to enhance tumor-specific migration. Like every treatment, there are benefits and adverse effects. Investigators have reported both pro- and anti-tumorigenic effects of MSC on tumor growth and progression. Understanding the potential long term effect of the MSC on the tumor microenvironment is important to the prospect of MSC as therapeutic delivery vehicles. Furthermore, understanding the MSC in the context of the tumor microenvironment may elucidate on the role of the endogenous MSC in tumor development as a precursor of stroma.

The objective of this study was to elucidate characteristics of the tumor stroma participants, particularly of the bone marrow derived MSC. Therefore, **we hypothesized that intracellular signaling via CD44 mediates the migration and incorporation of mesenchymal stem cells to the tumor microenvironment.** To investigate this hypothesis we proposed the following specific aims:

Aim I: To identify the MSC receptor(s) responsible for the migration of this stromal cell to the tumor microenvironment.

Primary human MSC were analyzed for the chemokine ligand and receptor expression changes under the influence of tumor conditioned medium revealing CD44 receptor. Migration of MSC toward tumor conditioned media was inhibited *in vitro* and *in vivo*. Mechanistic data revealed that tumor stimulated MSC can activate Twist expression leading to increased migration.

AIM II: Elucidate the stromal contribution of the MSC to the tumor microenvironment as tumor associated fibroblasts in the context of MSC expressed CD44

MSC admixed with tumor cells and engrafted *in vivo* show enhanced tumor growth through angiogenic and structural support in the form of tumor/carcinoma associated fibroblasts (TAF/CAF) as identified by surface markers. Utilizing transgenic CD44 knockout mice, a series of tumor engrafting studies were carried out with both endogenous and exogenous bone marrow derived stromal populations. Harvested tumors were analyzed for size as well as TAF markers and angiogenesis. We determined that MSC expressed CD44 is necessary for efficient TAF support within the tumor microenvironment. Furthermore, we confirmed that CD44KO bone marrow derived cells are less capable of tumor contributing to FAP+/FSP+ tumor development but that host derived WT stromal tissues compensate for the deficient FAP+/FSP+ TAF population within the tumor.

2.0 Materials and Methods

2.1 Cell culture

Murine E0771 breast cancer cells were generously donated by Dr. F.M. Sirontak of the Memorial Sloan-Kettering Cancer Center in New York, New York. Murine 4T1 cells were stably transduced with a lentivirus expressing renilla luciferase (4T1-rLuc) and donated by Dr. J. Ling of MD Anderson Cancer Center. Tumor cell lines including PANC-1, Skov-3, MDA-468, MCF7, MDA-231 cells were purchased from American Type Culture Collection (ATCC, Manassas, VA). MDA-231 and Skov-3 cells were maintained in alpha-minimum essential medium (α -MEM; HyClone, Waltham, MA), containing 10% fetal bovine serum (FBS; Invitrogen, Carlsbad, CA), sodium pyruvate, nonessential amino acids, vitamin solution (Life Technologies, Grand Island, NY), L-glutamine (Gibco/Invitrogen, Carlsbad, CA) and penicillin-streptomycin (Gibco/Invitrogen, Carlsbad, CA). E0771 and 4T1 cells were maintained in Roswell Park Memorial Institute medium (RPMI-1640; HyClone, Waltham, MA) supplemented with 10% FBS, penicillin-streptomycin and L-glutamine. Finally, PANC-1, MDA-468 and MCF7 cells were maintained in Dulbecco's modified eagle medium (DMEM, HyClone, Waltham, MA). Tumor conditioned media was made by incubating 30-80% confluent cells in 2% α MEM for 48 hours.

2.2 Isolation and propagation of MSC

2.2.1 Human MSC

Human MSC (hMSC) were obtained from bone marrow aspirates of normal donors undergoing bone marrow harvest for allogeneic bone marrow transplantation upon informed consent, according to institutional guidelines under the approved protocol, as described previously (9). Following a Ficoll-Hypaque density gradient (Sigma, St. Louis, Mo) and mononuclear cells were re-suspended in MSC medium: α -MEM, 20% FBS, L-glutamine and penicillin-streptomycin. The suspension was plated in 10 ml MSC medium in a 180 cm² dish. Non-adherent cells were removed three days after culture establishment and the adherent layer was washed with phosphate

buffered saline (PBS) before the MSC medium was replaced. Adherent monolayers were cultured until they reached 80-90% confluence, at which time they were trypsinized (0.25% trypsin/0.1% EDTA; Gibco/Invitrogen, Carlsbad, CA) and sub-cultured at 5,000-6,000 cells/cm². MSC media was replaced every three days. Cells were used for experimental procedures at passages 3-5.

2.2.2 Murine MSC

Murine MSC (mMSC) were isolated as described previously (142). Femurs, tibias, and iliac crests were isolated from 6-10 week old mice. Muscle and connective tissue was removed from bones with scalpel and the bone were crushed with a mortar and pestle in PBS containing 2% FBS to release the marrow. The marrow was collected and stored in MSC medium in a 10cm dish. The crushed bones were further diced with a scalpel and suspended in 3mg/ml Collagenase Type I (Worthington Biochemical Corporation, Lakewood, NJ) using 2 ml/mouse. The suspension was placed in a 37°C shaker at 300 rpm for 45 minutes. After incubation, bones were filtered out and cells were washed in PBS. Cells from the bone were combined with those plated from the marrow in MSC medium in a 10cm dish according to the same procedure used for hMSC culture. Cell density was maintained between 2,000 and 6,000 cells/cm².

2.3 Differentiation assays

2.3.1 Osteoblast differentiation

22,500 hMSC or mMSC were plated sub-confluently in a 12 well plate in NH OsteoDiff Medium (Miltenyi Biotec, Auburn, CA) and cultured for 3 weeks with twice weekly media replacement. After 3 weeks, osteoblasts were fixed with pre-cooled 100% methanol and then washed with PBS. Cells in each well were stained with either chromogenic alkaline phosphatase substrate, SIGMA FAST BCIP/NBT (Sigma Aldrich, St. Louis, MO) incubated at 37° for 10 minutes, or with Alizarin Red S solution (Sigma Aldrich, St. Louis, MO) for calcium staining. Alizarin Red S solution was added to washed cells and incubated at room temperature for 10

minutes. All wells were then washed with water and osteoblasts were visualized and photographed on an Olympus BX41 microscope (Olympus, Center Valley, PA).

2.3.2 Adipocyte differentiation

20,000 hMSC or mMSC were plated in a 12 well plate in 20% α MEM. After the cells reached confluence they were maintained in adipogenic induction medium for 48-72 hours (DMEM, 10%FBS, penicillin, streptomycin, L-glutamine, 10 μ g/ml insulin, 500 μ M 3-isobutyl-1-methylxanthine, 1 μ M dexamethasone, and 200 μ M indomethacin (last four chemicals purchased from Sigma Aldrich)). After 72 hours, cell media was changed to adipogenic maintenance medium (DMEM, 10%FBS, penicillin, streptomycin, L-glutamine, and 10 μ g/ml insulin) for 24 hours. The round of 72 hour induction followed by 24 hour maintenance was repeated for three rounds. After the third round, cultures were maintained in adipogenic maintenance medium for 10 more days with twice weekly media changes. Adipocytes were then visualized by staining with Oil Red O (Sigma). Cultures were fixed in 10% formalin. After one hour, formalin was washed off with 60% isopropanol, and cultures were dried. Twice filtered (0.22 μ m syringe filter) Oil Red O working solution (4 ml water + 6 ml of 0.35% Oil Red O dissolved in 100% isopropanol) was placed on dry adipocytes for 10 minutes. Cells were washed with water and let dry. Red stained lipid vacuoles were then visualized and photographed within adipocytes on the Olympus BX41 microscope.

2.3.3 Chondrocyte differentiation

350,000 cells were pelleted in a 15 ml polypropylene Falcon tube. Cells were resuspended in chondrocyte differentiation medium consisting of DMEM, penicillin, streptomycin, L-glutamine, 50 μ g/ml ascorbic acid, 100nM dexamethasone, and 10ng/ml transforming growth factor β 3 (TGF- β 3). The suspension was pelleted again and placed into 37°C incubator with the cap on but loosened for gas exchange. Without disturbing the pellet, the chondrocyte differentiation medium was replaced 3 times a week. 10ng/ml TGF- β 3 was added daily. The pellets were cultured for 21 days, before they were rinsed in PBS and fixed in 10% formalin.

They were then paraffin embedded and sectioned for histology. Sections were deparaffinized in xylene and rehydrated in a series of alcohols. Mucopolysaccharides associated with chondroblast differentiation were stained with 1% Alcian Blue in 5% acetic acid for 30 minutes. After rinsing with tap water and distilled water, sections were counterstained with Nuclear Fast Red (Lab Vision Corporation, Fremont, CA) and mounted in aqueous mounting medium. Sections were visualized and photographed on the Olympus BX41 microscope.

2.3.4 CFU-F assay

5×10^5 whole Bone marrow cells were plated in MSC medium in a 12 well dish. Medium was changed twice per week for 2 weeks. Wells were then washed with PBS and fixed in ice cold methanol. Giemsa staining solution was applied to fixed wells for 10 minutes. Wells are washed with water and then imaged.

2.4 Flow cytometry

For analysis, cells were trypsinized, washed and resuspended in ice cold PBS supplemented with 2% FBS and 1% BSA (106 cells/100 μ l/staining reaction). 1 μ g of each antibody was added to the cell suspension and incubated at 4°C for 30 minutes. Cells were washed two times in PBS and resuspended in 250 μ l for analysis or 100 μ l for secondary antibody staining (PE-secondary antibody for 15 minutes on ice). Cells were washed two more times before being resuspended in 250 μ l of PBS on ice for analysis on a BD LSRII Flow Cytometer (Becton Dickinson, San Jose, CA) with FACS Diva software (MDACC Core Flow Cytometry Facility) or on a Beckman Coulter Gallios with Kaluza Software (Beckman-Coulter). Human antibodies utilized for flow cytometry included: CD105, CD90, CD140b, CD73, CD116, CD146, CD44, CD31, and CD34 (BD Bioscience, San Jose, CA). Antibodies for mouse antigens included: Sca-1, CD11b, CD31, CD34, CD44, CD106, CD140b, CD45 and c-kit (eBiosciences, San Diego, CA).

2.5 Fluorescence activated cell sorting (FACS)

Cells were sorted based on GFP expression. Cells were trypsinized, washed, filtered and resuspended in ice cold PBS supplemented with 2% FBS. Cells were sorted into GFP⁺ and GFP⁻ sub-populations (BDFACS Aria).

2.6 Migration assays

2.6.1 Transwell assay

MSC migration was assayed using 8µm pore, 6.5mm transwell inserts in a 24 well plate. The 18hr serum-starved MSC were plated at 4×10^4 cells per well, with tumor cell conditioned media, serum media, or serum free media. For migration inhibition, MSC were pre-incubated with neutralizing antibodies for 45 minutes prior to plating. MMP inhibitor V (cat#444285) was purchased from EMD Chemicals (Gibbstown, NJ) After 24 hours, the media was removed, the cells were fixed, stained and excess cells were wiped from the top layer of the transwell insert and inserts were dried overnight. Only the cells within the membrane were analyzed using a 3 step staining method (Fisher Scientific, Pittsburgh, PA) comparable to the Wright-Giemsa method. Manual cell counts and images were captured (Olympus BX41 microscope with an Olympus DP70 camera attachment), and followed by a quantitative analysis measuring the amount of staining on each membrane. The transwell membranes were placed in 300µl 2% deoxycholic acid until dye was fully solubilized (3-8 hours). A fixed wavelength of 595nm was used to obtain a quantitative measurement from each sample (Beckman Du 640 Spectrophotometer).

2.6.2 Scratch assay

MSC were grown to a confluent monolayer in a 12 or 24 well dish. Using a p200 pipette tip a 5mm long “scratch” was made along the bottom of the dish. The location of the scratch was referenced on the dish—but outside of the field of view on the microscope.

The wells were gently rinsed with serum media to clean the edges of the scratch and discard debris. 1% serum MSC media was added to the wells as base media.

Neutralizing antibody, full serum, IgG antibody, small molecule inhibitors or tumor conditioned media was added to sample wells. Cells were incubated at 37°C. Images were acquired on a fluorescence or phase contrast microscope at select time points over the duration of the incubation—every 60 minutes over a 48 hour period. Using image analysis software, the distances between the scratch and the migrating cells can be quantitatively compared using Slidebook, Image Pro-Plus software (Media Cybernetics) or a freeware (<http://rsb.info.nih.gov/ij/>).

2.7 Tube formation assay

HUVEC (ATCC, Manassas, VA) were cultured in EGM2 (Clonetics, Workingham, UK). 3×10^4 HUVEC were plated per well into a 24 well plate in triplicate. Media was replaced 12 hours later with MSC conditioned media. Wells were imaged and analyzed with an Olympus Ix81 microscope with a DSU confocal attachment and Slidebook software (Center Valley, PA). 4 images were taken per well, tubes were manually counted and averaged between groups.

2.8 Western blot

Cells were lysed in protein lysis buffer (50mM HEPES (238.3g/mol), 300mM NaCl (58.4 g/mol), 2mM EDTA (372.24 g/mol), 50mM NaF (41.99 g/mol), 2mM Sodium Orthovanadate (183.91 g/mol), 10% (v/v) glycerol, 2% (v/v) NP40, 1% (v/v) Triton X-100 and a cocktail of protease and phosphatase inhibitors). After 1-2 hours on ice, lysates were spun down for 30 min at 13,000rpm, lysate supernatant was quantified by Bradford assay (Bio-Rad, Hercules, CA) and then lysate was boiled with loading buffer and loaded onto a 12% SDS-PAGE gel (Bio-Rad, Hercules, CA). After electrophoresis, proteins were transferred onto Hybond-P membranes (Amersham Pharmacia Biotech), or nitrocellulose odyssey membranes (Licor Biosciences, Lincoln, NE) followed by immunoblotting. Signals were detected using ECL-Plus (Bio-Rad, Hercules, CA), alternatively, if fluorophore-conjugated secondaries were used the immunoblot signals were detected on the Odyssey infrared imaging system (Licor Biosciences, Lincoln, NE).

2.9 Chromatin Immunoprecipitation assay (ChIP)

1×10^7 MSC were grown to 80% confluency in 15cm plates. Cells were subjected to Skov-3 conditioned media before being fixed in 1% formaldehyde for 10 minutes at room temperature. Glycine (125mM final concentration) was added to stop the cross-linking reaction. After PBS wash, cells were scraped in PBS+protease inhibitor cocktail and centrifuged (650xg for 5 min). Cells were resuspended in lysis buffer and protocol was continued according to manufacturer's details (GA-101 ChampionChIP, SABiosciences, Frederick, MD). Briefly, chromatin was sheared on ice and then pre-cleared. Fractions were immunoprecipitated including negative and positive controls as well as CD44 (ab65829; Abcam, Cambridge, MA). Twist promoter primers listed in Table 1.

2.10 Immunocytochemistry

200 MSC per well were plated in an 8-well chamber slide (Lab-Tek, Naperville, IL). Cells were subjected to 24 hours of serum free media before conditioning with tumor conditioned media (Skov-3, MDA-231, or PANC-1) or MMP inhibitor V (444285; EMD Chemicals, Gibbstown, NJ) or small chain hyaluronan oligomer (100 μ g/mL of oHA from Dr. B. Toole) for 24 hours. After conditioning, cells were fixed in 3% formaldehyde, blocked in 3% BSA and stained with primary (listed in flow section) antibody at 4°C overnight. Secondary antibodies, Alexafluor[®] 488, Alexafluor[®] 594 or Alexafluor[®] 647 (Molecular Probes, Carlsbad, CA), were used at a 1:1000 dilution for 8 hours at 4°C or 1 hour at room temperature. 5 mg/ml DAPI (Sigma, St. Louis, MO) stain was used at a dilution of 1:10,000 for 1 minute. Glass coverslip was applied over Dako Fluorescent Mounting Media (Dako, Denmark) and let dry in the dark before edges were sealed with nail hardener. Image analysis was performed using an Olympus Ix81 microscope with aDSU confocal attachment and Slidebook software (Center Valley, PA).

2.11 Immunohistochemistry

Tissue sections were deparaffinized in a series of xylene and ethanol gradient incubations before subjected to incubation in boiling sodium citrate solution. Tissue

sections were stained with CSA II IHC kit (Dako, Denmark). Briefly, sections were blocked in peroxidase for 5 minutes, before being washed and blocked with a species specific protein block. Primary antibody was added for 15 minutes followed by 3x wash. Anti-mouse (or species secondary in use) IgG-HRP was added for 15 minutes followed by 3x wash. For low expressing proteins, an amplification reagent was used prior to anti-fluorescein HRP followed by DAB chromagen substrate. Slides were counterstained with hematoxyalin stain (Dako, Denmark) before being dehydrated in a series of ethanol incubations and then were finally cover-slipped with working oil mounting media.

2.12 Immunofluorescence

Paraffin embedded tissue sections were deparaffinized in a series of xylene and ethanol gradient incubations before subjected to incubation in boiling sodium citrate solution. Frozen tissue sections were fixed in ice cold acetone for 10 minutes, rinsed in PBS and then incubated in blocking buffer (3%FBS, 1%BSA and 3% goat serum) for 1 hour at room temperature. Primary antibody was added at optimal dilution in diluted blocking buffer overnight at 4°C. Slides were washed three times in PBS with 0.05% Tween-20 (PBST). Secondary Alexafluor antibody was added at a 1:1000 dilution in diluted blocking buffer and placed on the slide for 1 hour at room temperature. Slides were washed three times in PBST before being stained with the nuclear marker 5mg/mL DAPI at a 1:10,000 dilution for 1 minute. Slides were washed three more times in PBST, and covered with glass coverslip over Dako Fluorescent Mounting Media (Dako, Denmark) and left to dry in the dark before edges were sealed with nail hardener. Multispectral images were obtained using a CRi attachment on an Olympus Ix81 microscope with a DSU confocal attachment using Nuance software, and images were analyzed using InForm software (CRi, Woburn, MA).

Data analysis was performed with InForm software. Briefly, regions of interest were defined on 4 images, and the recognition software was trained to classify all images based on stroma versus parenchyma versus background. Then, based on DAPI

fluorescence, the nuclei were defined and classified followed by cytoplasm definition surrounding each defined nuclei. Fluorescence data (pixels) was quantified for each nucleus and cytoplasm for every cell in every image. Nuclear and cytoplasmic pixel signals exported and summated to give per cell quantitation of pixel count for each fluorochrome per cell (nucleus+cytoplasm). Numerical cutoffs based on isotype controls were used to define combination of either Alexa Fluor 488+ or Alexa Fluor 594+ cell populations. Each image was evaluated on a percent positive basis. 10 images per slide were quantified and averaged at 3 different depths within the tissue section which were in turn averaged to give a final percent across each tumor. 3 tissue sections were analyzed in this manner per experimental group.

2.13 Molecular analysis

All cells subject to PCR analysis were extracted with either DNAeasy or RNAeasy kits (Qiagen, Valencia, CA) according to manufacturer's protocol. Nucleic acid concentration was measured using Nanodrop 2000c (ThermoScientific, Wilmington, DE). DNA was used at 0.25µg per reaction and RNA was used at 1µg per reverse transcription reaction.

2.13.1 PCR

Maxima Hot Start 10x buffer, 25mM MgCl₂, 25mM dNTP and 5U Taq was purchased from Fermentas Life Sciences (Glen Burnie, MD). Primers purchased from Integrated DNA Technologies (Coralville, IA) were prepared into 10µM stock solutions and are listed in Table 1.

2.13.2 RT-PCR

Inflammatory chemokine and cytokine arrays were purchased from SA Biosciences (Frederick, MD). After 24 hour conditioning, RNA was collected (RNAeasy; Qiagen, Valencia, CA) and reverse transcribed using cDNA kit (SABiosciences, Frederick, MD). Data was analyzed using SABiosciences spreadsheet to calculate fold change based on delta Ct.

For all other RT-PCR, 1µg RNA was reverse transcribed using a kit from Signalway Biotechnology (Pearland, TX). 20µL of cDNA was diluted with 100µL of distilled RNase/DNase free water. Sybr-green master mix was purchased from Applied Biosystems. 0.5µL-1.0µL cDNA was used per reaction on an assay dependent basis. 0.5µL forward and reverse primer (both at 10µM stocks) 10µL distilled water and 12µL Sybr-green master mix was added per well for a total volume of 25µL. All reactions were done in triplicate and carried out in a 96well fast plate in an ABI7900HT Thermocycler (Applied Biosystems). Relative expression was calculated by normalizing samples to GAPDH (human) or 18s (murine) and then compared between control and sample sets using the delta-delta Ct method. All data is presented as fold change over control ($2^{-\Delta\Delta C_t}$).

Table 1. Primers

Protocol name	Primer name	sequence (5'-->3')
CD44-Twist ChIP proximal	Twist prox prom F	CGG GGG AGG GGG ACT GGA AAG C
	Twist Prox prom R	AGG CCT CCT GGA AAC GGT GCC G
CD44-Twist ChIP distal	Twist Dist prom F	TAC TCC AGC GCG GTG CAC AAA ACT
	Twist Dist prom R	AAC GAA GAG CCC CAA AGA GGG TGT
CD44-CD44 ChIP promoter	CD44 promoter F	AGG GCT CTG AAG ATA GCG CCA GG
	CD44 promoter R	AAT GCA CCC AGC CAT CCC CCT
CD44 expression	CD44 F open	GGG AGC TGG GAC ACT TAA CA
	CD44 R open	GGG CCC TAA TTT CAG AAA GC
Twist expression	Twist RT F	GGA GTC CGC AGT CTT ACG AG
	Twist RT R	TCT GGA GGA CCT GGT AGA GG
VegfA expression	VegfA F	CTT GCC TTG CTG CTC TAC C
	VegfA R	CAC ACA GGA TGG CTT GAA G
VegfC expression	VegfC F	TGC CGA TGC ATG TCT AAA CT
	VegfC R	TGA ACA GGT CTC TTC ATC CAG C
EGF expression	EGF F	CCT GCC TAG TCT GCG TCT TT
	EGF R	CAC AAT ACC CAG AGC GAA CA
IL-8 expression	IL-8 F	ATG ACT TCC AAG CTG GCC GTG GCT
	IL-8 R	TCT CAG CCC TCT TCA AAA ACT TCT C
OPN expression	OPN F	GCC AGT TGC AGC CTT CTC A
	OPN R	GCA AAA GCA AAT CAC TGC AAT T

2.14 Transfections

Transfections were carried out using JetPrime reagent (VWR, West Chester, PA) or Amaxa electroporation (Lonza Biotech, Walkersville, MD). Lentiviral transduction was done using BES transfection buffer (1.5mL of 2x BES: 50mM BES, 280mM NaCl, 1.5mM Na₂HPO₄ in water at 6.96pH) with 150μL of 2.5M CaCl₂ with 10μg DNA plasmid, 10μg pPax and 10μg pMD2 plasmids in 1.35mL distilled water. Solution was aerated for 30 seconds using 5mL pipettaid/tip before being added to fresh 10mL DMEM supplemented with 10% FBS and 10% PSG on HEK-293T.

2.14.1 siRNA

siRNA CD44 and negative control #1 siRNA purchased from Ambion (Austin, TX). siRNA was transfected into MSC using JetPrime Transfection reagent as per manufactures instruction (VWR, West Chester, PA) After 48 hours, cells were subjected to assay of choice

2.14.2 Luciferase reporter assay

The CD44 PGL3 luciferase promoter construct was obtained from Addgene (Cambridge, MA). Luciferase assay was performed in a 96 well plate according to manufactures instructions (Promega, Madison, WI). Tumor conditioned media was obtained from tumor cell lines grown for 2 days at 50-80% confluency and filtered through a 0.2μm syringe filter to remove cell debris. MSC in a 96 well plate (1x10⁴ cells/well) were conditioned with the media for 1, 12 and 24 hours. MSC proliferation was measured after 12, 24 and 36 hours following breast cancer conditioning using CyQuant Proliferation assay protocol (Molecular Probes, Carlsbad, CA).

2.15 Viral transduction

2.15.1 Adenoviral vectors

Soluble CD44 Adenoviral vector was obtained from Dr. B. Toole, amplified in 293T cells, and concentrated in a cesium chloride gradient. Firefly luciferase and renilla luciferase constructs were made in house. A recombinant adenoviral (Ad) vector

expressing firefly luciferase (ffLuc) or renilla luciferase (rluc) possessing an RGD-modified fiber (AdLuc-F/RGD) was prepared, purified, and titered as described previously (143). Adenoviral transductions of cell lines were carried out using a cell-specific multiplicity of infection (MOI) in serum free medium when cells were 70% confluent. Human MSC were incubated with AdLuc/RGD at 3,000 MOI for 4 hours, C57bl/6 MSC were incubated with AdLuc/RGD at 5,000 vp/cells for 6 hours in serum-free medium and tumor cells were incubated with AdLuc/RGD at 3,000 MOI for 6 hours in serum-free medium. After incubation serum containing media was added to the culture. Transduction efficiency was routinely above 95%, as previously reported (143). MSC were assessed for luciferase expression by plating increasing numbers of transduced cells into 96 well plates and adding 1 μ l of substrate solution (Caliper Life Sciences [Xenogen], Hopkinton, MA) per well containing media. 30 sec later cells were placed into the imager for detection. A standard curve could be generated between the number of cells plated and the photon count per well detected by the IVIS imager. ffLuc labeled MSC were also assayed for maintenance of adipogenic, osteogenic and chondrogenic potentials as described above.

2.15.2 Lentiviral vectors

Five GIPZ shRNA (clone ID: 1-V2LHS_111680; 2-V2LHS_111682; 3-V2LHS_111684; 4-V3LHS_334831; 5-V3LHS_334830) lentiviral constructs against CD44 and one negative control shRNA (RHS4346) (Open Biosystems, Huntsville, AL) were transfected into HEK-293T cells with pPax and pMD2 plasmids using JetPrime Transfection reagent or BES. Supernatants were collected and filtered after 72 hours and a subsequent 48 hours thereafter for a total of 40mL. Virus was concentrated in 8.5% polyethylene glycol (8.4mL PEG- from 50% stock solution) and 0.3M sodium chloride (3.75mL NaCl- from 4M stock solution) and balanced with PBS to equal volume. Solution was placed on a shaker at 4°C for 90 minutes. Solution was spun down at 4°C at for 45minutes. Pellet was resuspended in 300 μ l PBS, snap frozen and stored at -80°C. For transduction, 20ul of each concentrate were combined with 5ul of 5mg/ml polybrene stock in 10mL of fresh 20% serum

media. Media was changed 24 hours post transduction. Cells were sorted by FACS for GFP positivity.

ffLuc/cGFP co-expressing vector was made by subcloning the ffLuc from pGL4.51[*luc2*/CMV/Neo] Vector (Promega, Madison, WI) into pCDH-CMV-MCS-EF1-copGFP_CD511B-1 (System Biosciences, Mountain View, CA).

2.16 Animals

C57Bl/6 mice expressing either GFP under the control of the ubiquitin promoter, tdTomato under the control of the ROSA26 promoter, or CD44 KO mice expressing LacZ under the CD44 promoter were purchased from Jackson Labs, and bred in house to maintain colonies. Additionally, severe combined immune disorder (SCID) mice were purchased from Jackson Lab (NOD.CB17-*Prkdc*^{scid}/J; Bar Harbor, ME). All mice were housed in accordance with institutional standards, and treated under approved protocols. Mice were allowed food and water ad libum and in accordance to the facility were healthy and free of opportunistic organisms.

2.16.1 Exogenous MSC migration study

SCID mice were anesthetized and then injected SC with 5×10^5 rLuc labeled Skov-3 cells suspended in 100 μ L of PBS into both hind limbs. Mice were divided into 4 groups (n=20), all receiving rLuc-Skov-3 tumor cells. Tumor engraftment was confirmed by bioluminescent imaging (IVIS-Xenogen 100 system; Caliper Lifesciences, Hopkinton, MA) 56 days post injection. Confirmation of engraftment was followed by tail vein injections of 1×10^6 ffLuc labeled MSC; mice received either normal MSC (black and blue groups) or MSC expressing the soluble CD44 adenovirus (green and red groups). The blue and red groups received an intratumoral injection of the soluble CD44 expressing adenovirus (heretofore known as, Ad-s44) in the right limb 48 hours prior to IV MSC administration. Bioluminescent imaging was conducted for 5 consecutive days post MSC administration. Images were acquired over a 3 minute period to detect and quantify the ffLuc expression (MSC) and 2 minute for rLuc expression (tumors).

2.16.2 Tumor growth study

Wild type and transgenic CD44 knockout (Jackson Laboratory, Bar Harbor, ME) murine MSC were isolated as previously described (66) and stably labeled with GFP-lentivirus. 1×10^6 MSC were admixed with 1×10^6 4T1 tumor cells and injected into the mammary fat pad of SCID mice. 3 weeks following injection, mice were sacrificed and tumors and organs removed for immunohistochemical analysis.

2.16.3 Bone marrow transplantation study

Ubiquitous-expressing DS-Red C57/B6 wild type and transgenic CD44 knockout (Jackson Laboratory, Bar Harbor, ME) murine bone marrow were isolated as previously described (142). 2×10^6 total bone marrow cells were tail vein injected into lethally irradiated ubiquitously expressing GFP C57/B6 mice. Recipient mice (n=10) received either tdTomato bone marrow (n=5) or CD44 KO bone marrow (n=5), one mouse received PBS injection as control for lethal radiation dose. The control mouse died at day 18. At day 24, mice were bled and transplant was confirmed by flow. Day 25, the right dorsal side of anesthetized recipient mice was shaved and cleaned with alcohol. Then, 2×10^5 EO771 tumor cells suspended in 50 μ l of PBS were injected adjacent to the fat transplant site. Following 29 days of tumor engraftment, mice were sacrificed and tumors and organs removed and placed in formalin or snap frozen in OCT compound for subsequent immunohistochemistry or immunofluorescent staining.

2.17 Bioluminescent imaging

Images were captured using Xenogen's IVIS 200 system and Living Image Software (Caliper LifeSciences, Hopkinton, MA). The ffLuc substrate, d-Luciferin (100 μ L of 4mg/mL in PBS; Biosynth International Inc, Itasca, IL) was injected IP 5 minutes prior to imaging. The rLuc substrate, coelenterazine (Biotium, Inc., Hayward, CA) was resuspended and diluted in PBS injected IP 5 minutes prior to imaging. Bioluminescent images were acquired between a 10 second and 10 minute period to detect and quantify the ffLuc or rLuc expression depending on the expression system and the place of signal within the animal. Analysis of the

bioluminescent imaging was carried out by creating a standard region of interest (ROI) around the right and left hind legs to calculate the flux (photons per second; p/s) of the target signal in the given area. Relative quantification of the MSC number and tumor size were then calculated by normalizing the MSC flux against the tumor flux in order to achieve a comparable number of migrated MSC toward each tumor individually. Statistical significance was determined by the Student's T-test.

2.18 Statistical Analysis

Numerical data were expressed as means \pm standard error. Statistical differences between the means for the different groups were evaluated with Prism 4.0 (GraphPad software) using either the Student's T-test or analysis of variance (ANOVA), with the level of significance at $p < 0.05$ with the exception of the bone marrow transplant experiment where significance was set at $p < 0.1$.

3. Results

3.1 Characterization of MSC

MSC were isolated, expanded and characterized by passage three by surface marker expression by flow cytometry and by differentiation capabilities into adipocytes, osteoblasts and chondrocytes.

Human MSC were characterized based on the positive expression of CD90, CD105, CD44, CD73, CD140b, CD146 and CD166, and the negative expression of hematopoietic marker CD45, endothelial markers CD31 and CD34 and macrophage marker CD11b (Figures 2A). Murine MSC were characterized based on the positive expression of Sca-1, CD106, CD44 and CD140b and the negative expression of CD45, CD31, cKit and CD11b (Figures 2B).

To confirm their multipotent potential, human and murine MSC were subject to differentiation assays. Naïve human MSC, or adenoviral transduced Ad-MSC both show trilineage differentiation potential. Furthermore, lentiviral transduced shRNA CD44 MSC and shNeg transduced MSC were also subject to trilineage differentiation. shCD44 MSC displayed diminished capacity for adipocytes differentiation (Figure 3). Murine MSC showed comparable differentiation into bone, cartilage or fat. The murine CD44 KO MSC displayed bone and cartilage potential but hindered adipocyte differentiation potential. Additionally, adenoviral infected MSC do not lose their differentiation potential (Figure 4). Osteoblasts were identified by alkaline phosphatase and Alizarin Red S staining. Adipocytes were identified by Oil Red O stained lipid vacuoles. Chondrocytes were identified by Alcian Blue stained mucopolysaccharides.

Figure 2. MSC characterization by flow cytometry. Phenotypic surface marker expression was evaluated on (A) human MSC and (B) murine MSC.

Figure 2

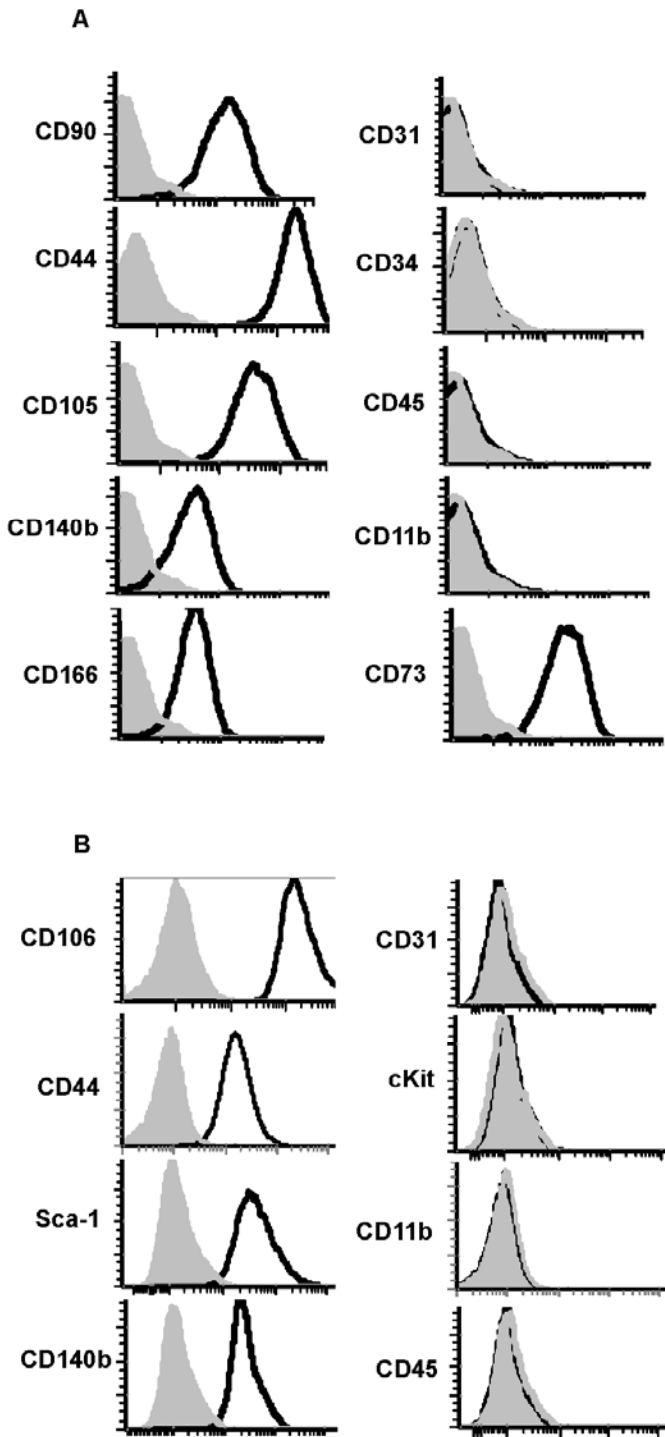


Figure 3. Human MSC trilineage differentiation potential. MSC cultured in adipocyte, chondrocyte or osteoblast differentiation medium. **(A)** Oil Red O stain verified the presence of mature adipocytes. **(B)** Alkaline phosphatase substrate and **(C)** Alizarin Red S stained for mature, calcium-producing osteocytes, and **(D)** Alcian Blue stained for mature chondrocytes.

Figure 3.

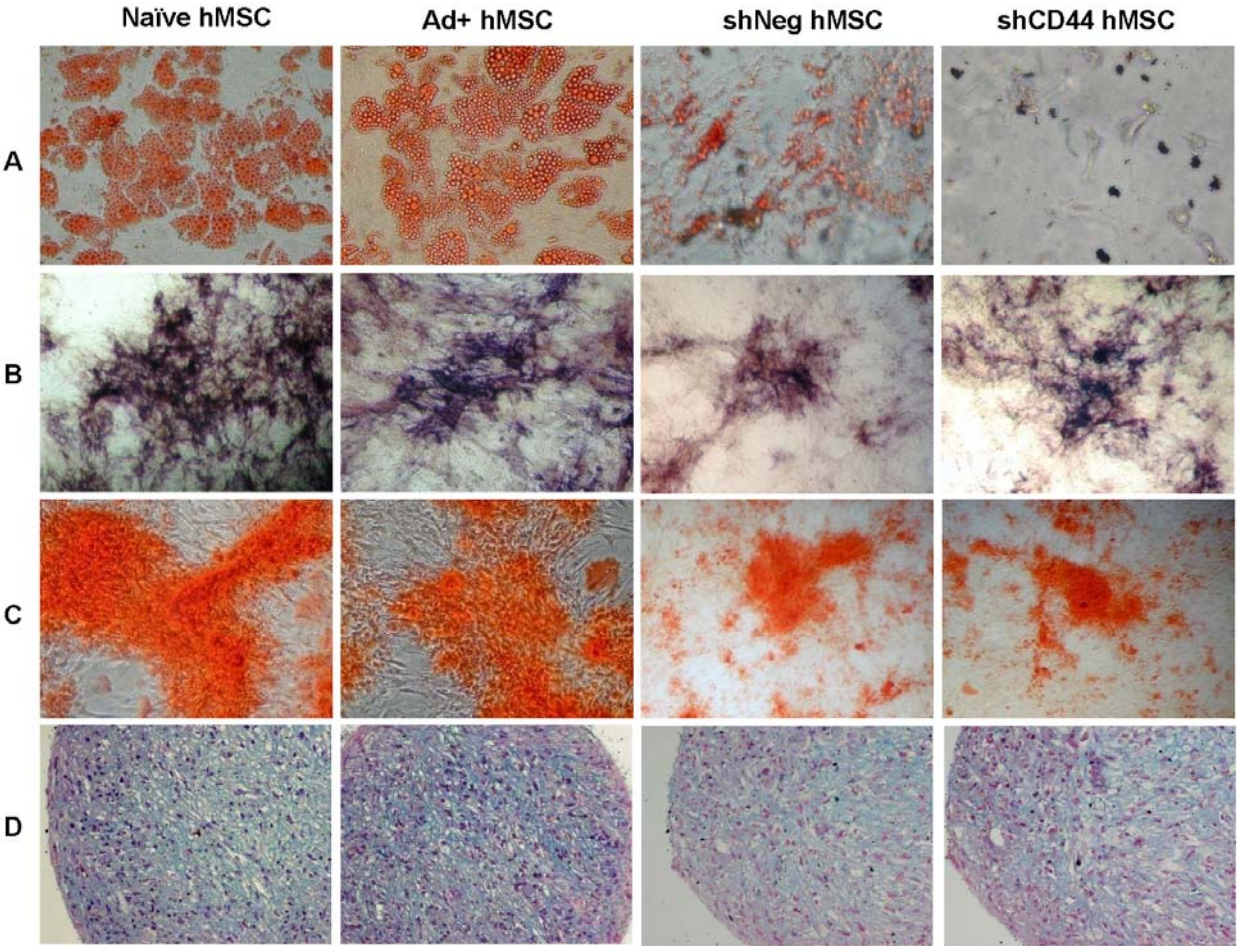
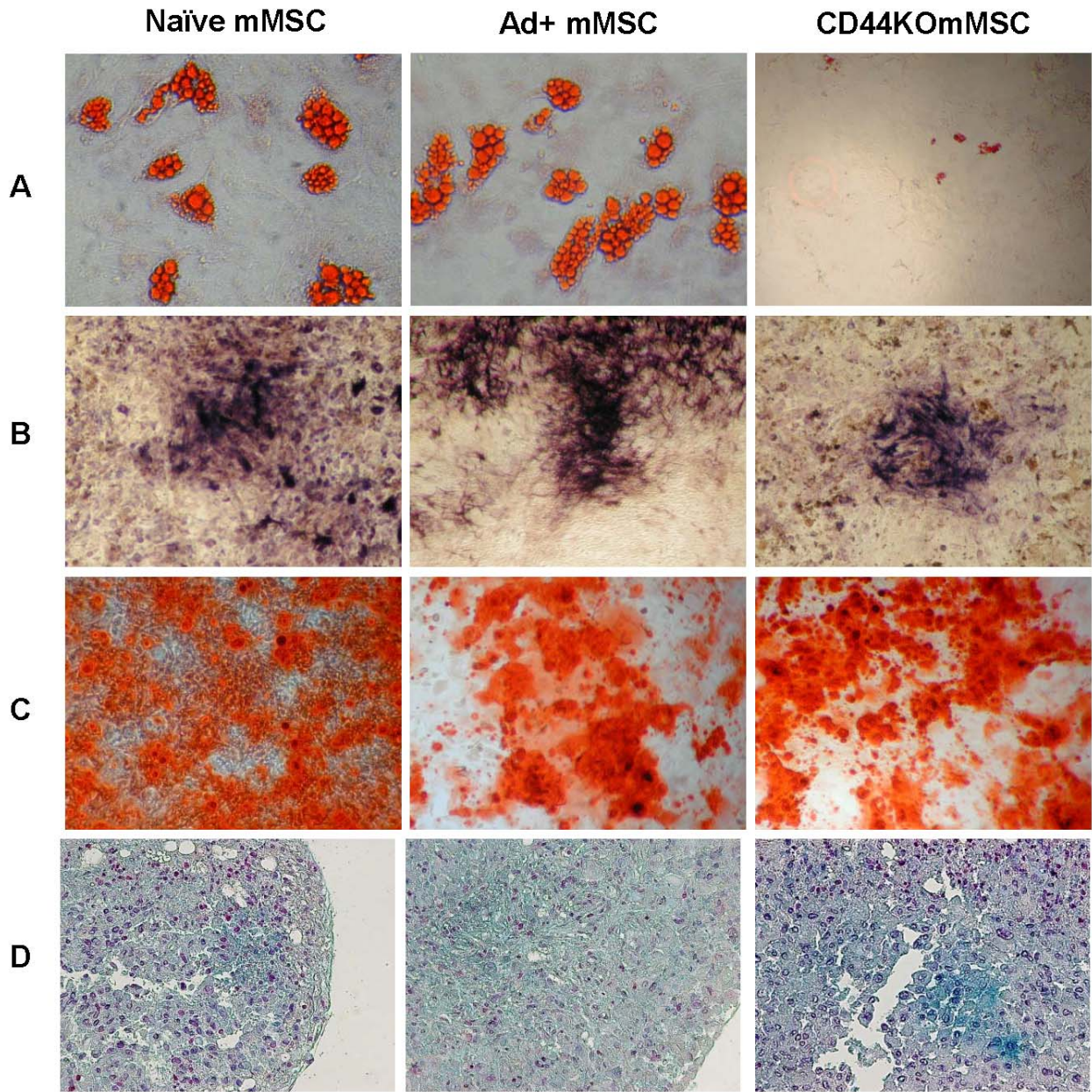


Figure 4. Murine MSC trilineage differentiation potential. Naïve and viral transduced MSC cultured in adipocyte, chondrocyte or osteoblast differentiation medium. **(A)** Oil Red O stain verified the presence of mature adipocytes. **(B)** Alkaline phosphatase substrate and **(C)** Alizarin Red S stained for mature, calcium-producing osteocytes, and **(D)** Alcian Blue stained for mature chondrocytes.

Figure 4.



3.2 Defining characteristics of tumor tropic MSC

3.2.1 Chemokine and cytokine expression profiles

RNA was extracted from MSC stimulated with tumor conditioned media for 24 hours. cDNA was synthesized and run on a SABiosciences chemokine/cytokine array. Both human and murine MSC were stimulated with breast (MDA-231, 4T1), ovarian (Skov-3, ID8), prostate (PC-3) and pancreatic (Panc-1) tumor cell lines to analyze the MSC autocrine response to tumor stimulation. Resulting chemokine expression up regulated by tumor conditioning varied between tumor models, although there were a few overlapping expression profiles including IL8, IL1, CXCL1, CXCL5 and C3. Then, tumor cell lines were analyzed for chemokine and cytokine expression in order to compare autocrine and paracrine chemokine expression. One factor that was unique to tumor paracrine stimulation in the Skov-3 ovarian cell line compared to chemokines expressed by other tumor cell lines was osteopontin (OPN; Figure 6A). This ligand was further pursued because our previously published data showed Skov-3 tumor cells are highly attractive to MSC compared to other adenocarcinoma cell lines both *in vitro* and *in vivo* (60). By ELISA, we show the Skov-3 tumor cell line secretes OPN (40ng/ml \pm 3) as compared to no secretion by Panc-1 or MDA-468 tumor cells and limited secretion by MSC (1ng/ml) and HUVEC (2ng/ml). 12 additional breast and pancreatic tumor cell lines were negative for OPN secretion. (data not shown) Furthermore, tumor cell lines and MSC conditioned by tumor cell lines were analyzed for gene expression of OPN by PCR. MSC express OPN which is increased following tumor conditioning by both high (Skov-3) and low (MDA-468 and MCF7) expressing cell lines (Figure 6C). Then tissue sections from tumor-burdened mice were analyzed for OPN expression by immunofluorescence. Three xenograft and two syngenic tumor models showed varied OPN staining; all tumor sections had patches of strongly positive OPN staining (Figure 6D). Furthermore, the majority of the normal tissue of a tumor-burdened mouse stained was negative for OPN with exception of the liver. OPN positive stain per slide section was quantified and averaged across each tissue section (Figure 6E).

Figure 5. Chemokine and cytokine expression by tumor stimulated MSC. Real-time PCR was conducted on human and murine MSC lysates extracted after 24 hour stimulation with **(A)** MDA-231, **(B)** 4T1, **(C)** Skov-3, **(D)** ID8, **(E)** Panc-1 or **(F)** PC-3 tumor cell conditioned media.

Figure 5

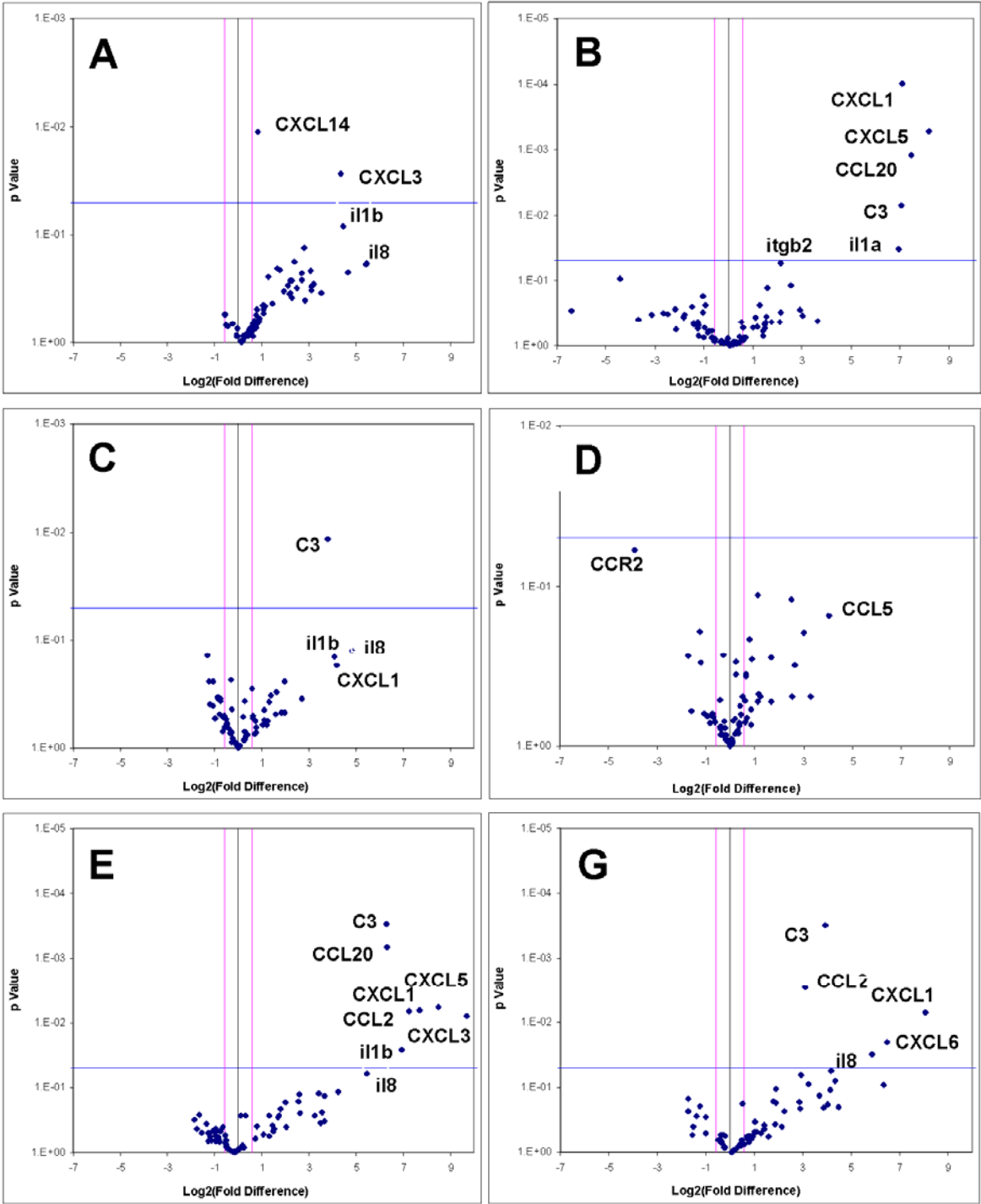
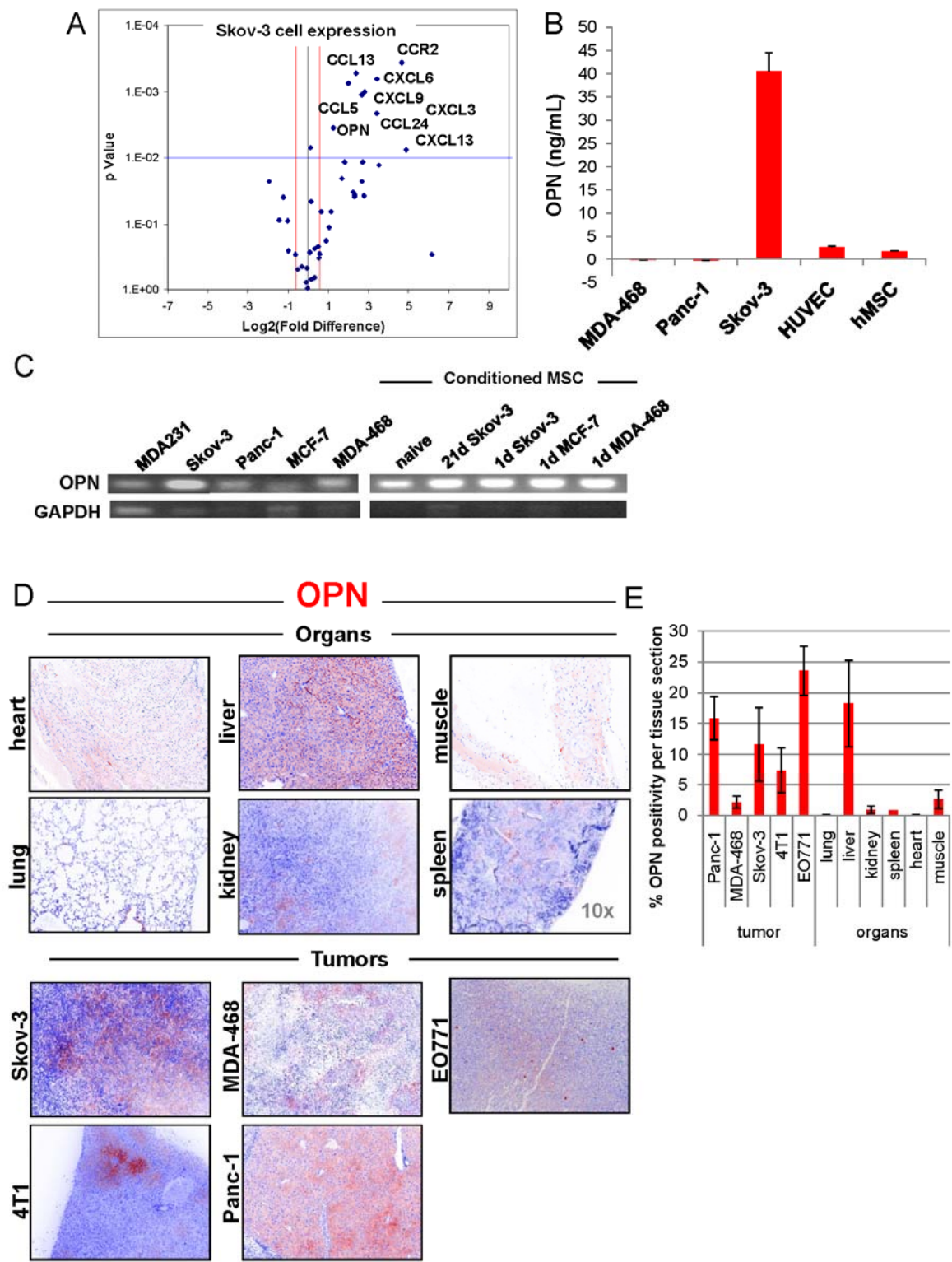


Figure 6. Expression of CD44 ligand in tumor cell lines and tissues. (A) Osteopontin (OPN) was among the chemokines expressed by Skov-3 tumor cells by RT-PCR chemokine array (SA Biosciences). **(B)** OPN secretion by breast (MDA-468), ovarian (Skov-3) and pancreatic (Panc-1) tumor cells was confirmed by ELISA and compared against normal cell lines including endothelial cells (HUVEC) and MSC. **(C)** OPN gene expression was analyzed in tumor cell lines, MSC, and tumor conditioned MSC **(D)** OPN positive tissue sections were confirmed by IF and **(E)** quantified using InForm software (CRi, Woburn, MA).

Figure 6



3.2.2 *In vitro* migration of MSC

Tumor-secreted paracrine factors are chemoattractive to MSC. A scratch assay showed the visible difference in MSC motility subjected to Skov-3 conditioned media versus serum or serum free media. The difference was empirically measured by defining the edge of the scratch at time zero and calculating the distance of enclosure at 6, 12 and 24 hours. The Skov-3 conditioned MSC were able to permeate the demarcated scratch border faster than the serum or serum free conditioned MSC (Figure 7A). Then, we compared conditioned media from two highly invasive and aggressive tumor cell lines: Skov-3 and MDA-231. Tumor conditioned media (TCM) is as attractive as full, 20% serum media. 10-fold dilutions in conditioned media correlate with less MSC migration (Figure 7B). Furthermore, the Skov-3 cells were more attractive than the MDA-231, which may be explained by the dramatic difference in OPN secretion by the Skov-3 cells (Figure 6B).

Next, blocking antibodies for a number of chemokine receptors corresponding to the chemokines expressed by the tumor cells were used to inhibit MSC transwell migration toward Skov-3 conditioned media (SCM). Among the neutralizing antibodies tested, blocking CD44 severely inhibited MSC migration (Figure 7C).

Cell surface expression of CD44 was confirmed before and after SCM stimulation. Interestingly, by flow cytometry, the cell surface expression of CD44 was consistently decreased compared to the serum free control (Figure 8A). However, by both western blot and by immunocytochemical staining for CD44, there was no decrease in total CD44 level (Figure 8B and C). To resolve this discrepancy, we transfected MSC with a CD44 luciferase promoter construct and then subjected them to TCM. We chose breast cancer cell lines (conditioned media generously given to us by Dr. M.C. Hung) with variable levels of invasiveness as well as the Skov-3 and Panc-1 cell lines.

Figure 7. Migration of hMSC to tumor conditioned media. (A) MSC under Skov-3 conditioned media (SCM) permeate (leading edge identified by red line) the demarcated (black dotted line) “scratch” earlier than the serum or serum free (SF) stimulated MSC indicating enhanced motility. **(B)** MSC migration toward Skov-3 and MDA-231 conditioned media in 10-fold dilutions. **(C)** Neutralizing antibody inhibition of MSC toward Skov-3 conditioned media blocks chemokine receptors corresponding to the tumor secreted chemokines.

Figure 7.

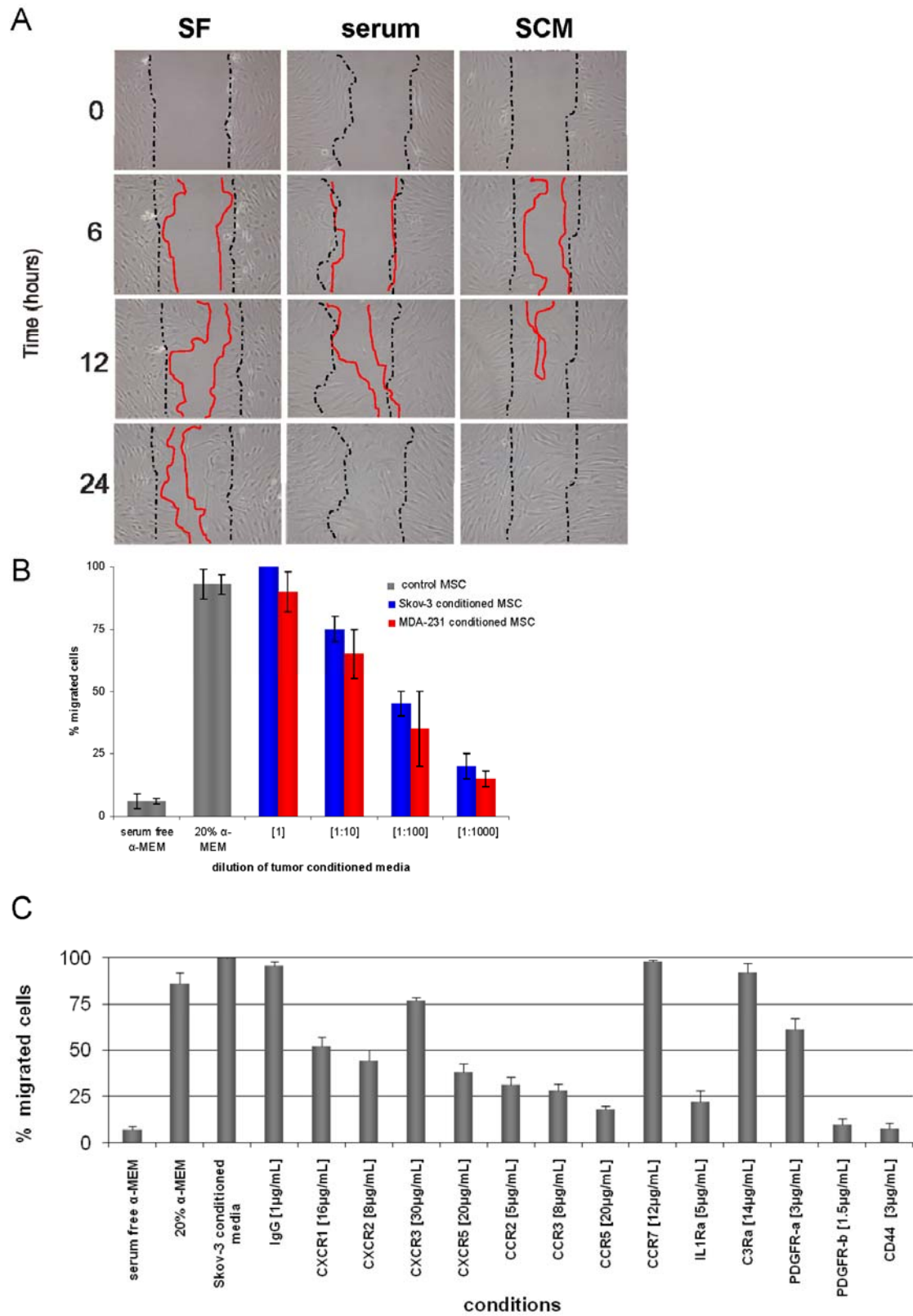
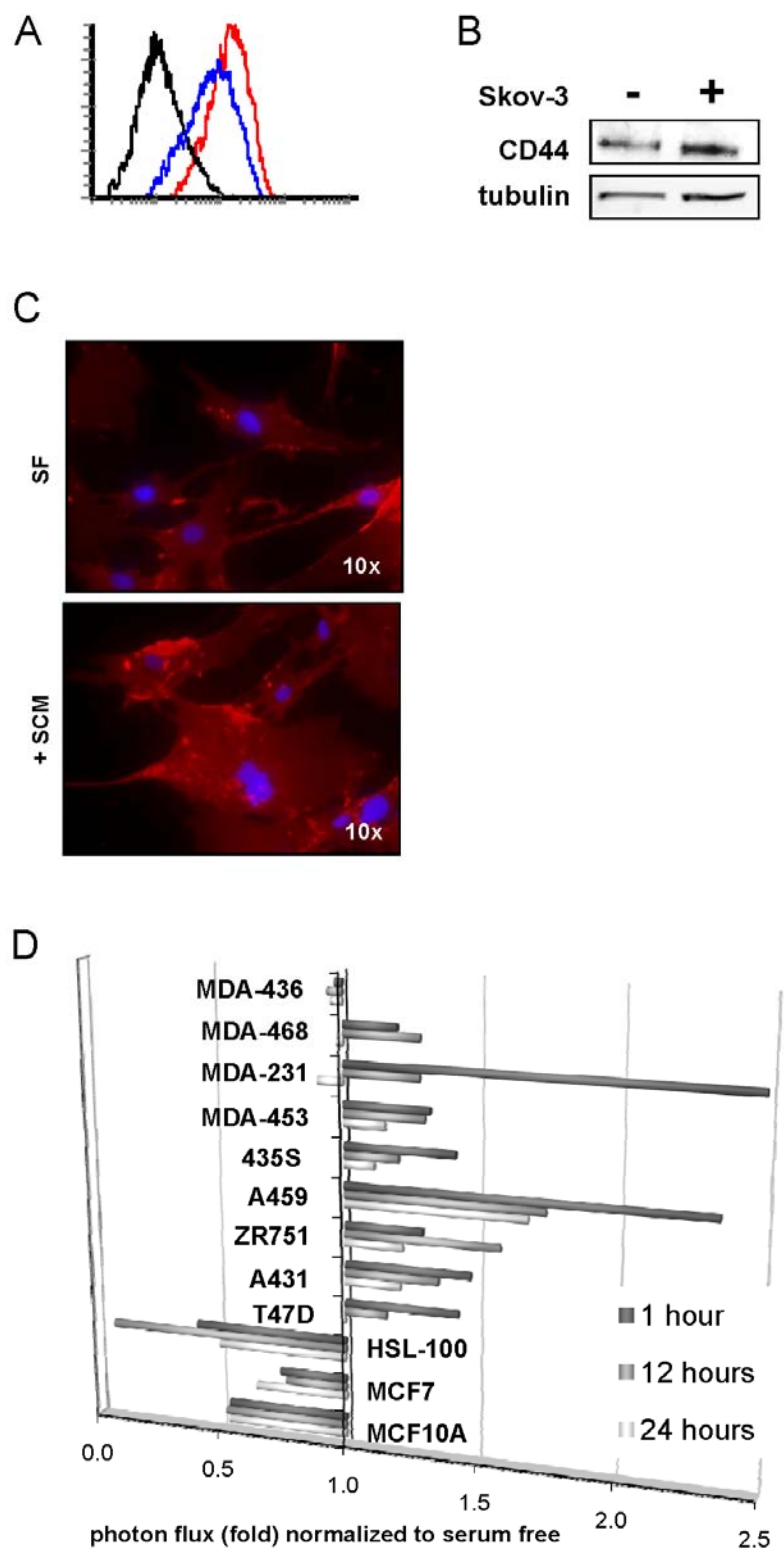


Figure 8. CD44 expression on human MSC. CD44 expression was evaluated after 24 hours of Skov-3 conditioning and compared to naïve MSC. **(A)** Flow cytometric analysis of CD44 before (red) and after Skov-3 conditioning (blue). **(B)** Western blot of CD44 expression in MSC. **(C)** IF staining of MSC with CD44 (Alexa-594). **(D)** CD44 promoter activity in MSC following tumor conditioning measured by relative luciferase activity.

Figure 8.



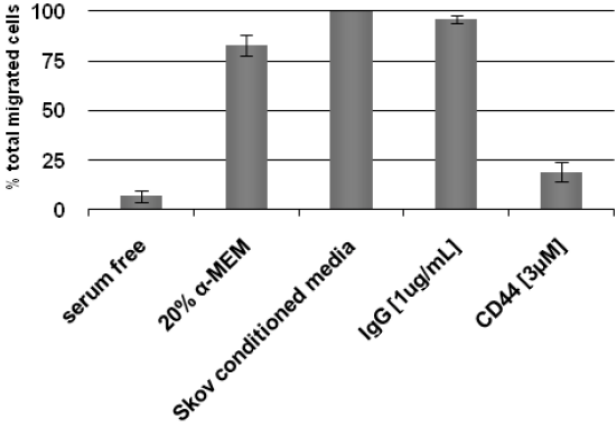
3.2.3 Blocking CD44 inhibits tumor-tropic MSC migration

MSC expressed CD44 was blocked using several different methods. First, CD44 neutralizing antibody was used to block migration towards SCM by 80% \pm 4% (Figure 9A). Then, MSC transiently transfected with siRNA against CD44 showed 60% \pm 11% reduction in migration towards SCM as compared to the naïve control (Figure 9B and 9C). Furthermore, stable knockdown of CD44 in MSC was achieved using a combination of four shRNA hairpins (Open Biosystems, Huntsville, AL). The stable knockdown shows similar migration inhibition to the transient knockdown of CD44, 68% \pm 5% (Figure 9D and 9E). Alternatively, using a small Hyaluronan oligomer (oHA) that competitively inhibits CD44 also inhibits migration by 60% \pm 4% (Figure 9F). Finally, we used an adenoviral expressed soluble CD44 (s44) as an inhibitor of CD44. We tested the adenovirus secretion of s44 by expressing it either from the Skov-3 tumor cells producing the conditioned media (Figure 9G) or the migrating MSC (Figure 9H). Whether the s44 was expressed in the SCM or the MSC, there was a significant inhibition in migration at an MOI of 5000. This was the MOI chosen for subsequent *in vivo* experiments.

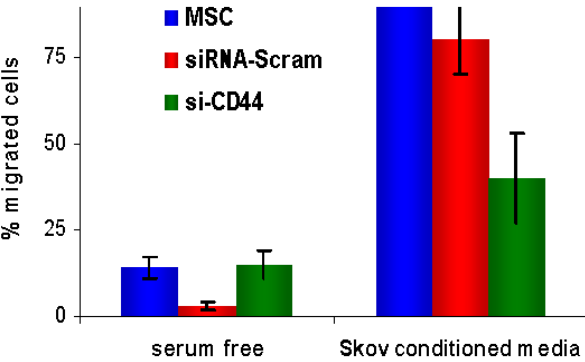
Figure 9. Migration inhibition of MSC toward Skov-3 conditioned medium. MSC migration was blocked using **(A)** neutralizing antibody and **(B)** siRNA against CD44. **(C)** Western blot shows degree of transient knockdown in MSC; **(D)** Stable knockdown of CD44 shows migration inhibition similar to transient knockdown; **(E)** Western blot shows the degree of stable knockdown in MSC **(F)** HA oligomer inhibits MSC migration at 100µg/mL. **(G)** Conditioned media from s44 expressing Skov-3 tumor cells or **(H)** s44 transfected MSC also inhibit MSC migration toward Skov conditioned media.

Figure 9.

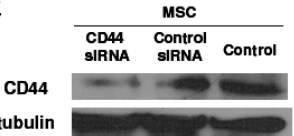
A



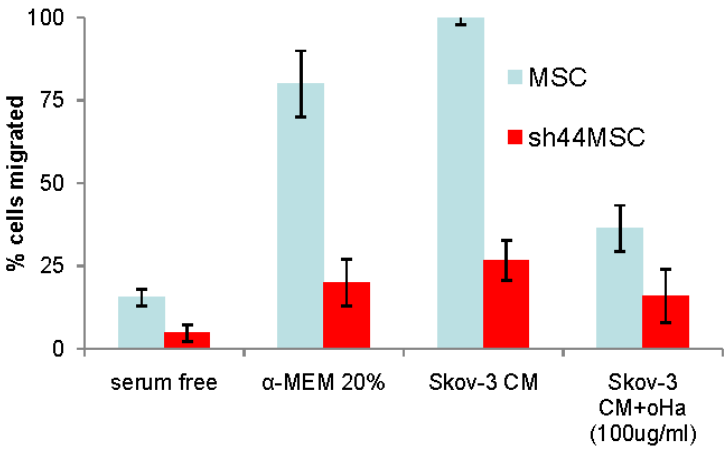
B



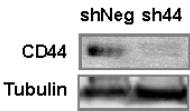
C



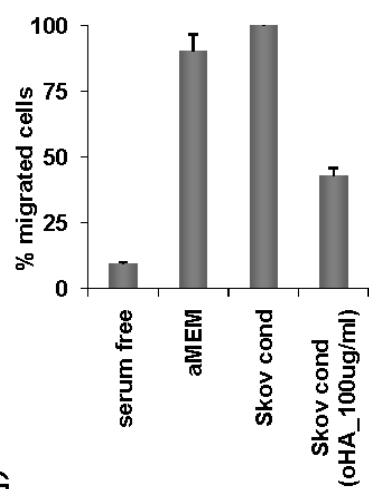
D



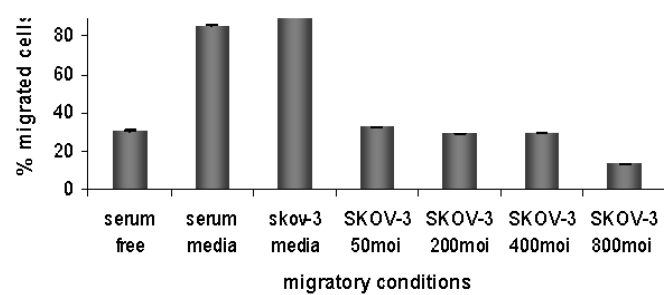
E



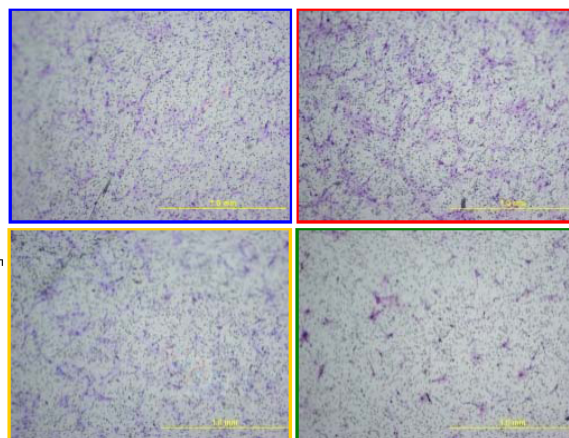
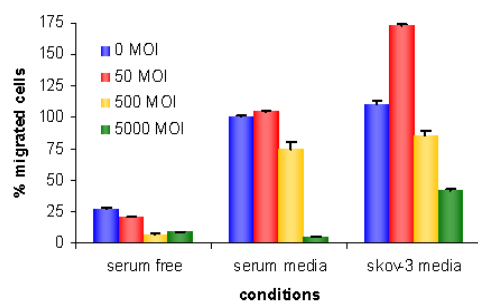
F



G



H

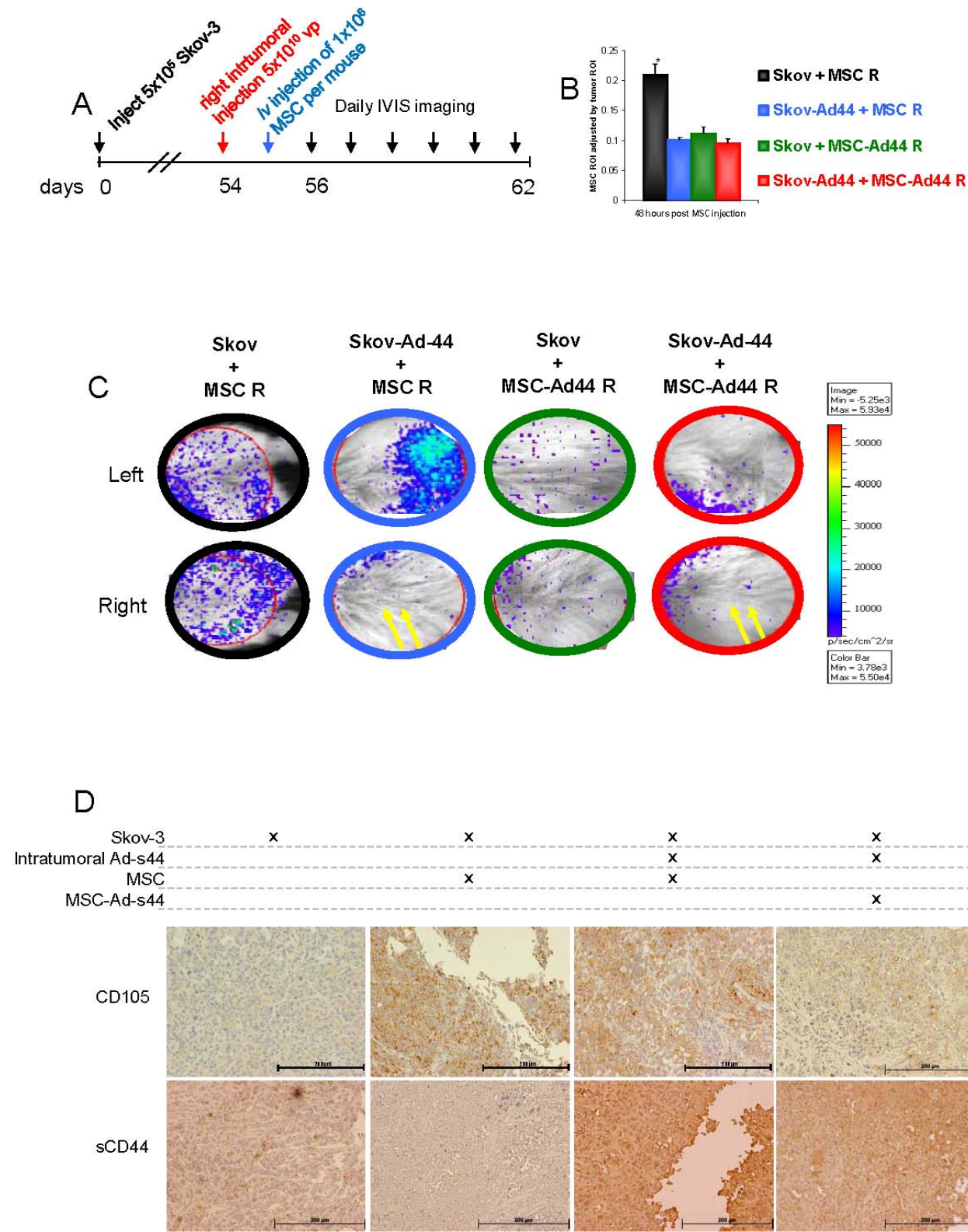


3.2.4 Inhibition of tumor tropic MSC migration *in vivo*

5×10^5 Skov-3 cells were subcutaneously (SC) injected bilaterally to the inguinal fat pads of SCID mice. Following tumor engraftment, 54 days after injection, mice were separated into four groups of mice ($n=5$). Two groups of mice (blue and red in Figure 10) were given intratumoral injections of 2.5×10^{11} vp of Ad-s44 in the right leg. Tail vein injections of 1×10^6 MSC were given 48 hours later. Two groups of mice (black and blue in Figure 10) received control MSC and the other two groups, green and red, received Ad-s44 expressing MSC. Mice were imaged consecutively for 5 days post MSC injection and were then sacrificed on day 6. Day 2 had the greatest influx of MSC as quantified with BLI, and displays a statistically significant ($p < 0.01$) decrease in MSC migration into the tumors that expressed sCD44 (blue and red) and into the tumors belonging to the mice that received the Ad-s44 MSC (green and red). The mice receiving both the intratumoral Ad-s44 injection and the Ad-s44-MSC (red) were not significantly different from those mice that received one or the other (Figure 10B). The control mice (black) with normal Skov-3 tumors and normal MSC showed a normal and equal localization of MSC to the bilateral tumor sites, whereas the mice receiving MSC infected with Ad-s44 did not. Figure 10C shows the region of interest surrounding each tumor-burden corresponding with the left and right tumors in each of the four groups. Immunohistochemical staining of the right tumors shows the infiltration of MSC by CD105 staining. Those mice that received both intratumoral Ad-s44 injections and Ad-s44-expressing MSC had less MSC compared to the control tumor evident by immunohistochemical staining for CD44 and CD105 (Figure 10D).

Figure 10. *In vivo* tumor-tropic migration of MSC is inhibited by s44. MSC were injected systemically into bilateral xenograft Skov-3 tumor burdened NOD/SCID mice in the presence or absence of the Ad-s44. **(A)** Time line of the mouse experiment. **(B)** BLI average of the right ROI in each group shows that any mouse receiving s44 had a decrease in tumor tropic MSC migration. **(C)** Representative ROI of each tumor. Yellow arrows indicate the tumors that received intratumoral injections of Ad-s44. **(D)** Immunohistochemical staining of tumor sections shows the presence of MSC by CD105 staining, and the presence of s44.

Figure 10.



3.2.5 CD44 signaling in MSC migration

To begin to understand the mechanism of MSC migration through CD44, we used the oHA oligomer on MSC with 6 or 24 hours of SKM and analyzed CD44 expression by confocal microscopy. Using InForm software to quantify the mean CD44 fluorescent pixels within the nucleus versus the cytoplasm we were able to determine that oHA blocks the nuclear localization of CD44 under tumor conditioning (Figure 11A). Because matrix metalloproteinases are an integral part of invasion and migration, we looked at MMP2 and 9 levels in MSC with and without tumor conditioning. We saw an increase in MMP2 and MMP9 activation in MSC under tumor conditioning (Figure 12A). Using an MMP inhibitor against MMP14 (and MMP2 and MMP9 at lower concentrations), we saw a decrease in migration comparable to that achieved with s44 (Figure 12B). To elucidate whether CD44-induced migration could be dependent on MMP, we analyzed CD44 expression by western blot, using the MMP inhibitor and tumor conditioning. At a concentration of 1 μ M, MMP inhibition leads to visible changes in MSC CD44 cleavage products (Figure 12C). The extracellular membrane portion can be found ~34kDa and the intracellular membrane portion can be found at ~17kDa. Figure 12D illustrates the structure of CD44. When we use an MMP inhibitor we see ablation of the CD44 cleavage products, suggesting that MMP14, MMP9 or MMP2 are involved in CD44 cleavage in response to tumor conditioning.

Figure 11. MSC expressed CD44 localized to the nucleus following stimulation with SCM. (A) Mean pixel density of Alexa594-labeled CD44 co-localizing with nuclear-DAPI in MSC following 6 or 24 hours of Skov-3 conditioning. Tumor induced nuclear localization of CD44 is blocked by oHA in MSC. **(B)** Representative images of oHA treated Skov-3 conditioned MSC.

Figure 11

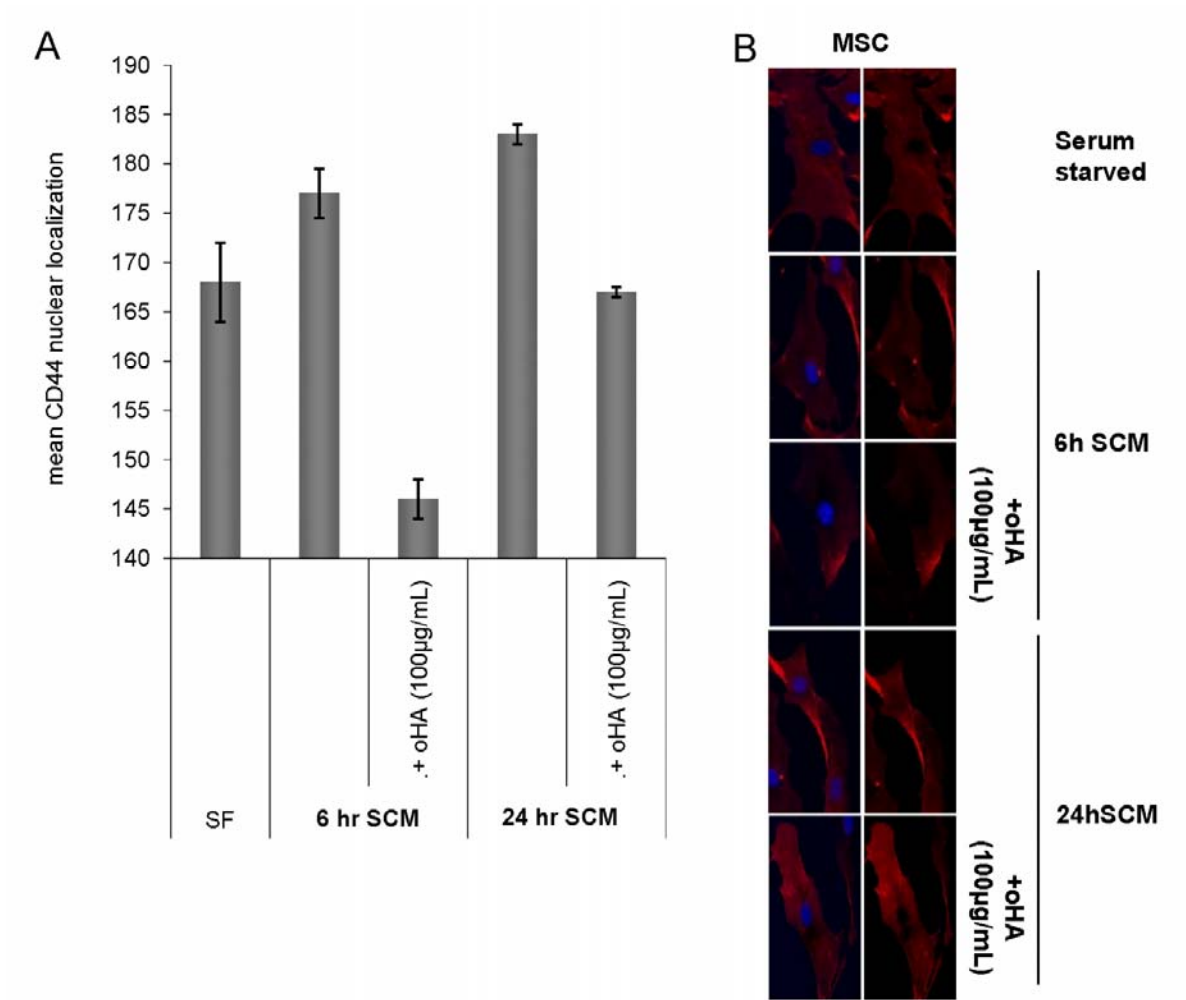
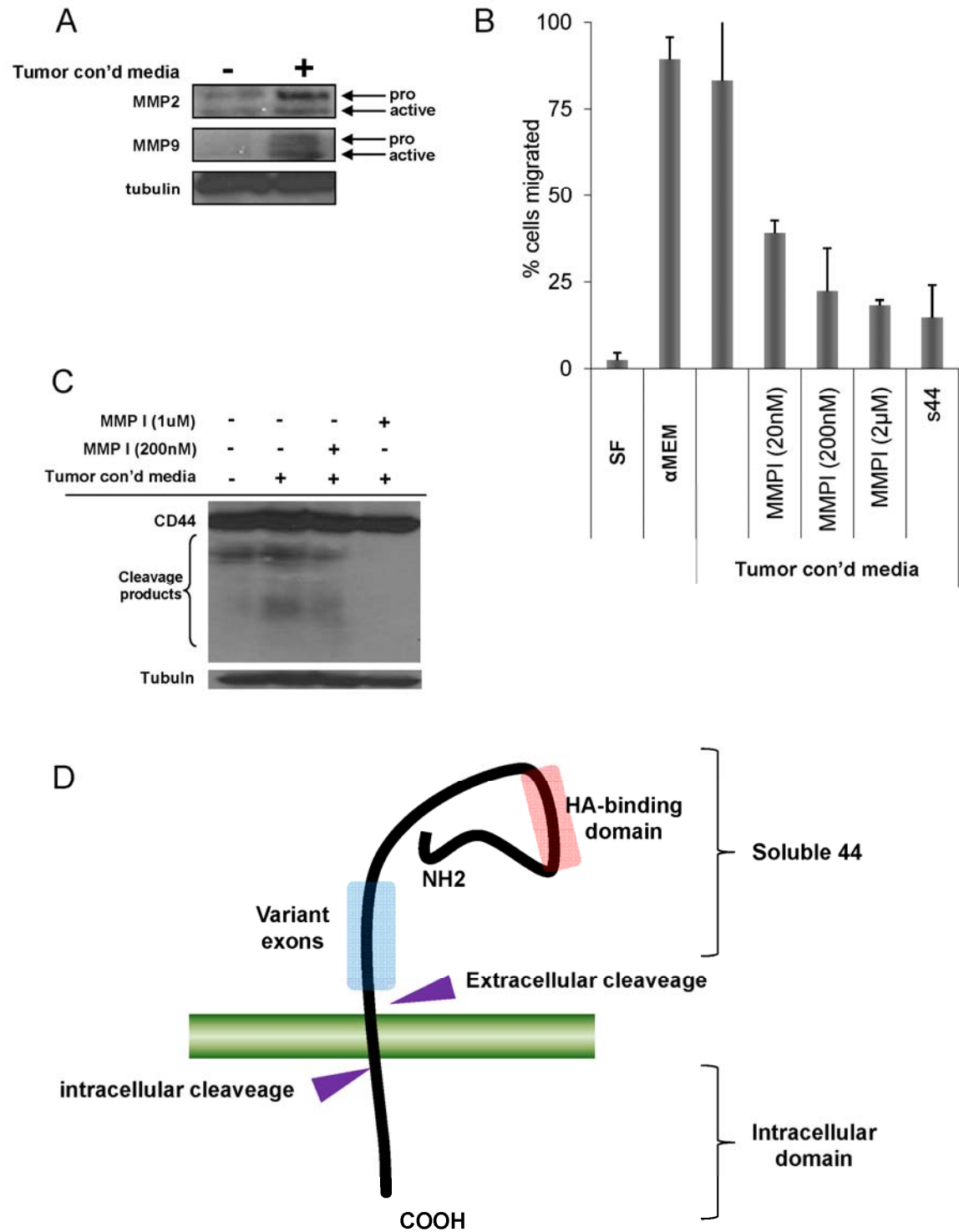


Figure 12. MMP activation in tumor conditioned MSC drives migration partially through CD44. **(A)** MMP expression is up regulated in tumor conditioned MSC. **(B)** Using an MMP inhibitor to block MMP2 at 20nM, MMP9 at 200nM and MMP14 at 1μM. MSC migration was inhibited to a level consistent with that of s44 inhibited migration. **(C)** Western blot shows that MMP inhibition at 1μM is able to inhibit the CD44 cleavage products including 34kDa extracellular portion and the 17kDa intracellular portion. **(D)** Illustration of CD44 receptor including the extracellular and the intracellular cleavage sites, the region containing the CD44 variants and the only known ligand binding domain.

Figure 12



3.2.6 CD44 activation by TCM induces twist expression

To elucidate potential downstream targets of the nuclear CD44, we analyzed potential transcriptional targets involved in both mesenchymal cell phenotype and migrational phenotype. Expression of the transcription factor Twist down regulated in the presence of s44 even when stimulated by SCM (Figure 13A). We then decided to look at Twist expression following MMP inhibition as shown in Figure 12C—the MMP inhibition that blocked CD44 cleavage products. Twist expression was slightly decreased in the MSC in lane 4 (Figure 13B).

Knocking down expression of CD44 in human MSC using four shRNAmir hairpins in pGIPZ vectors (OpenBiosystems, Huntsville, AL); we were able to suppress CD44 expression in MSC by greater than 95%. Furthermore, the protein expression of Twist in the shCD44 MSC is decreased in the tumor conditioned MSC at both 30minutes and 24 hours (Figure 13C). The twist expression levels were also confirmed by real time RT PCR. Twist expression is down regulated in tumor conditioned shNeg MSC that were treated with s44 or with 1 μ M MMPI. This down regulation is similar to that observed from the shCD44 MSC with or without tumor conditioning (Figure 13D).

The shCD44 MSC were previously subjected to a transwell migration assay that confirmed deficient migration towards tumor conditioned media. Next, we transfected shNeg MSC or shCD44 MSC to exogenously express HA-tagged Twist. There was a 130 fold increase in Twist expression by RT PCR (Figure 13E) and HA the presence of HA is evident by western (Figure 13F). These Twist expressing shCD44 MSC were subjected to a transwell migration assay toward tumor conditioned media. The exogenous expression of Twist showed a 12% increase in migration of the shCD44MSC compared to no Twist. The shNeg MSC transfected withTwist showed a significant decrease in migration as compared to the control cells. There was no migratory inhibition of shCD44MSC with or without Twist in the presence of 100 μ g/mL oHA (Figure 13G).

Next, ChIP was performed to assess the transcriptional regulation of Twist by CD44. Primers to the distal and proximal promoter regions of Twist were used to confirm CD44 complex with Twist promoter. The proximal promoter region was pulled down with CD44 following 24 hours of tumor conditioning (Figure 14A). The assay was performed at an earlier time point to confirm CD44 binding to the Twist proximal promoter following 30 minutes of tumor conditioning (Figure 14B). Furthermore, we also assessed the binding of CD44 to the Twist promoter under the stimulation of soluble CD44 and tumor conditioning. Under these conditions, there is a decrease in association between CD44 and the Twist promoter (Figure 14C).

Figure 13. Inhibition of CD44 on MSC leads to decreased Twist expression. (A) MSC gene expression of Twist by MSC is decreased in the presence of s44 and tumor conditioned media as compared to tumor conditioned media alone. **(B)** MMP inhibition of tumor conditioned MSC leads to decrease in Twist protein expression after 24 hours. **(C)** CD44 shRNA knockdown of human MSC shows decrease in Twist expression following 30minutes and 24 hours of tumor conditioning. **(D)** Gene expression of Twist by RT PCR is lower in shCD44 transduced MSC (red) compared to shNeg transduced MSC (blue) and is comparable to the shNeg MSC treated with s44 or with 1 μ M MMPI. **(E)** Exogenous expression of Twist in shNeg MSC (green) or shCD44 MSC (yellow) was increased by >130 fold compared to non-transfected MSC. **(F)** HA-tagged Twist-transfected MSC shown by western blot. **(G)** Transwell migration assay of Twist transfected shCD44MSC shows a 12% gain of migration towards tumor conditioned media compared to the shCD44MSC without Twist.

Figure 13

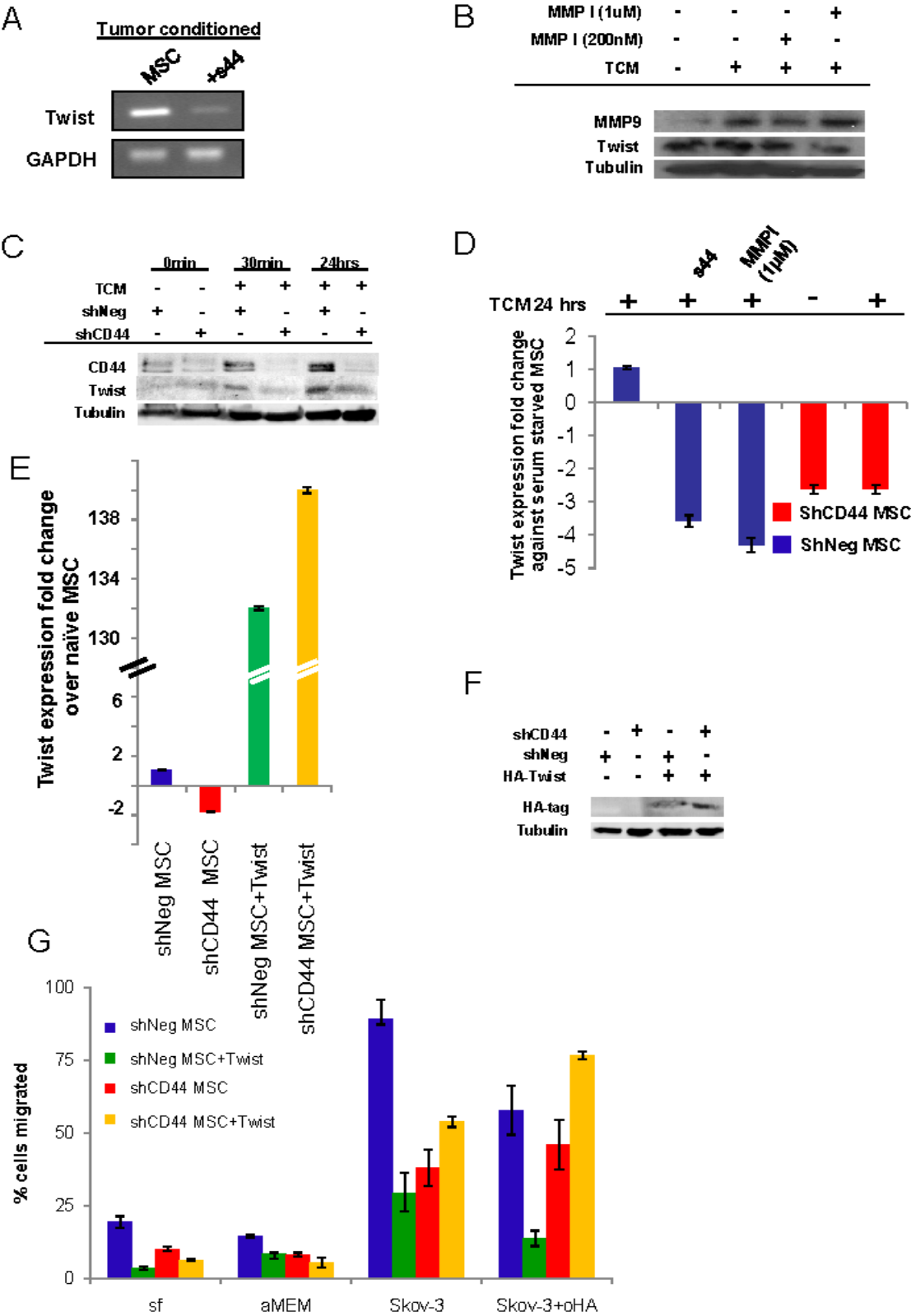
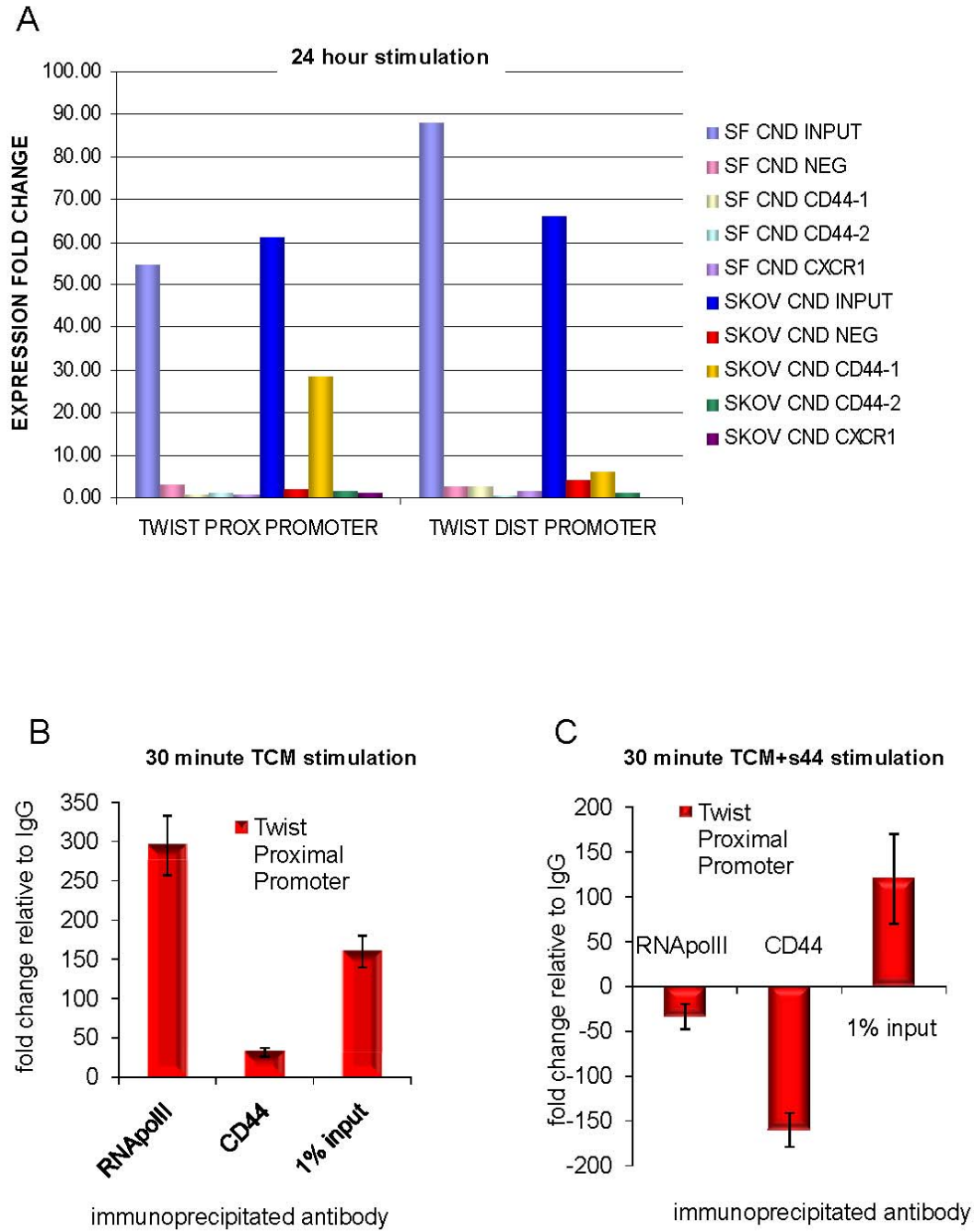


Figure 14. Tumor conditioned MSC induce CD44 binding to Twist promoter by ChIP. (A) Initial ChIP assay was done after 24 hours of tumor conditioning. Only Twist Proximal promoter primers showed expression fold changes by RT-PCR. **(B)** Using only the Twist proximal primers, Twist promoter could be associated with CD44 pulldown at 30 minutes following stimulation. **(C)** Additionally, a large decrease in binding is seen between naïve MSC and MSC stimulated with TCM and soluble CD44.

Figure 14



3.3 Incorporation of MSC within the tumor microenvironment

3.3.1 Tumor conditioned MSC differentiate into activated fibroblasts

An activated fibroblast is a fibroblast conditioned by a pathogenic incident. Within the tumor microenvironment, these fibroblasts are known as tumor (carcinoma) associated fibroblasts (TAF or CAF). The heterogeneous population of TAF can be currently defined by a group of markers that characterize aggressiveness by ECM-altering protein expression, vascularization potential by pro-angiogenic proteins expressed and secreted and growth potential by the growth factors secreted (Figure 15A). MSC that are conditioned over a period of 21-31 days *in vitro* are differentiated into TAF as defined by expression of Tn-C, TSP1 and FSP, and an increase in expression of FAP, α SMA, and desmin (Figure 15B).

Similarly, IV injected MSC that home to tumors, or MSC admixed with tumor cells prior to tumor engraftment show a marked increase in TAF-associated expression. Following three months *in vivo*, Skov-3 xenograft tumors that had been admixed with MSC were removed and analyzed for the expression of activated fibroblast expression of FAP and FSP (Figure 16A and B), aggressive/invasive markers Tn-C, TSP and SL1 (MMP3) (Figure 16C-E), neovascularization markers α SMA, desmin and VEGF (Figure 16 F-H) and finally growth factor expression of HGF, EGF and IL6 (Figure 16 I-K).

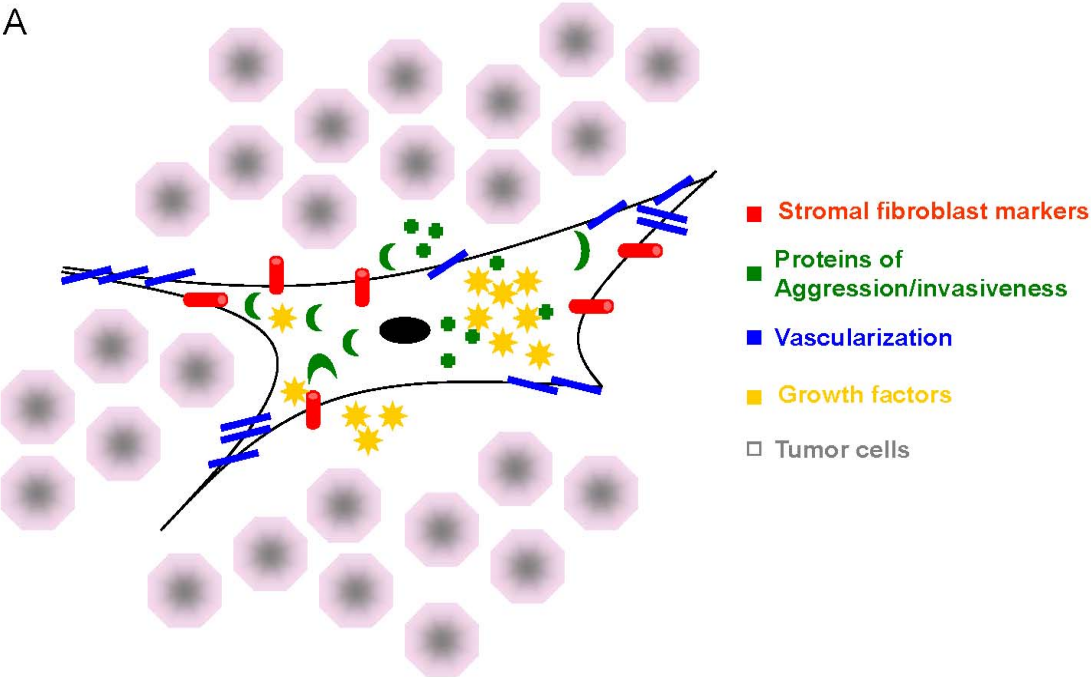
Furthermore, MSC incorporation as tumor stroma is not exclusive to one tumor type. While we focus primarily on Skov-3 ovarian carcinoma, we briefly show the potential for the MSC to incorporate into both breast (MDA-231) and pancreatic (Panc-1) tumors (Figure 16L-P).

Figure 15. MSC can differentiate into TAF. (A) The expression of several markers defines the heterogeneous population of the TAF. **(B)** After 21 days in tumor conditioned medium, MSC differentiate into TAF, as defined by the appearance of FSP, TSP1 and Tn-C, and the increase in α SMA, FAP and desmin.

* Figure published in PlosOne 2009, Spaeth *et al.*

Figure 15

A



B

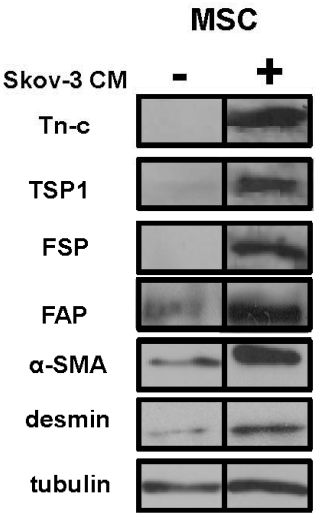
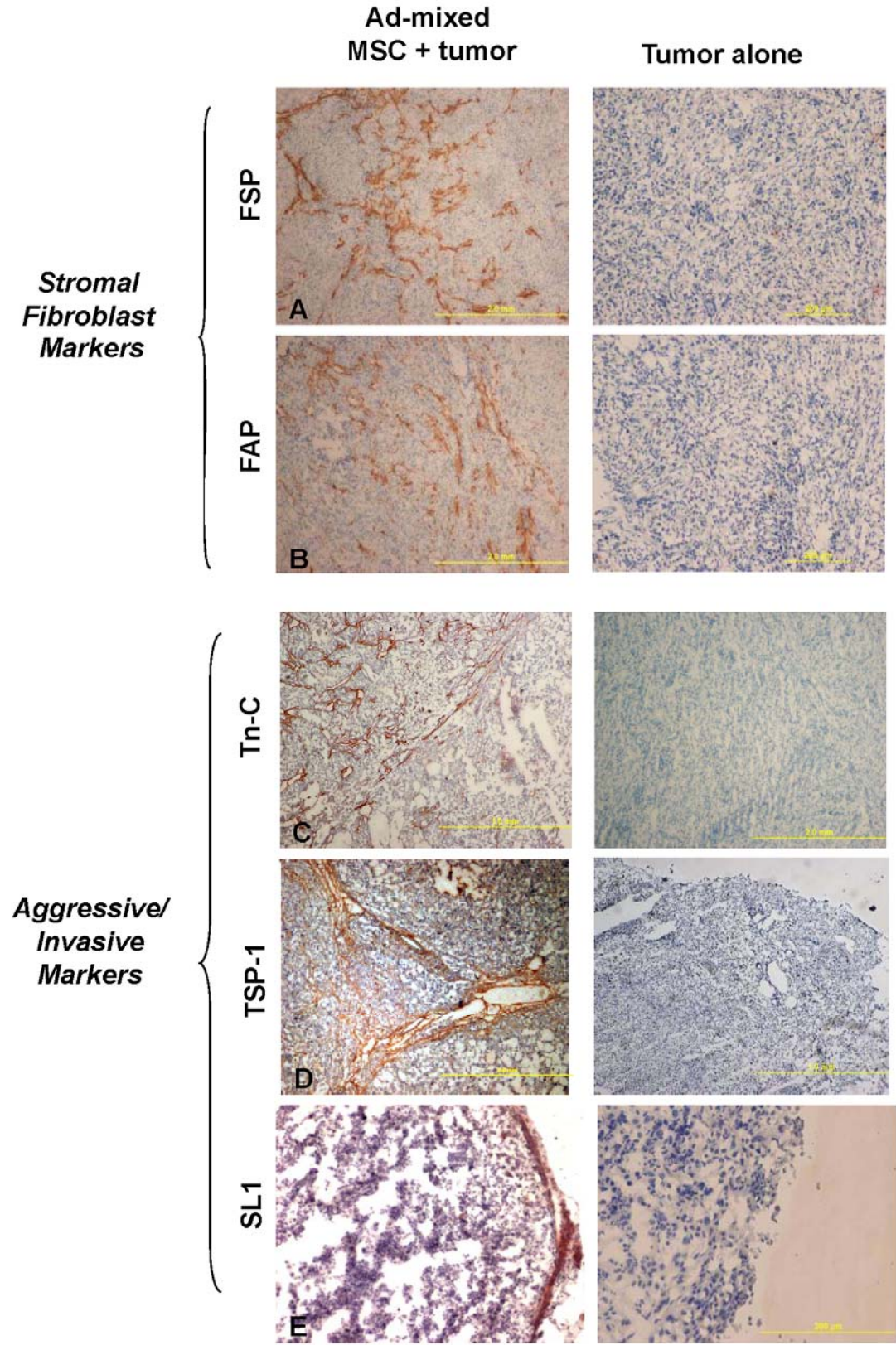


Figure 16. Expression of TAF markers in MSC-admixed Skov-3 tumors *in vivo*.

Following three months of tumor engraftment, excised tumors were analyzed by IHC for the presence of TAF markers. Activated fibroblast proteins **(A)** FSP, **(B)** FAP were scattered in a non-uniform branching network. The ECM-modifying proteins **(C)** Tn-c and **(D)** TSP1 are found throughout the tumor whereas **(E)** SL1 is found localized to the leading edge of the tumor. The myofibroblast markers including **(F)** α SMA and **(G)** desmin are found throughout the tumor and are associated with neovascularization as endothelial-supportive cells and the growth factor **(H)** VEGF is more highly expressed in localized regions of the admixed tumor. Additional growth factors expressed within the tumor microenvironment at higher levels than in the tumor alone include **(I)** HGF, **(J)** EGF and **(K)** IL6. **(L)** Expression of MSC marker, Thy1 shows co-localization in adjacent tumor sections with **(M)** α -SMA + stained Skov-3, MDA-231 and Panc-1 xenograft tumors. Additional TAF markers shown include: **(N)** desmin **(O)** TSP1 and **(P)** Tn-C.

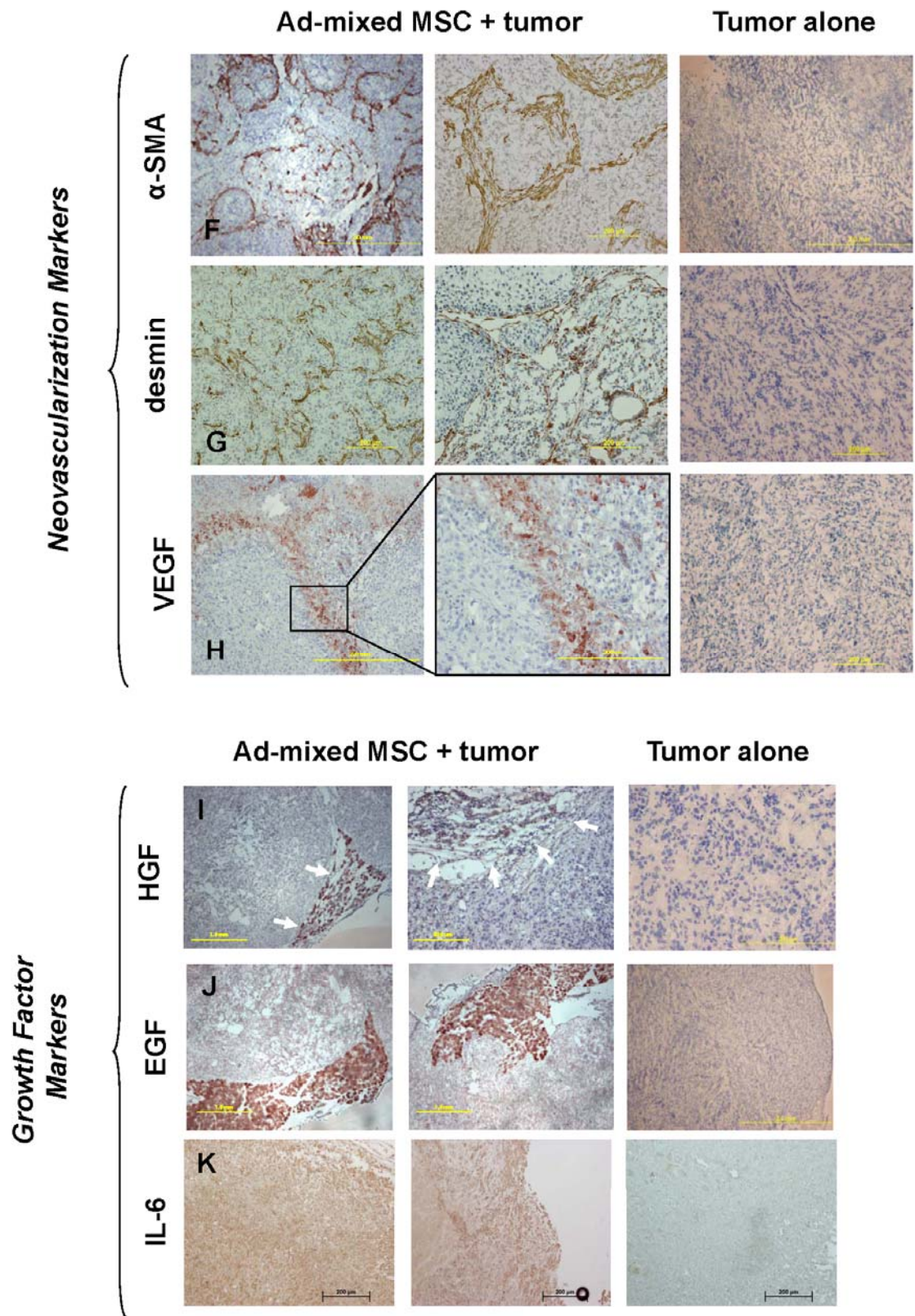
* Figure published in PlosOne 2009, Spaeth *et al*.

Figure 16



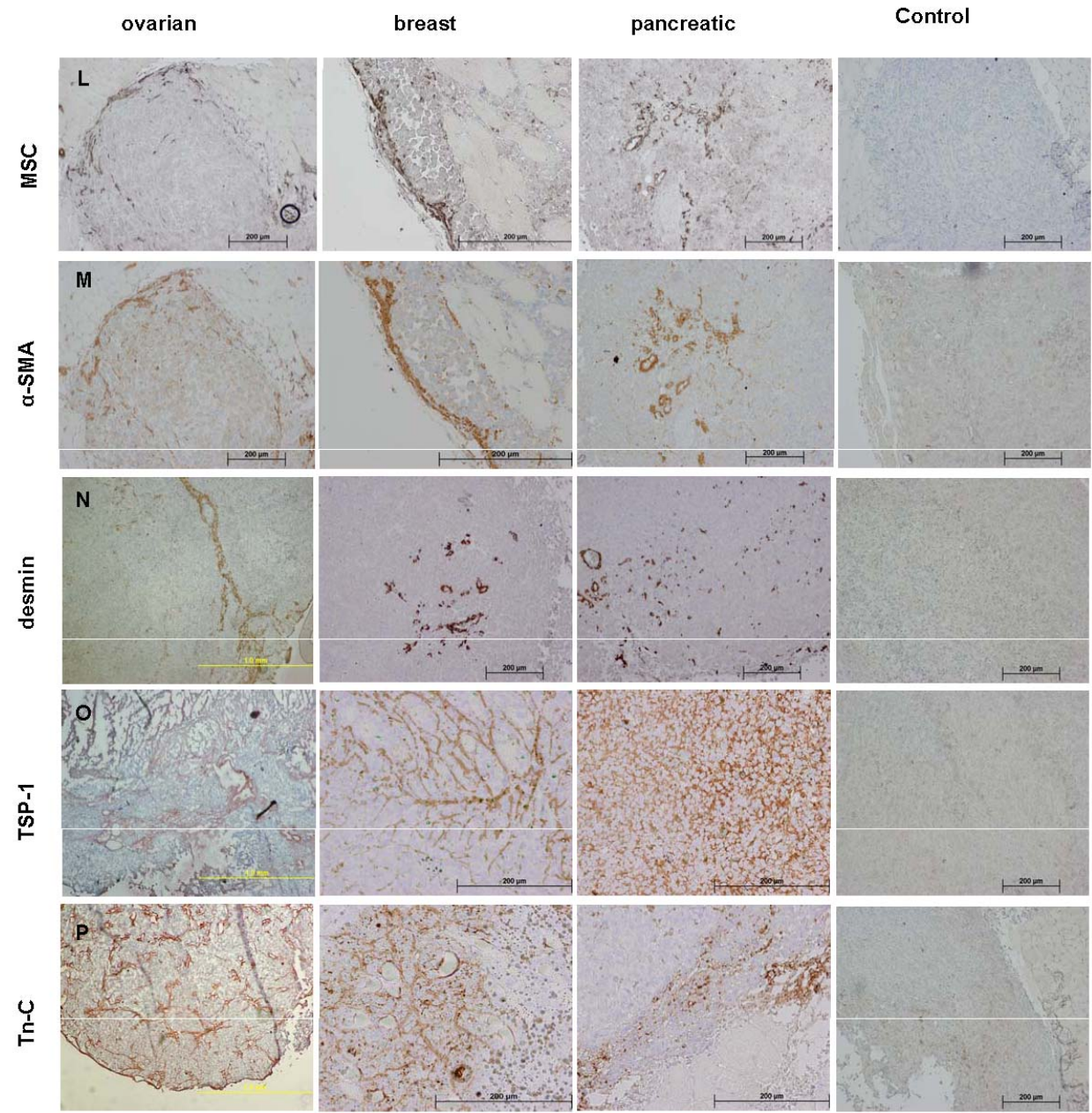
Spaeth et al.2009. PLoS ONE 4(4): e4992

Figure 16 cont.



Spaeth et al.2009. PLoS ONE 4(4): e4992

Figure 16 cont.



Spaeth et al.2009. PLoS ONE 4(4): e4992

3.3.2 MSC as TAF contribute to tumor growth

In vivo, we showed the presence of growth factors by IHC (Figure 16). *In vitro*, MSC express and secrete multiple growth factors, chemokines and cytokines when stimulated by tumor conditioned media. Measuring IL-6, TGF β , VEGF and HGF expression by ELISA from both the MSC stimulated by the SKM (Figure 17A) or from the Skov-3 tumor cells stimulated by the MSC conditioned medium (Figure 17B) we see an increase in growth factors within the medium in all cases with the exception of HGF which is not induced in MSC by SKM. VEGF is not significantly up regulated and the increased presence of HGF is due to HGF secreted by the MSC.

The MSC within the tumor microenvironment give rise to TAF which are supportive and capable of enhancing tumor growth *in vivo*. Comparing Skov-3 only tumors to Skov-3/MSC admixed tumors, there is a significant although delayed growth advantage (Figure 17C). Furthermore, we attribute this growth advantage to the human MSC and not the mouse stromal MSC participation. In an *in vitro* tumor growth assay, Skov-3 cells were admixed with a BALB/c, c57 murine MSC cell lines or with fibroblasts and compared against the human MSC. The human MSC provided a significant growth advantage to the Skov-3 tumor cells over a period of eight days (Figure 17D).

An *in vitro* tumor growth assay was used to assess the MSC secreted growth factor that was driving Skov-3 tumor cell proliferation. First, Skov-3 tumor cell proliferation was analyzed alone, with MSC conditioned media or with the exogenous addition of FGF, HGF, TGF- β , VEGF, EGF or IL-6. EGF and IL-6 showed the most potent proliferative advantage next to MSC conditioned media (Figure 17E). Next, to determine whether the MSC conditioned media was the source of the IL-6 and EGF that was promoting cell proliferation, the same assay was set up with MSC conditioned media that had had EGF or IL-6 immunoprecipitated out of solution. By immunoprecipitating IL-6, but not EGF out of the MSC conditioned media, the proliferative advantage of the Skov-3 cells was significantly hindered (Figure 17F).

Figure 17. Growth advantage of tumors admixed with MSC. Growth factors potentially attributing the growth advantage of Skov-3 tumors admixed with MSC were measured by ELISA. **(A)** IL-6, TGF β and VEGF are all increased in MSC supernatant following SCM. Likewise, **(B)** IL-6, TGF β , VEGF and HGF were increased in Skov-3 supernatant following MSC conditioning. **(C)** *In vivo* tumor growth advantage of admixed tumors was delayed yet apparent after day 80. **(D)** Neither murine MSC nor fibroblasts have the same growth advantage as human MSC do on Skov-3 tumor cell proliferation in an *in vitro* tumor growth assay. **(E)** Skov-3 proliferation was analyzed in a tumor growth assay using MSC conditioned media or growth factors alone. **(F)** immunoprecipitation (IP) of EGF or IL-6 from MSC conditioned media showed that Skov-3 cell proliferation is inhibited with the removal of MSC secreted IL-6.

* Figure published in PlosOne 2009, Spaeth *et al.*

Figure 17

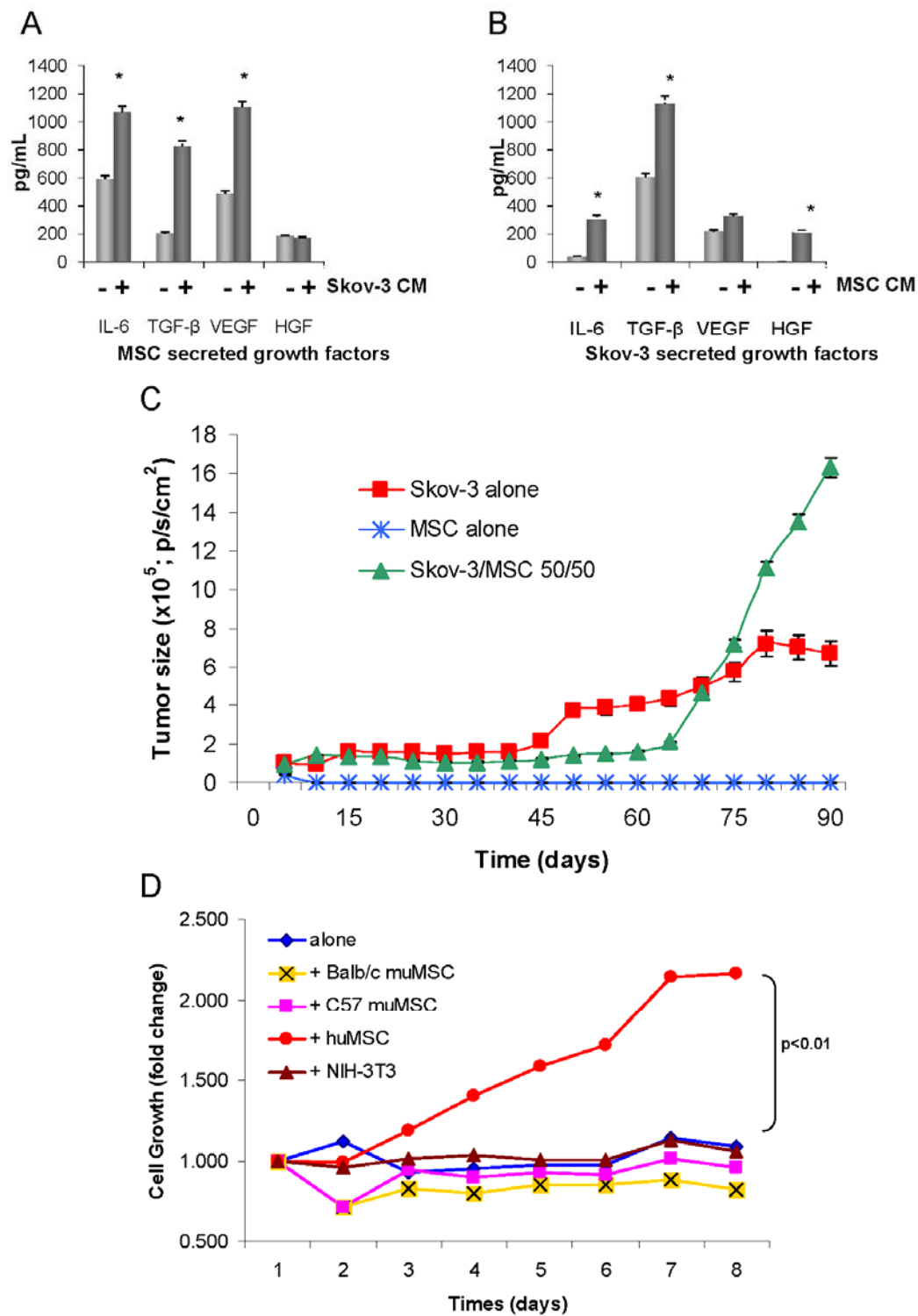
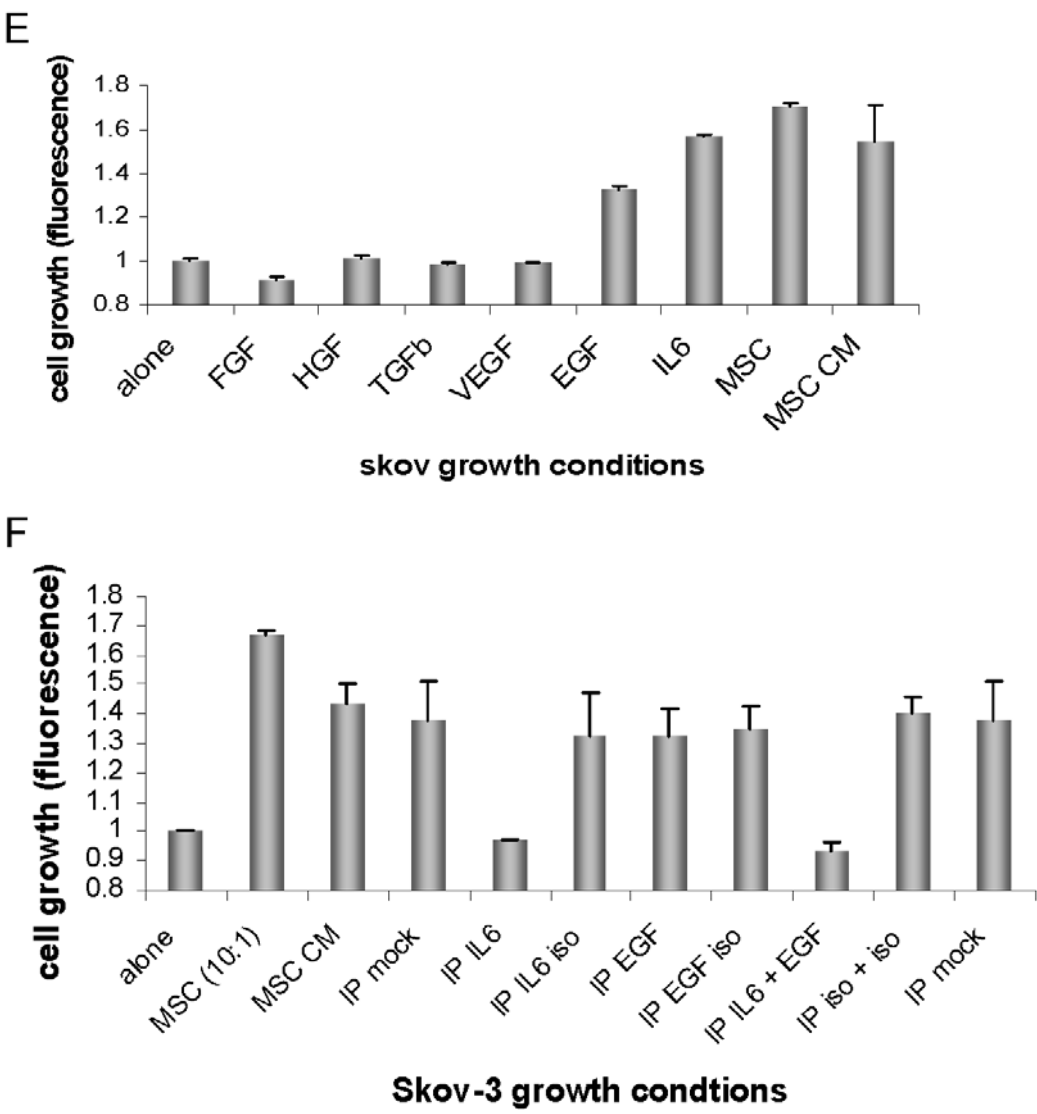


Figure 17 cont



3.4 CD44 deficient MSC become inadequate TAF

3.4.1 sh44 MSC are deficient as a supportive stromal cell

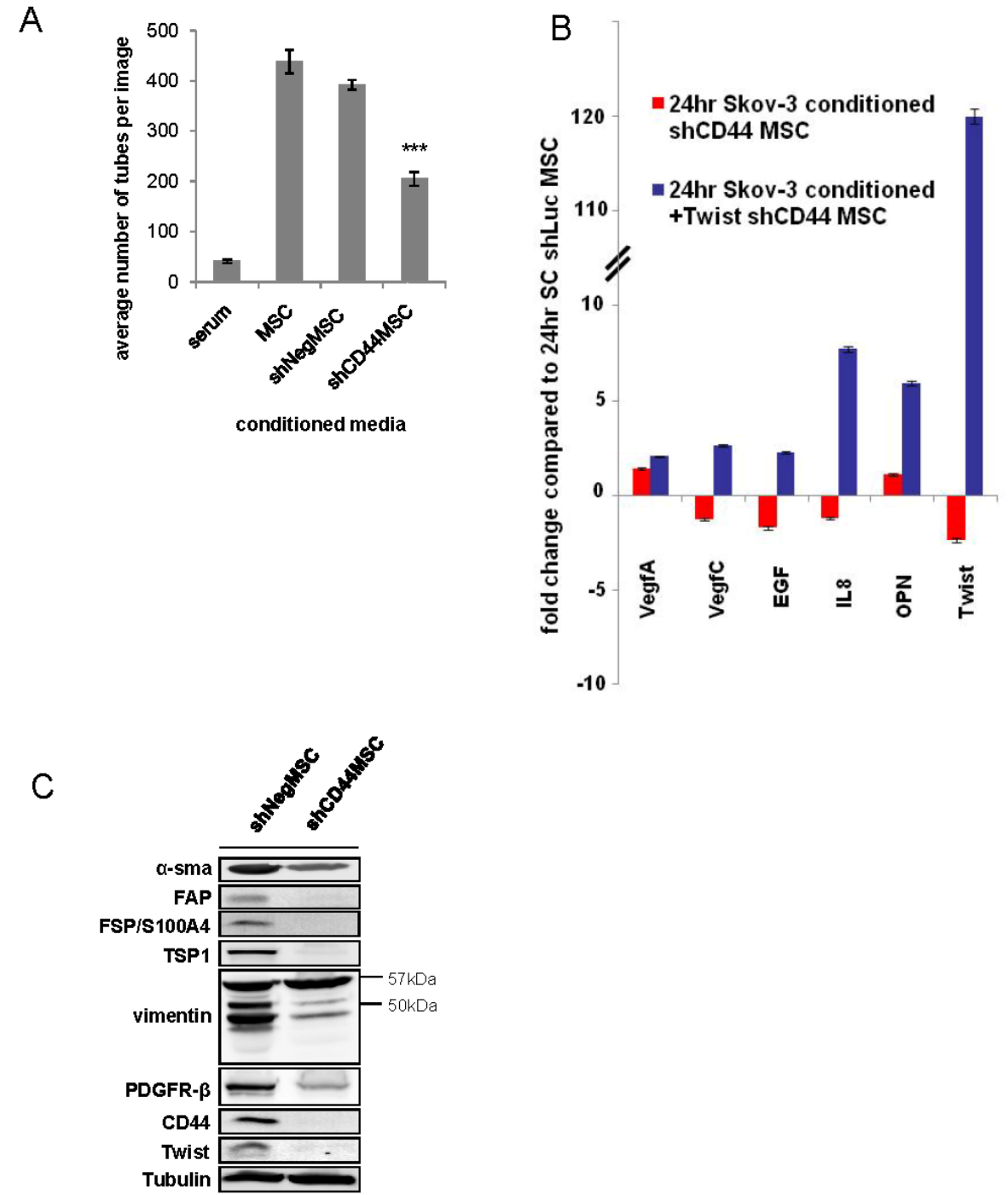
The MSC, as a stromal cell is able to support cell growth and maintenance through the production of growth factors, chemokines and cytokines. Through paracrine stimulation, MSC are proangiogenic; they are able to induce *in vitro* endothelial tube formation. The stable shCD44 MSC cell line showed a decreased propensity to support endothelial (HUVEC) tube formation and stabilization *in vitro*. Naïve MSC can initiate and maintain endothelial tube formation including a large quantity of nodal structures after conditioning whereas shCD44 MSC conditioned HUVEC are not able to form as many nodal structures intersecting single tubes. These can be enumerated by manual counting of the tubes per field of view under the light microscope. Furthermore, the naïve MSC are able to sustain support beyond 10 days whereas the shCD44MSC media does not support or sustain tube formation in HUVEC past 8 days. By quantifying tube formation at day 7, the shCD44 MSC show a decreased capacity ($p < 0.001$) to induce and maintain HUVEC tube formation of 53% compared to naïve MSC (Figure 18A). To elucidate what proangiogenic growth factors could be affected by knockdown of CD44 in MSC, we evaluated the gene expression of growth factors including VEGF A, VEGF C, EGF, TGF α , IL-8 and OPN. The gene expression of VEGF C, EGF, TGF α and IL-8 is decreased in the shCD44MSC compared to shNeg MSC. Furthermore, when Twist was exogenously expressed in the shCD44MSC, the expression of all six growth factors increased in expression (Figure 18B).

Finally, we looked at the expression of TAF markers following long term (21 day) tumor conditioned sh44MSC compared to shNeg MSC. The expression of FAP, FSP and TSP1 are significantly decreased in the shCD44MSC population. The expression of α -SMA and PDGFR- β is decreased. And, while the levels of total vimentin are not different between the shCD44MSC and the shNeg MSC, the protease cleavage fragments of vimentin are less in the shCD44MSC. The

expression level of Twist is also decreased in the shCD44MSC following long term tumor conditioning (Figure 18C).

Figure 18. Deficient stromal supportive features of shCD44MSC. **(A)** *In vitro*, MSC (or shNeg MSC control) conditioned media induced tube formation on HUVEC up to 12 days in culture. HUVEC conditioned by shCD44MSC formed 53% fewer tubes compared to naïve MSC ($p < 0.001$). Tubes were manually counted under a light microscope (4 fields of view per well x3 wells). **(B)** Growth factor gene expression fold change of shCD44MSC (red) or shCD44MSC+Twist (blue) following 24 hour tumor conditioning. Fold change relative to tumor conditioned shNeg MSC. **(C)** TAF marker expression in long term (21 day) conditioned shCD44MSC compared to shNeg MSC showed decreased expression of nearly every TAF marker evaluated.

Figure 18

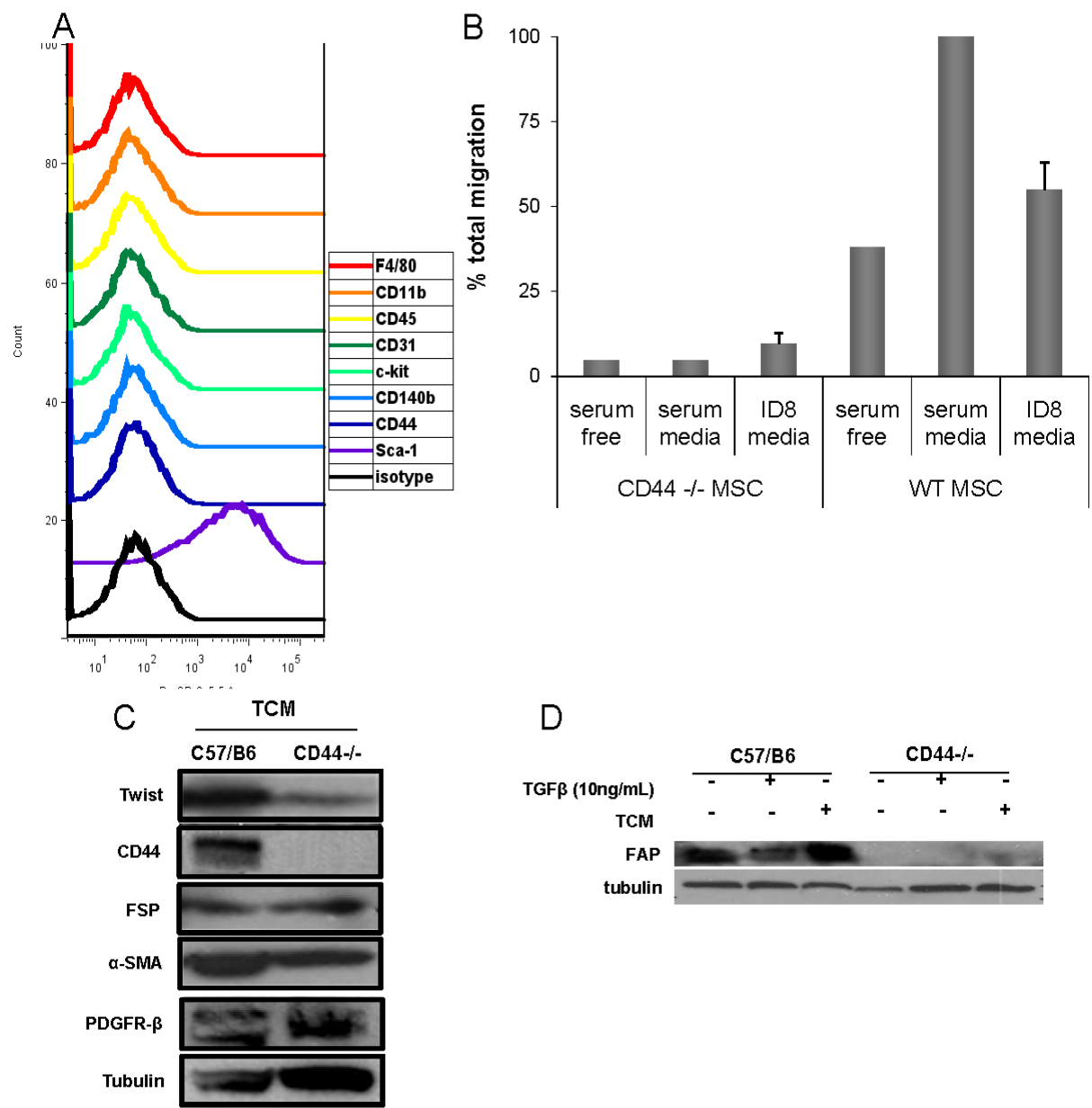


3.4.2 Characterization of CD44 deficient murine MSC

To further investigate the role of CD44 in MSC, CD44 knockout mice were purchased from Jackson Labs (Bar Harbor, Maine). MSC isolated from these mice express Sca-1, but not CD140b, CD106 or CD44 (Figure 19A). When compared to their wild type counterparts, the CD44KO MSC have impaired migratory capacity towards ID8 tumor conditioned media *in vitro* (Figure 19B). Next, we saw a decrease in basal levels of Twist expression in CD44KO MSC versus WT MSC in addition to a change in PDGFR- β bands (Figure 19C). Both of these changes were seen in the human sh44MSC. The most striking difference between the two MSC was the lack of detectable FAP expression in the CD44KO mice at basal levels, with tumor stimulation or with TGF- β stimulation (Figure 19D).

Figure 19. Characterization of murine CD44KO MSC. **(A)** Phenotypic surface marker expression of CD44KO MSC. **(B)** Overall migration capacity of CD44KO MSC compared to wild type C57/b6 MSC. **(C)** Comparison of marker expression of activated fibroblast markers under TCM (ID8) shows no CD44 expression and altered PDGFR β expression and the levels of **(D)** FAP expression could not be induced.

Figure 19

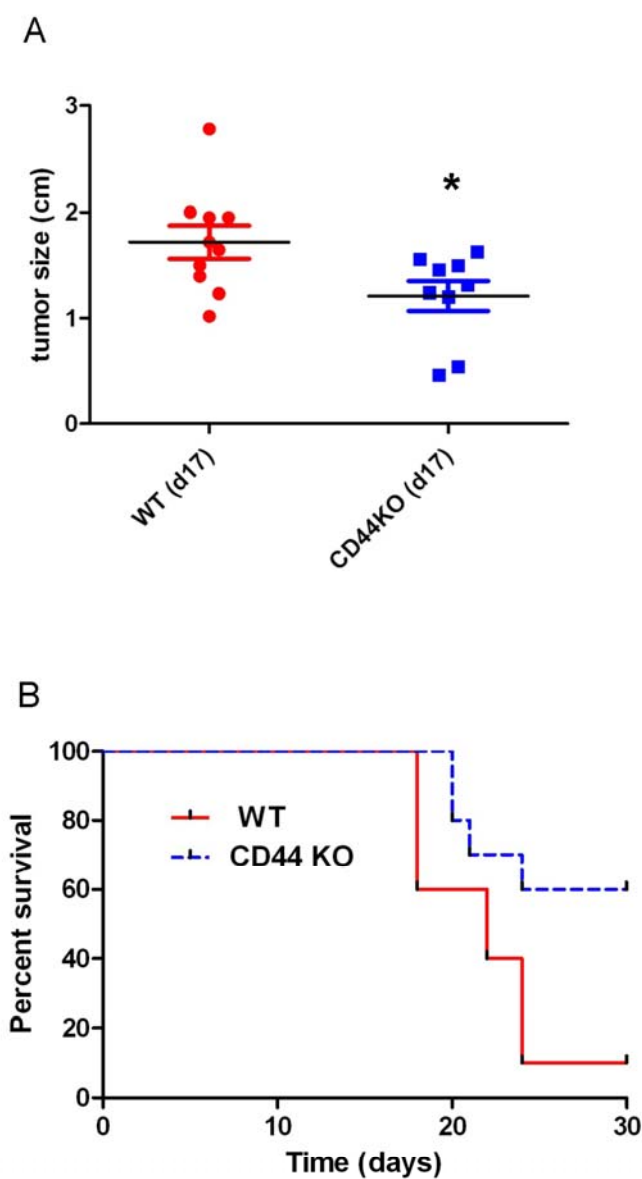


3.4.3 Delayed tumor progression in CD44KO mice

To elucidate whether CD44KO mice have less tumor promoting potential compared to WT mice, 2×10^5 EO771 tumor cells were engrafted SC into the CD44KO (n=10) or WT (n=10) mice. Tumor growth was followed by daily caliper measurements. The majority of tumors were palpable by day 8. On day 17 there was a significant difference ($p < 0.05$) between the size of the tumor in the WT mice compared to the CD44KO mice (Figure 20A). The first mice died in the control group on day 18. All of the mice were sacrificed due to tumor burden 30 days following tumor engraftment. At this time there were 6 mice remaining in the CD44KO group and only 1 remaining in the WT group. There was a significant difference in survival between tumor burdened WT mice and tumor burdened CD44KO mice by Log-rank test ($p < 0.05$; Figure 20B). One marked difference between the two groups was the size of the spleen in the CD44KO mice was consistently 2x larger than in the WT mice. Otherwise, all of the organs were similar in appearance. There were no signs of lung or lymph node metastases.

Figure 20. Tumor growth in CD44KO mice compared to WT mice. (A) Caliper measurements from the mice (n=20) were analyzed 17 days following tumor engraftment. Tumor size in CD44KO mice is significantly smaller ($p<0.05$) compared to WT mice. **(B)** Kaplan-Meier curve of WT versus CD44KO mice following EO771 tumor engraftment shows significant difference ($p<0.05$). All mice were sacrificed on day 30.

Figure 20



3.4.4 Tumor microenvironment impact of CD44KO MSC

Next, we asked whether the inability of the CD44 deficient MSC to support angiogenesis *in vitro* was associated with the vascularization potential of the MSC (or the tumor conditioned MSC, the TAF) *in vivo*. Briefly, murine CD44KO MSC or murine WT MSC were admixed with 4T1 tumor cells at a 1:1 ratio, a total of 2×10^5 cells, and engrafted into the mammary fat pad of SCID mice. Following 3 weeks of tumor engraftment, the mice were sacrificed and the tumors excised, paraffin embedded and processed for immunofluorescent staining. Compared to tumors with admixed wild type MSC, the tumors admixed with CD44KO MSC contained fewer stromal components that are normally provided by MSC-differentiated tumor associated fibroblasts. α -SMA expression, indicative of myofibroblast and pericyte presence and vessel stability in neoangiogenesis, is increased in MSC admixed tumors compared to tumor alone. In CD44KO admixed tumors, the expression level of α -SMA is reduced to the level seen in tumors without admixed MSC ($p < 0.001$; Figures 21A and B). Likewise, vessel presence was measured by the endothelial cell marker, CD31. Its expression is also decreased in the CD44KO MSC admixed tumors compared with the wild type MSC admixed tumors ($p < 0.05$; Figures 21C and D). Finally, the expression levels of FAP and FSP, proteins indicative of “activated” fibroblasts or tumor associated fibroblasts, are similarly decreased in the CD44KO MSC admixed tumors when compared to the wild type MSC tumors ($p < 0.001$ for both; Figures 21E-F).

Figure 21. CD44KO MSC/4T1 admixed tumors have less tumor associated fibroblast presence and less vascularization *in vivo*. Paraffin embedded 4T1 tumors alone or admixed with either CD44KO MSC or WT MSC were analyzed for the presence of myofibroblast marker **(A)** α -SMA, a marker of vascular support. **(B)** Quantitative analysis of α -SMA staining across all slides. **(C)** The presence of endothelial cells was confirmed by CD31 positive staining and **(D)** quantified. **(E-F)** FAP positive staining represents activated fibroblasts in the tumor stroma as does **(G-H)** FSP positive staining. In IF images, stained cells are shown in white but are shown in red in the mock-brightfield images.

Figure 21

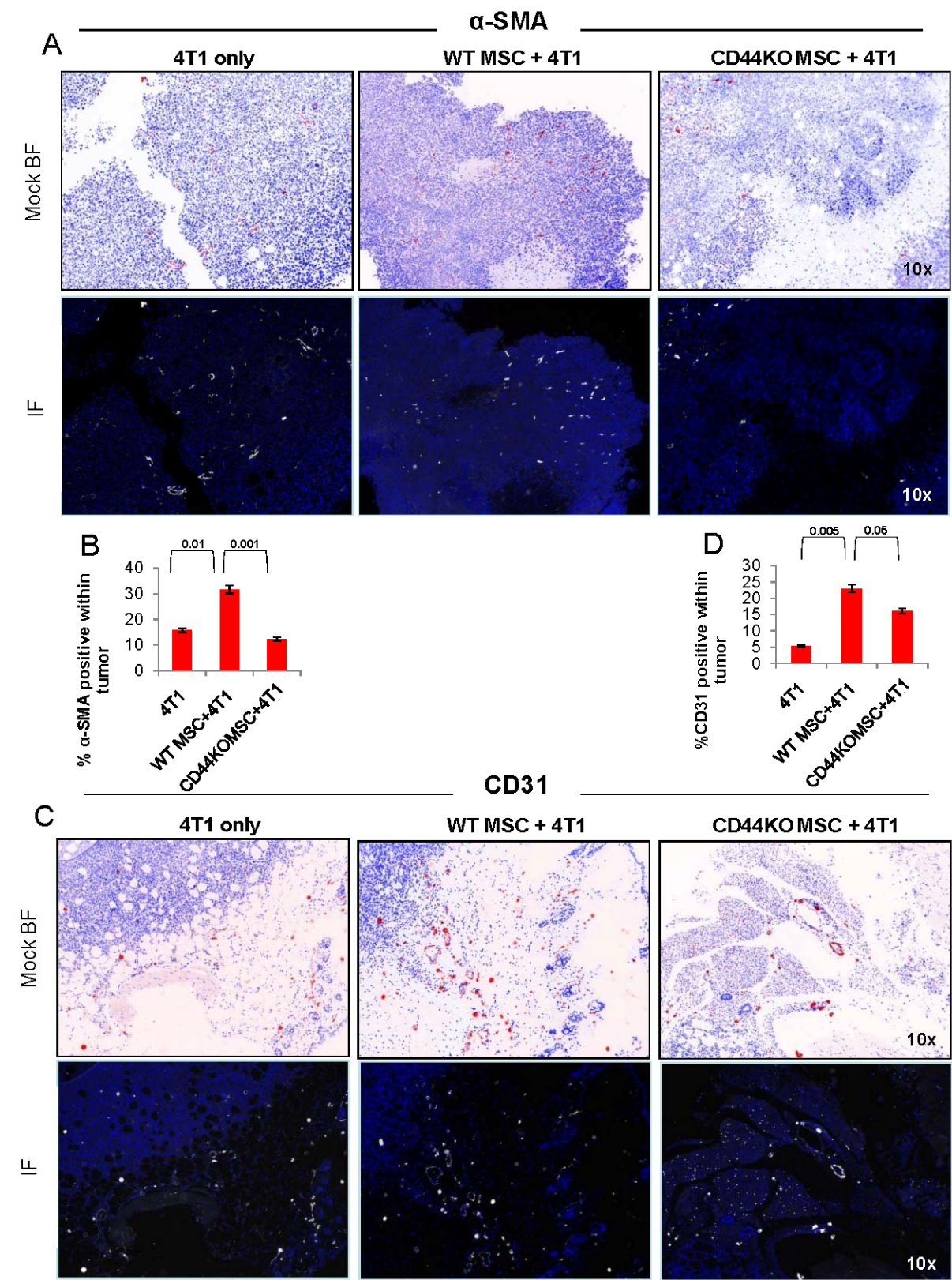
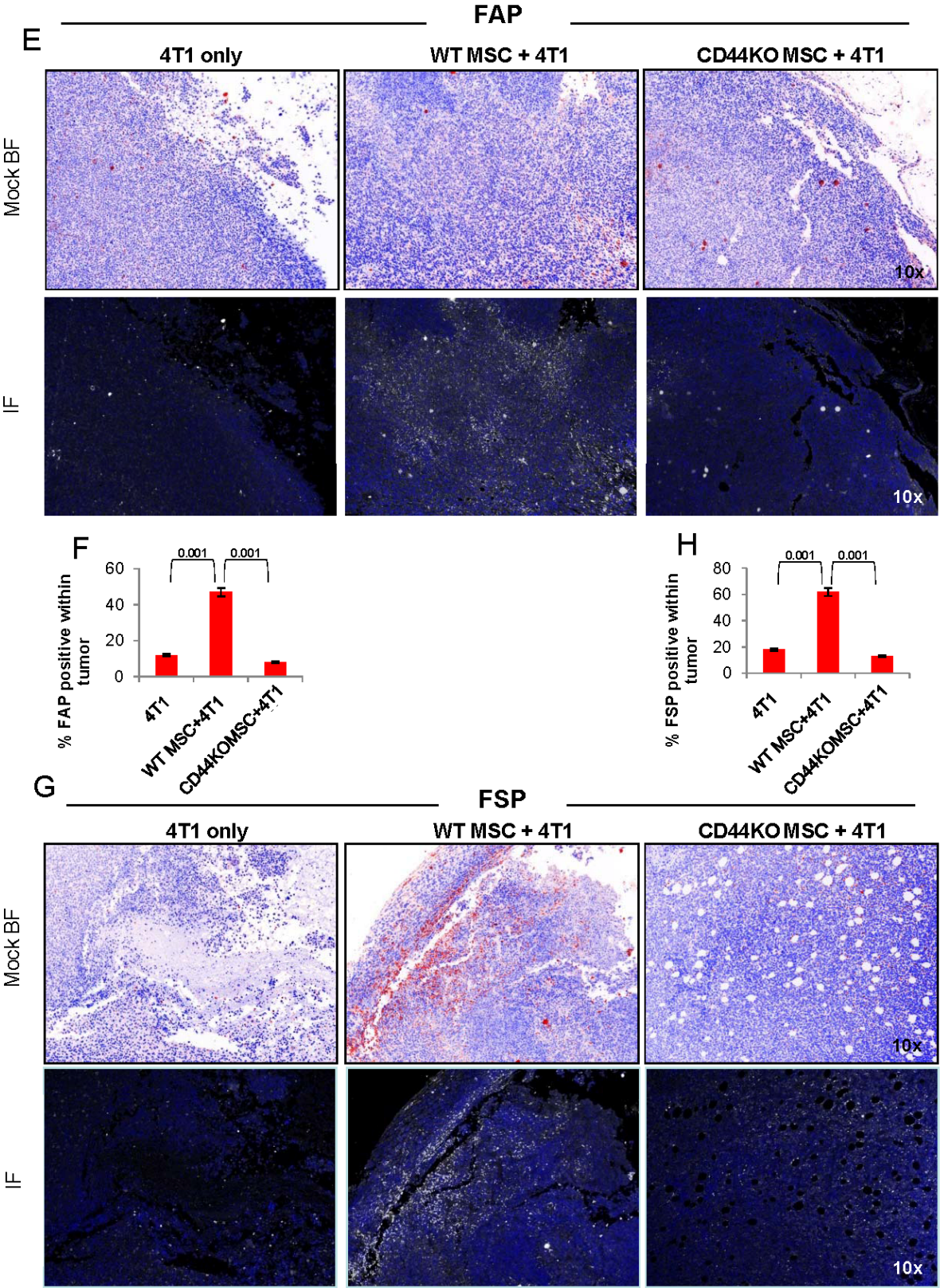


Figure 21 cont.



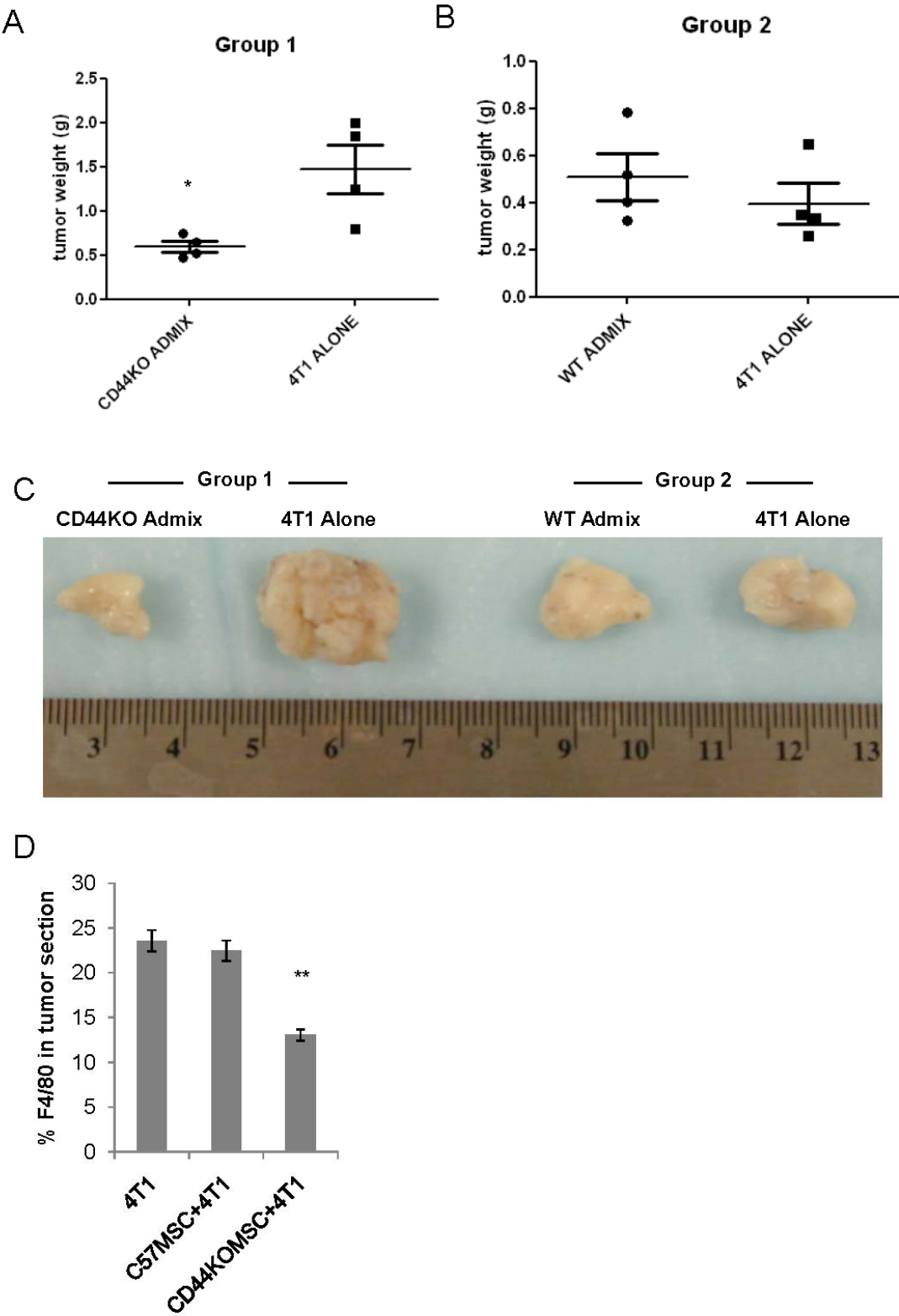
3.4.5 CD44-deficient stroma tumor growth deficiency

SCID mice were given contralateral tumor injections in the inguinal fat pads. The mice in Group 1 received a 1:1 admixture of CD44KO MSC and 4T1 (2×10^5 total) on the right and 2×10^5 4T1 cells alone on the left. Mice in group 2 received the same number of cells but a 1:1 admixture of WT MSC and 4T1 on the right and 4T1 alone on the left. Three weeks after engraftment, mice were sacrificed and tumors were weighed in order to compare discrepancies in tumor size. Group 1 resulted in 4T1 tumors significantly larger than the admixed 44KO MSC/4T1 tumors ($p < 0.05$; Figure 22A). In group 2, the WT MSC/4T1 tumors were larger than the 4T1 tumors ($p = \text{NS}$; Figure 22B).

Representative image of excised tumors shows the CD44KO Admixed tumors from group 1 were significantly smaller than the opposite tumor but not smaller than the tumors from the mice in group 2 (Figure 22C). One potential reason for the tumor size discrepancy between groups may have to do with the macrophage presence in the mice. Represented by F4/80 positive staining, 4T1 tumors and WT MSC/4T1 tumors did not have statistically significant differences in the macrophage marker whereas CD44KO MSC/4T1 tumors had 40% less infiltration (Figure 22D).

Figure 22. Differences in tumor size between CD44KO MSC/4T1 admixed and control tumors. Three weeks prior to tumor excision, mice received an injection of either CD44KO MSC/4T1 or WT MSC/4T1 bilateral to 4T1 alone. Tumor weight (g) was measured in both sets of mice. **(A)** Group 1 mice received CD44KO MSC/4T1 tumor bilateral to 4T1 were significantly smaller in tumor size ($p<0.05$). **(B)** Group 2 mice received WT MSC/4T1 tumor bilateral to 4T1 and did not show a significant difference between tumor sizes **(C)** Representative images of excised tumors from mouse in group 1 versus mouse in group 2. **(D)** The macrophage infiltration was depicted by F4/80 staining. Macrophage infiltration is less in the CD44KO MSC/4T1 ($p<0.01$) group and not altered between WT MSC/4T1 tumors and 4T1 alone.

Figure 22



3.4.6 Tumor recruitment of CD44KO bone marrow derived stroma

After evaluating the tumor stroma participation of the CD44KO MSC as TAF in the non-physiological 1:1 admixing experiment, we asked whether the TAF deficiencies would be similar in a physiologically relevant situation. Thus, bone marrow transplants were conducted using ubiquitous-expressing GFP recipient mice to evaluate the contribution of CD44KO bone marrow stromal populations to the tumor microenvironment. The GFP recipients were lethally irradiated (9Gy) and transplanted with whole bone marrow from LacZ labeled CD44KO mice or from mice expressing tdTomato (Red) under the gtROSA promoter (Figure 23A). Schematic diagram of the bone marrow transplant is shown in Figure 23B. Four weeks following engraftment, the bone marrow transplants were confirmed by Flow cytometry (Figure 23C). Then, 2×10^5 EO771 tumors were injected SC and allowed to engraft. Mice were sacrificed 35 days following tumor engraftment; tumors, lungs, liver, spleen and bone marrow were collected for analysis by immunostaining. There were very few differences between the transplant groups as seen by H&E staining (Figure 24A). The marked difference was observed between the tumors within the groups. The tumors engrafted in the CD44KO BMT mice displayed less stromal cell dispersion compared to those in the Red BMT mice. Furthermore, the calculated percentage of stromal cell engraftment in the two representative tumor images is 6.9% in the CD44KO BMT derived tumor compared to 20.1% in the Red BMT derived tumor. Percentage of stromal cell within the images was calculated based on the Eosin-positive staining using Nuance software (Figure 24C).

Figure 23. Bone marrow transplantation into GFP recipient mice. Whole bone marrow was collected from ubiquitously expressing tdTomato mice (red) or CD44KO mice (blue) and transplanted into lethally irradiated ubiquitously expressing GFP mice (green). **(A)** The color and CD44 status of the bone marrow was confirmed by flow cytometry prior to transplantation. **(B)** Schematic diagram of transplantation shows GFP recipient mice receiving either Red BMT (group1) or CD44KO BMT (group2). **(C)** Four weeks following engraftment, blood was drawn from each transplant recipient (Red BMT, n=5; CD44KO BMT, n=5) to confirm the status of the BMT.

Figure 23

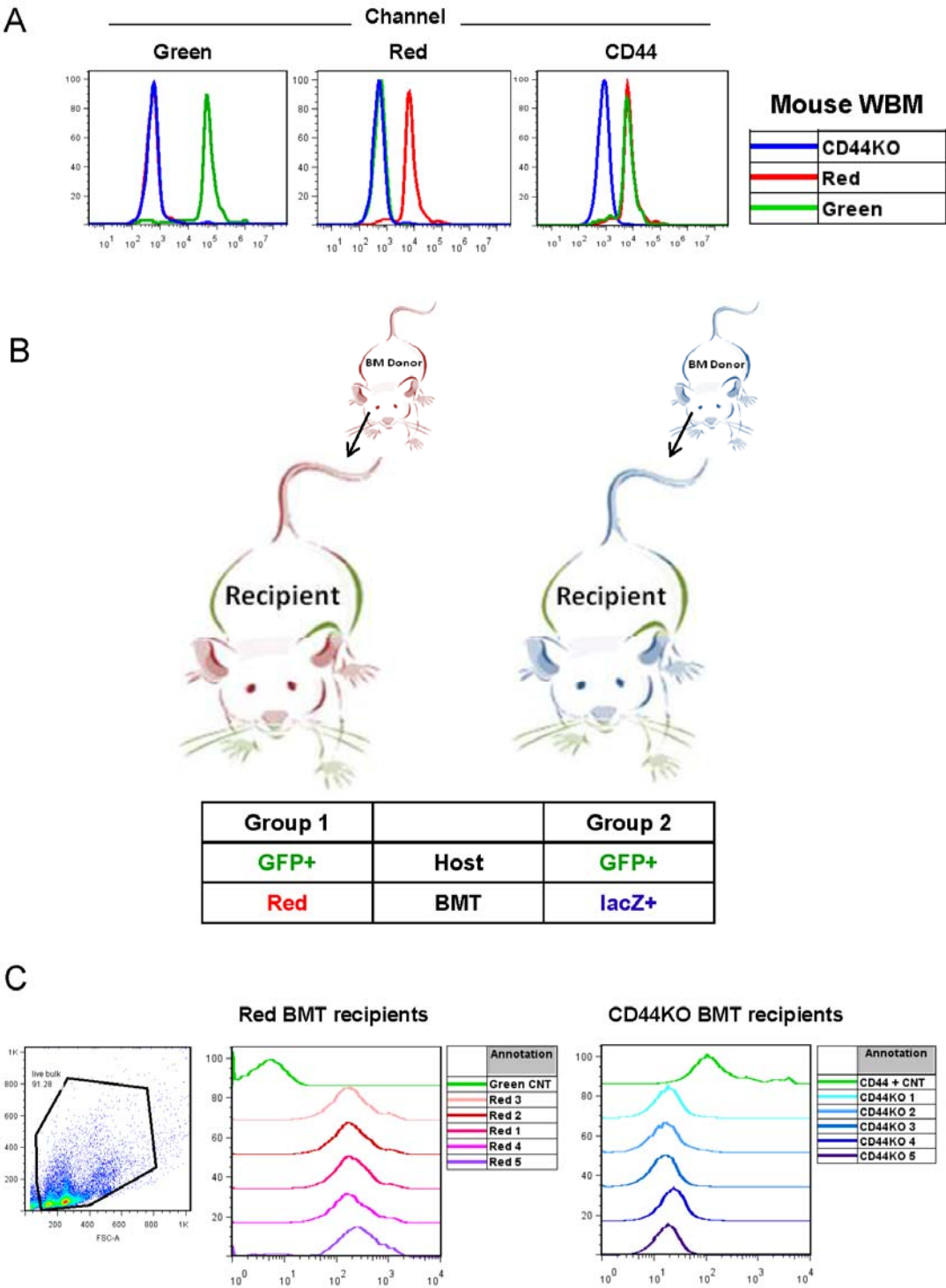


Figure 24. H&E stained organs and tumor sections of BMT mice. There is no visible difference between the organs of the Red BMT versus CD44KO BMT recipient mice as seen by **(A)** H&E staining of tumors and organs. Images are from two individual mice from each group. **(B)** However the H&E stained tumor from the CD44KO BMT mice exhibit less stroma incorporation compared to the Red BMT engrafted tumor. H&E staining colors were enhanced by InForm; light blue→darker blue and pink→red.

Figure 24

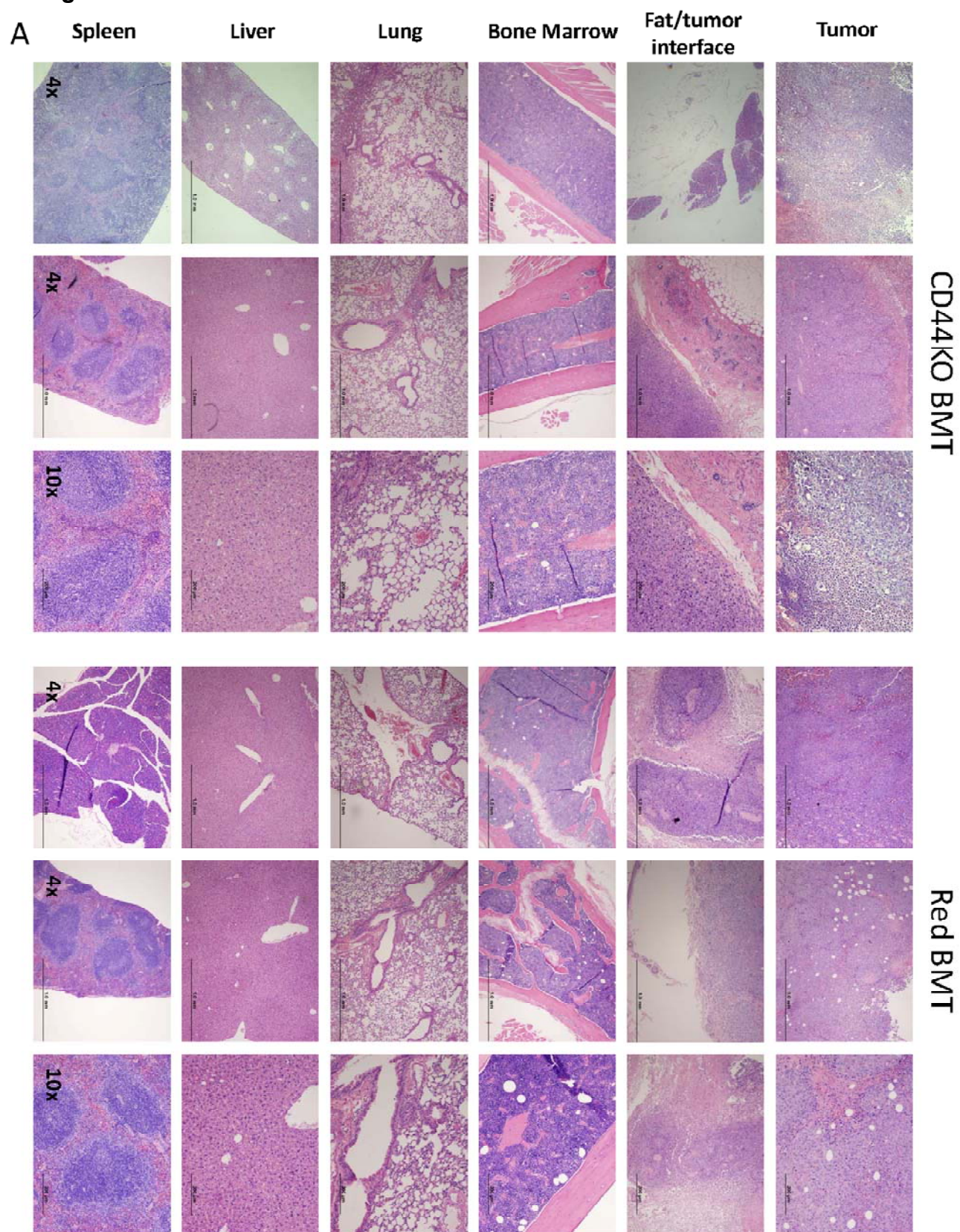
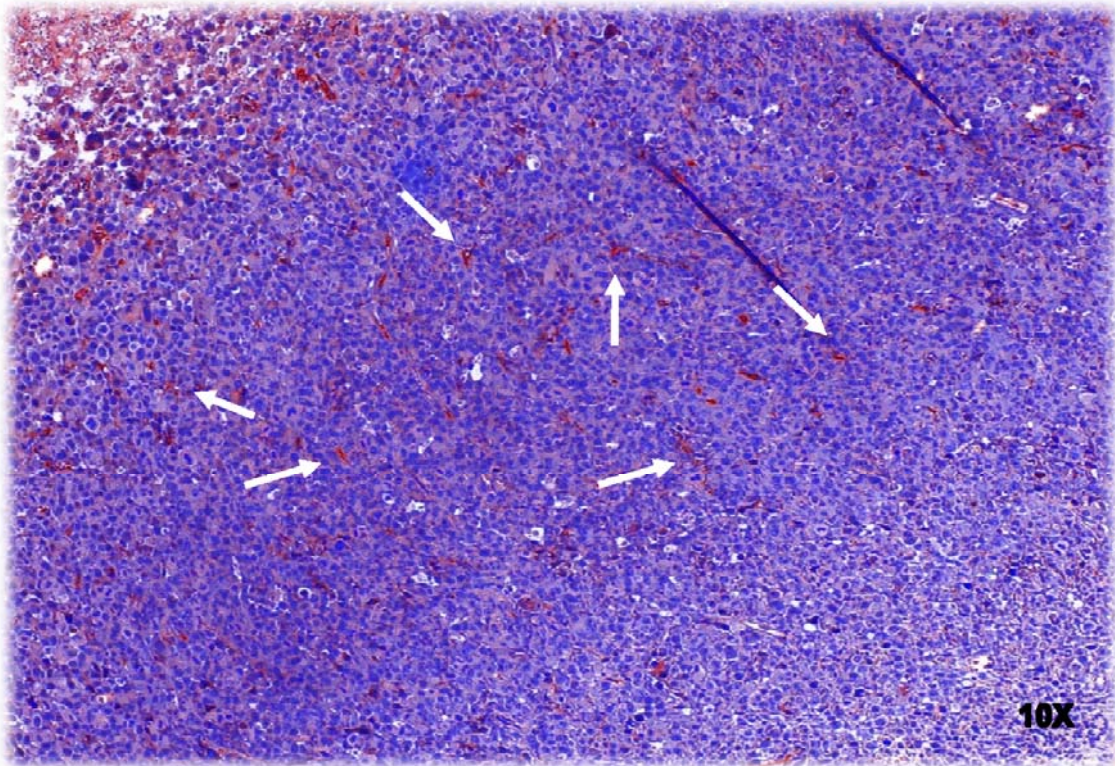


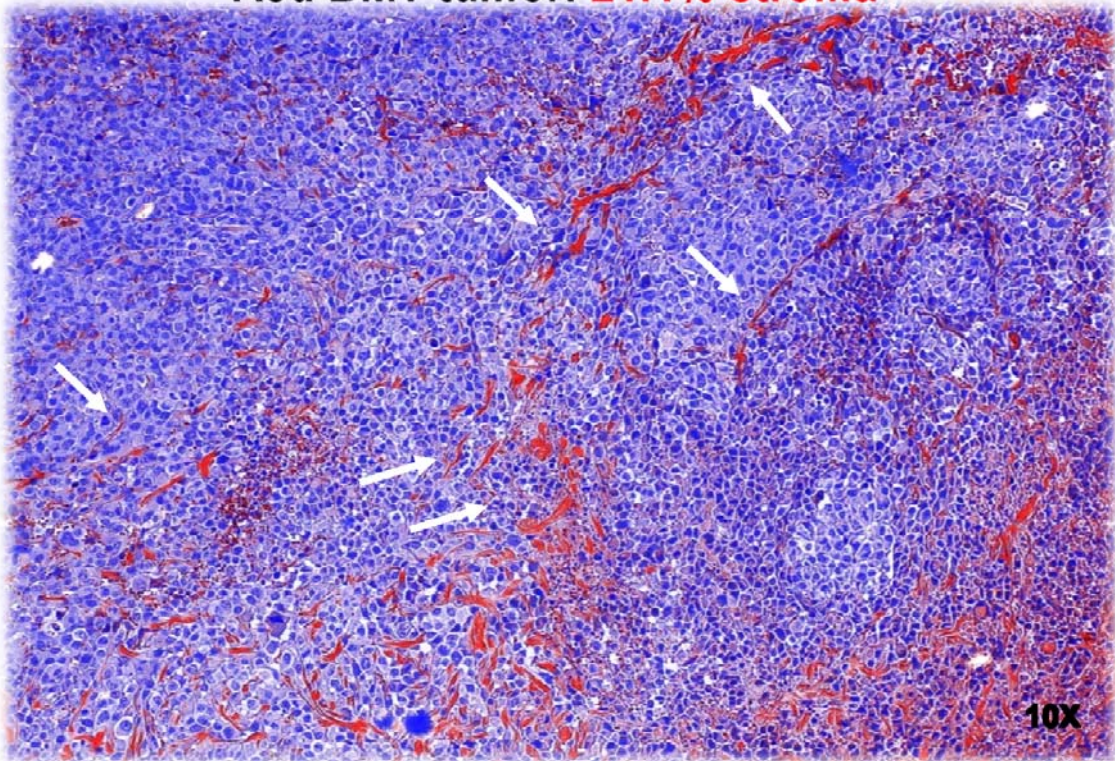
Figure 24 cont

B

CD44KO BMT tumor: 6.9% stroma



Red BMT tumor: 21.1% stroma



3.4.7 CD44KO stromal participation in the tumor microenvironment

Next, we needed to deduce the origin of the tumor stromal participants, whether bone marrow derived or host derived. The tumors from the tdTomato (Red) BMT were analyzed for the co-expression of RFP (to label the BMT cells) or GFP (to label the host cells) and the TAF markers FAP, FSP and α -SMA, and the endothelial marker CD31. Likewise, the CD44KO BMT were analyzed for the co-expression of LacZ (to label the BMT cells) or GFP (to label the host cells) and FAP, FSP, α -SMA and CD31. Co-expression was characterized using InForm software to identify immunostaining co-localization. Briefly, each cell was identified based on the expression of the nuclear stain DAPI (average of 2000 cells per image). Then, the fluorescent intensity of each fluorescent label per cell was enumerated. The fluorescent intensities were plotted (488 label on the Y axis and 594 on the X axis) and co-stained cells were quantified. Figure 25 illustrates the process of spectral unmixing, cell segmentation based on nuclear stain and the quantitation of an image stained with α -SMA+ and GFP+. Corresponding fluorescence intensity plot of co-stained cells correlates to the image (Figure 25I).

In tumors from both CD44KO BMT mice and Red BMT mice, the GFP host cells were found to co-express with the FAP (Figure 26A), FSP (Figure 26B), α -SMA (Figure 26C) and CD31 (Figure 26D) markers more than the respective β -gal+ or RFP+ bone marrow derived cells.

Briefly, the number of cells assessed (n) for the co-expression of each marker pair was 100,000 on average. The following percentages were calculated based on the co-stained cells in the numerator and the total number of cells (n) in the denominator. Red bone marrow derived stromal presence (RFP+) in the tumor was limited. The overall prevalence of the GFP+ cells expressing FAP, FSP, α -SMA or CD31 (6.1% \pm 2.3%) from the Red BMT mouse derived tumors was greater than the RFP+ cells expressing any of the four markers (0.7% \pm 0.3%; Figure 27A). There was a significant difference between the GFP+/CD31+ cells and the

RFP+/CD31+ cells within the tumor ($p < 0.001$) but no significant difference between any of the other markers. Again, percentages displayed in Figures 27A-C of GFP+ or RFP+ or β -gal co-stained cells in tumors from BMT mice were calculated averages of co-stained (double positive as explained in Figure 25I) cells per total number of cells per tumor image was calculated between 5 mice and 10 images per tumor.

CD44KO bone marrow derived stromal presence (β -gal+) in the tumor was overall less than control (RFP+) derived stroma but to no statistical significance (Figure 27A and B). Very few β -gal+ cells co-expressed FAP, FSP, α -SMA or CD31. However, the overall prevalence of GFP+ cells co-expressing FAP, FSP, α -SMA or CD31 in tumors ($9.6\% \pm 4.9\%$) of CD44KO BMT mice was greater than β -gal+ cells expressing FAP, FSP, α -SMA or CD31 in the same tumors ($0.6\% \pm 0.4\%$; Figure 27B). Furthermore, co-expression of both GFP+/FAP+ and GFP+/FSP+ cells was greater than β -gal+/FAP+ and β -gal+/FSP+ cells, respectively. But this trend did not reach statistical significance less than 0.05 (FAP+ comparison: $p < 0.1$; FSP+ comparison: $p < 0.06$).

Interestingly, there were more GFP+ co-stained TAF cells in the tumors from the CD44KO BMT mice as compared to the Red BMT (control) mice. The difference was significant ($p < 0.01$) when comparing co-stained GFP+/FSP+ cells between the two BMT groups. (Figure 27C) This suggests the host (GFP+) fibroblastic incorporation into the tumor microenvironment was enhanced in the CD44KO BMT mice compared to the Red BMT mice. There is less β -gal+ expressed FAP ($0.025\% \pm 0.02\%$) or FSP ($0.026\% \pm 0.01\%$) compared to RFP+ expressed FAP ($0.26\% \pm 0.08\%$) or FSP ($0.21\% \pm 0.06\%$); however, the difference was trending towards but never reached statistical significance less than 0.05 (Figure 27D).

Finally, without analyzing the origin of the cell, whether bone marrow or host derived, the total percentages of tumor supportive stromal markers (α -SMA, CD31, FAP and FSP) per tumor are lower overall in the CD44KO BMT mice as compared

to the WT Red BMT mice but none of the percentages reach statistical significance (Figure 27E).

Figure 25. Example analysis of marker co-expression by InForm Software.

Image was taken using 20x oil lense with CRi attachment and Nuance Software. Initial image was spectrally unmixed to show each image component by wavelength. In this case, fluorescent stains include DAPI, Alexa488 and Alexa594. **(A)** DAPI alone; **(B)** 594+DAPI; **(C)** 488+DAPI; **(D)** 488+594; **(E)** Complete image **(F)** zoomed in section shows 594+ and 488+ stain on a single cell. **(G)** Fluorescent intensity overlay is yellow wherever 594+ and 488+ are overlapped and is further depicted by white arrow. **(H)** Cell segmentation based on nuclear DAPI staining designates every cell with a circle highlighted by a surrounding membrane. **(I)** Individual fluorescent intensity for each cell in imaged are plotted. White box surrounds data points depicting co-localized intensities that were highlighted by white arrowheads.

Figure 25

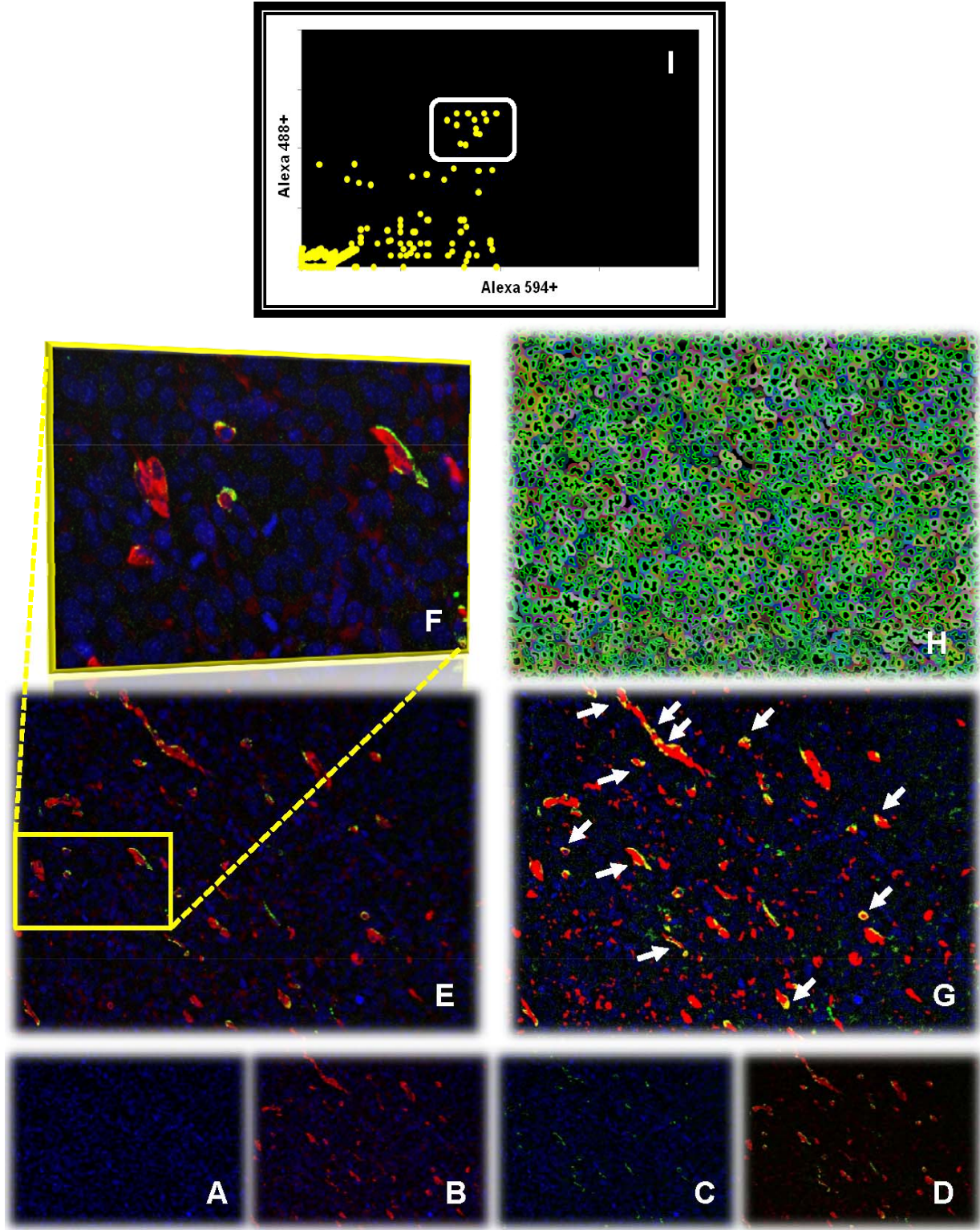


Figure 26. Fluorescent images of EO771 tumors in mice with CD44KO BMT or Red BMT. All images were spectrally unmixed and then subjected to a co-staining algorithm using InForm Software. The yellow color in the images is the enhanced image of the co-stained overlay. For each marker analyzed, there is a co-stain with the host (GFP) and the BMT (β -Gal for CD44KO and RFP for tdTomato). The markers used to assess double positive staining include: **(A)** FAP, **(B)** FSP, **(C)** α -SMA and **(D)** CD31.

Figure 26

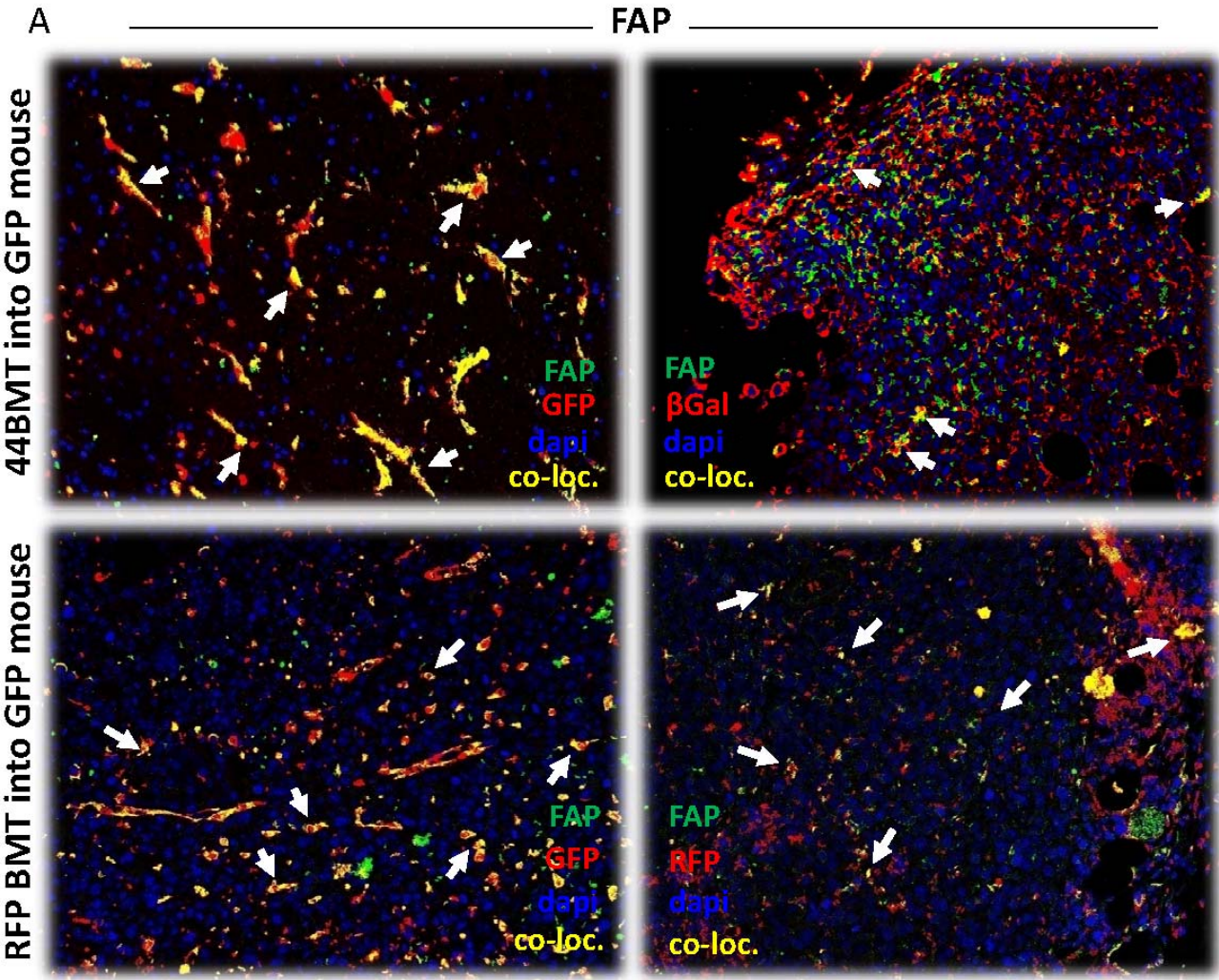


Figure 26 cont.

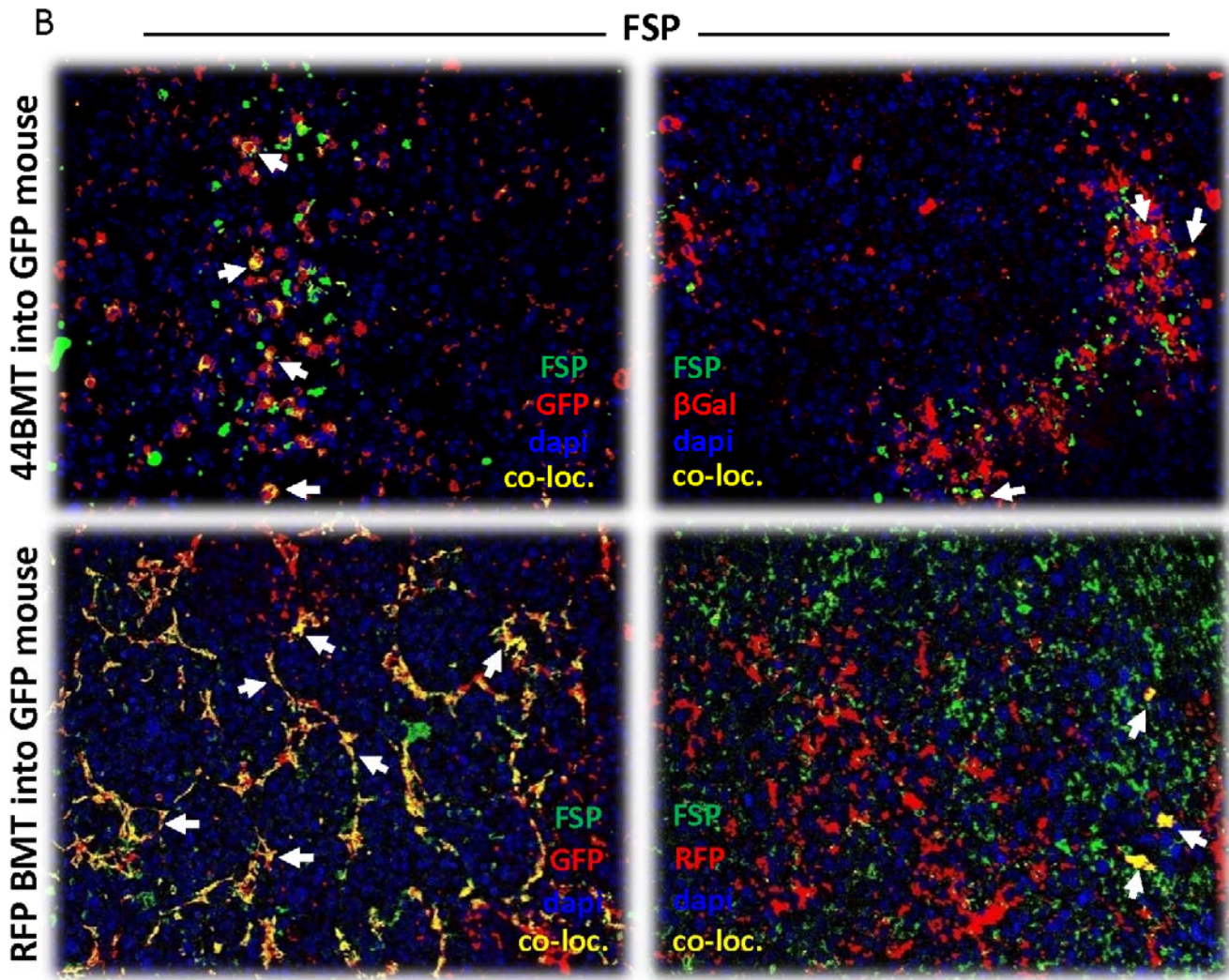


Figure 26 cont.

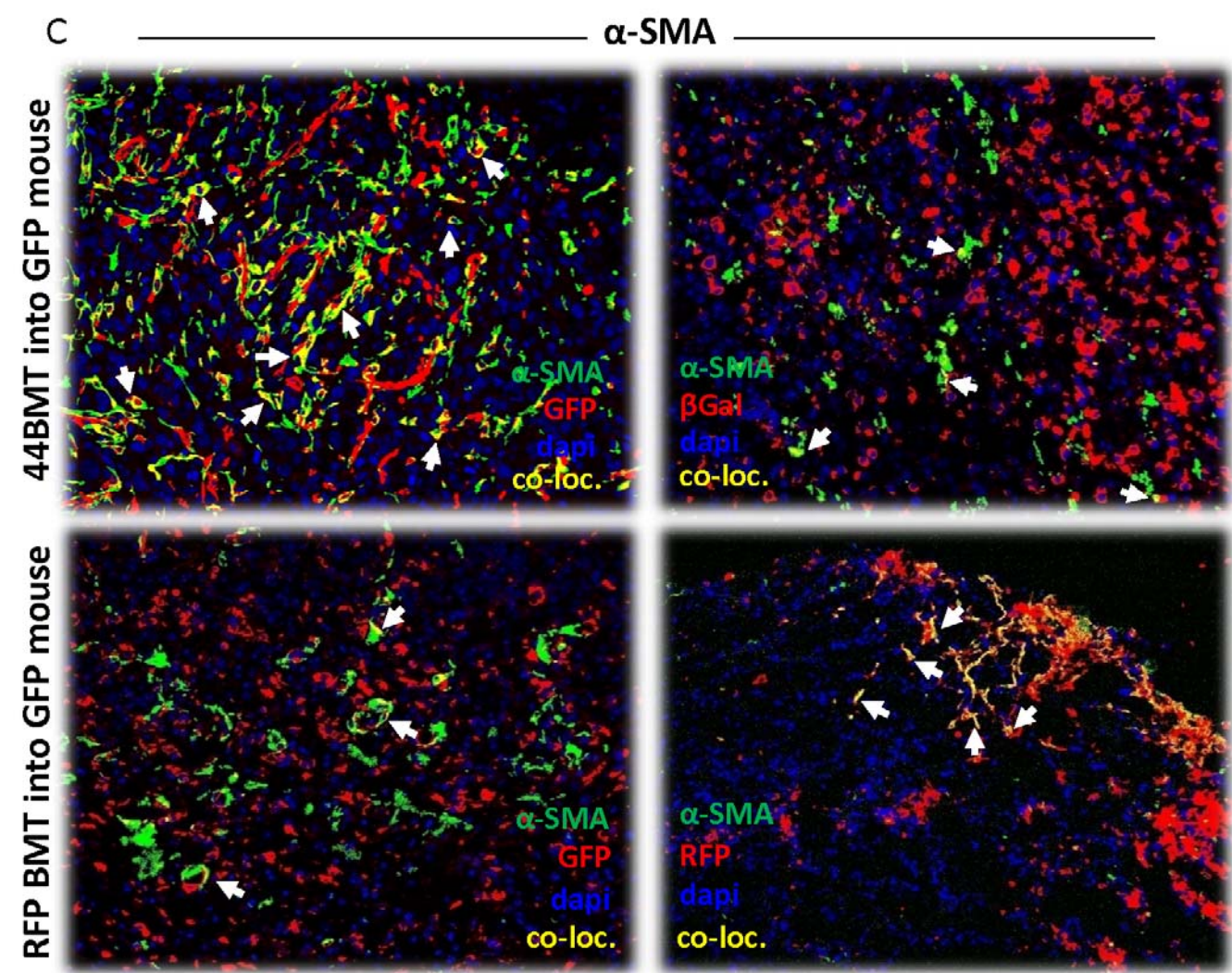


Figure 26 cont.

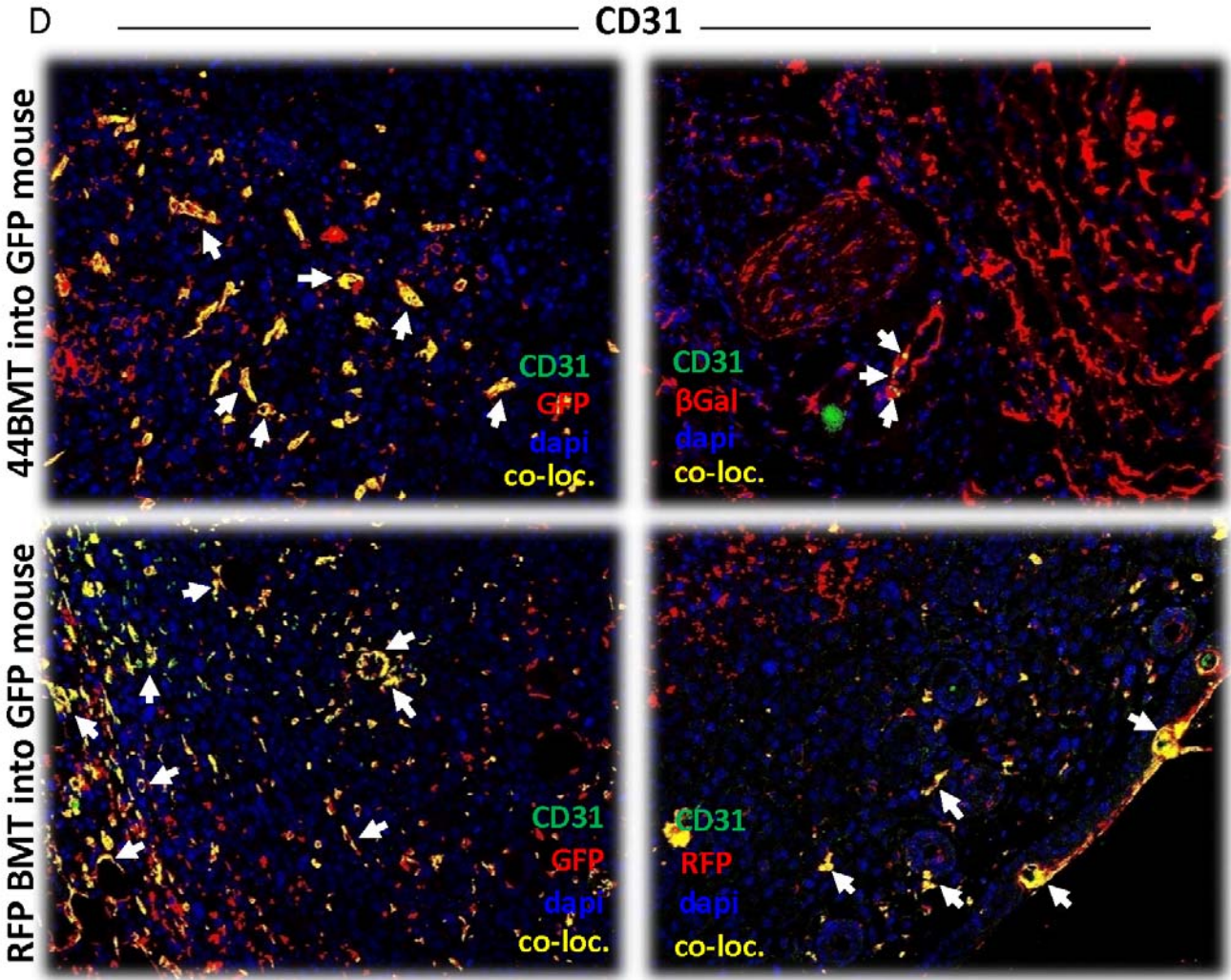


Figure 27. Statistical summary of tumor stroma origin. Percentage of total single stained or double positive (DP) cells per tumor was calculated across 5 tumors and 10 images per tumor. DP is defined as one cell origin marker (GFP+, RFP+ or β -gal+) plus one stroma marker (α -SMA, FSP, FAP or CD31) **(A)** Percentage of DP stained cells within the tumors engrafted in Red BMT recipient mice. There was a trend toward more GFP co-stained cells, however there was only a statistical significance between the CD31 co-stained GFP versus RFP($p<0.001$) **(B)** Percentage of DP stained cells within the tumors engrafted in the CD44KO BMT recipient mice. There was a trend toward higher number of GFP+ co-stained cells. GFP+/FAP+ versus β -gal+/FAP+ was not statistically significant ($p<0.1$) and GFP+/FSP+ versus β -gal+/FSP+ was not statistically significant ($p<0.06$). **(C)** The presence of GFP+/FSP+ co-stained cells was higher in the CD44KO BMT tumors than in the Red BMT tumors ($p<0.01$) **(D)** Neither the difference between β -gal+/FSP+ and RFP+/FSP+ cells nor the difference between β -gal+/FAP+ and RFP+/FAP+ cells reached statistical significance. **(E)** Average percentage of marker expression per image regardless of co-stain shows a trend toward more positive staining for every marker in the Red BMT tumors compared to the CD44KO BMT tumors, however, none reached statistical significance ($p>0.1$).

Figure 27

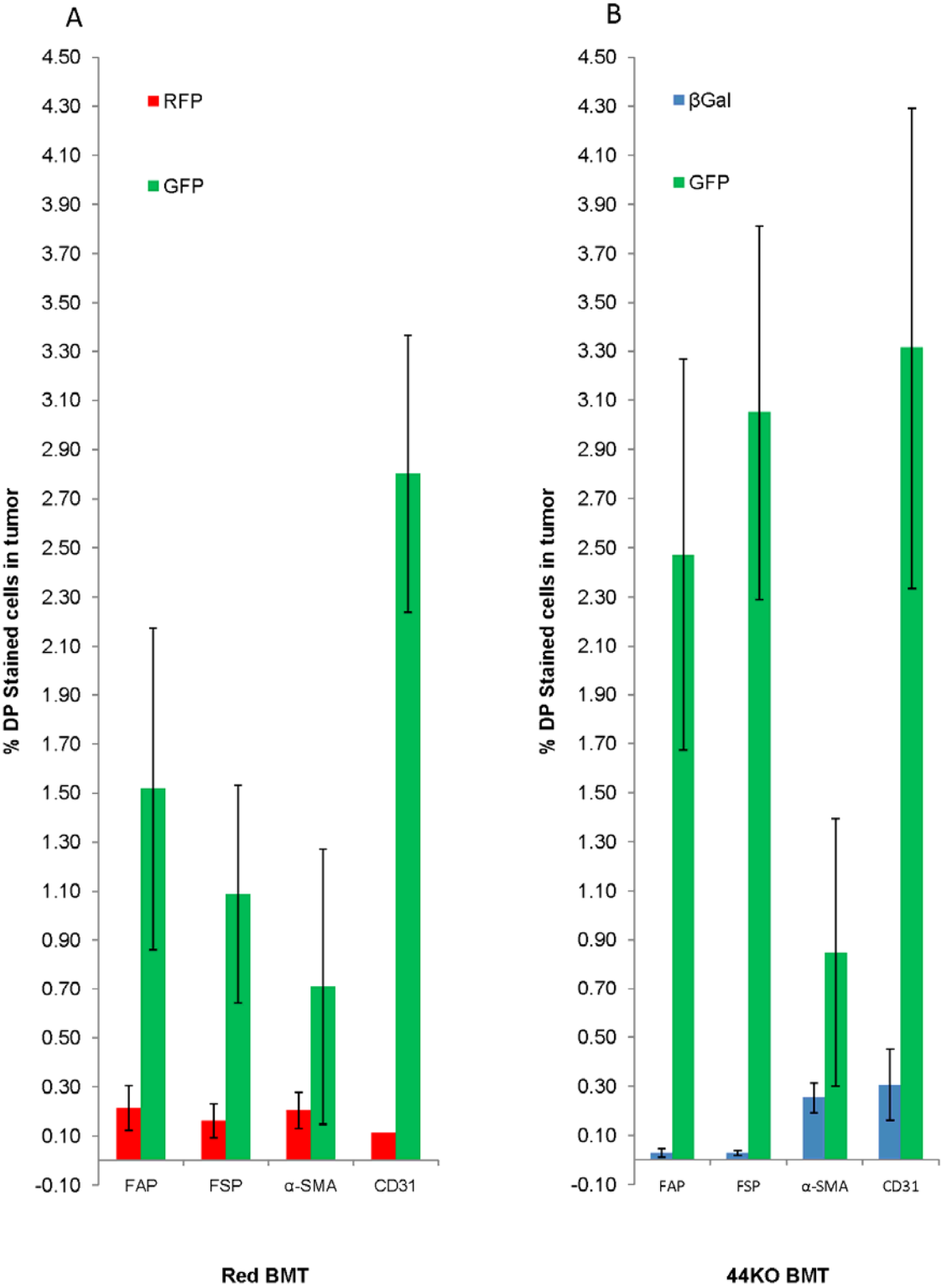
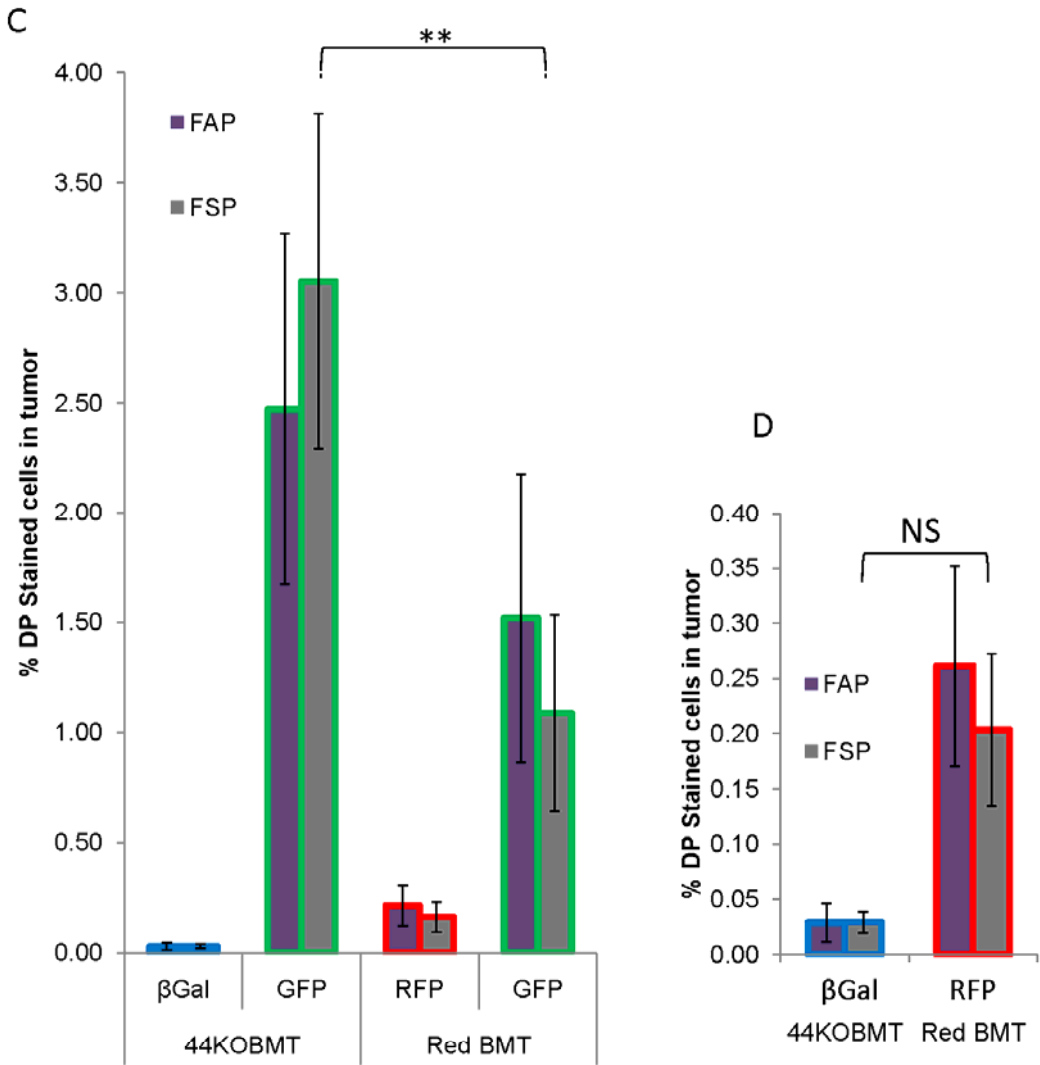


Figure 27 cont.



E

	aSMA			CD31	
	average	stdev		average	stdev
44KOBMT	2.12%	0.765873	44KOBMT	3.94%	1.941533
RedBMT	9.19%	2.215911	RedBMT	13.74%	5.34648

	FAP			FSP	
	average	stdev		average	stdev
44KOBMT	2.50%	0.84962	44KOBMT	2.28%	0.745333
RedBMT	4.47%	1.719278	RedBMT	6.67%	2.928454

4.0 Discussion

4.1 Role of CD44 in MSC tumor tropism

It is well established that MSC have an inherent tropism for sites of inflammation (112, 141, 144), including the tumor microenvironment (91, 110, 120, 145). However, the mechanism of migration has not yet been fully elucidated. In these studies, tumor tropic MSC migration was impeded both *in vitro* and *in vivo* through the inhibition of the cell surface receptor CD44. Several techniques were utilized in order to inhibit MSC migration including stable knockdown of CD44 and two CD44 antagonists: a soluble CD44 receptor (146) and a hyaluronan oligomer (147).

Similar to leukocyte migration, there are numerous factors that have the potential to induce chemotropic MSC migration. Several chemokines and growth factors have been identified to play a role in the migration of MSC towards tumors including CCL2, PDGFb, SDF-1, (68, 70, 115). Once recruited to the tumor microenvironment, the MSC themselves secrete a variety of chemokines to perpetuate the chemoattractive gradient. MSC initially were evaluated for the receptor expression level of respective chemotropic factors secreted by tumor cells. CD44 was ultimately chosen for further study for two reasons; first, because of the discrepancy in receptor expression levels between flow cytometry and western blot data and second, because of the elevated levels of OPN expressed from the highly chemoattractive Skov-3 tumor cells. A categorical data analysis of over 200 clinical papers has shown OPN over-expression to be associated with tumor progression and poor survival among patients in several cancers including lung, breast, prostate and head and neck (148). Furthermore, in triple negative breast cancers that have a large population of mesenchymal-like cells within the tumor, OPN levels are significantly higher than non-triple negative (149). Lastly, OPN has been shown to be chemotactic factor important in the migration of MSC to bone fractures (104).

In the first set of experiments, we sought to inhibit MSC migration *in vitro* through a series of methods using a transwell migration assay. MSC migration toward SCM

was inhibited between 55-80% compared to control MSC using both transient and stable knockdown of CD44 in MSC, or using neutralizing antibody, s44 or oHA. These data are in accord with previously published data that showed the significance of CD44 in wound-induced fibroblast migration (150).

Next, we used the soluble CD44 receptor to inhibit the migration of MSC to bilateral engrafted Skov-3 tumors in SCID mice. Analyzed by bioluminescent imaging, ffLuc-labeled MSC migrated towards rLuc-labeled Skov-3 but in the presence of the soluble CD44 migration was inhibited by 50%.

To further elucidate a mechanism of migratory inhibition, CD44-labeled MSC were analyzed by confocal microscopy in the presence and absence of SCM with and without oHA. Nuclear localization of CD44 increased in MSC under SCM however not in the presence of oHA. In order for nuclear translocation to occur, CD44 must undergo a proteolytic extracellular cleavage followed by a γ -secretase cleavage of the intracellular domain (151-154). We used an MMP 14 inhibitor in combination with SCM to show the inhibition of CD44 cleavage products in MSC. Under those same conditions, MSC migrated 75% less than control MSC.

Nuclear translocation of CD44 has been shown to form a complex with Stat3 and p300 under to modulate Cyclin D and CD44 transcription (98, 152). Therefore, we screened the gene expression of factors involved in cellular migration to ask whether CD44 could influence migration through transcriptional regulation. The transcription factor, Twist was found to be up regulated in MSC under SCM by RT-PCR and Western blot. This protein is typically expressed in mesenchymal-like cells and has been associated with migration, invasion and angiogenesis (125, 126, 155-157). Using our shCD44 MSC, we are able to show a decrease in Twist gene expression similar to the inhibition achieved with s44 or MMP inhibitors compared to naïve MSC under SCM. This decrease in Twist expression is also visible at the protein level between shNeg MSC and shCD44 MSC under SCM. Furthermore, tumor tropic migration can be partially restored in shCD44 MSC with the ectopic

expression of Twist. Finally, we show the association between CD44 and the Twist proximal promoter by ChIP at 24 hours, and a stronger association at 30 minutes following SCM.

MSC migration toward the tumor microenvironment is a double edged sword. Inducing a better migratory response could be beneficial to the therapeutic potential of the MSC as targeted gene therapy delivery vehicle (77, 135, 145, 158, 159). And alternatively, inhibition of naïve MSC migration toward the tumor microenvironment could be beneficial in the reduction of tumor progression by impeding supportive stromal cell accumulation (25, 160). In this regard, the manipulation of CD44 on the surface of MSC may be used to either enhance or inhibit the migration to the tumor microenvironment.

4.2 MSC contribution to the tumor microenvironment through TAF

Tumors acquire their stroma through four different proposed mechanisms: the recruitment of **(1)** local tissue-derived stem cells, **(2)** local tissue derived fibroblasts, **(3)** bone marrow derived stromal cells and **(4)** epithelial to mesenchymal transitioned tumor cells (7, 92, 161, 162). In these experiments, we show the potential for MSC participation as tumor stroma (TAF) through differentiation under long term SCM both *in vitro* and *in vivo*. Moreover, we show the potential for the TAF to promote tumor growth and proliferation within the tumor as compared to tumors without exogenously added MSC.

TAF are a heterogeneous population of cells that have several functions within the tumor microenvironment (28):

- 1)** to maintain a supply of growth factors;
- 2)** to support angiogenesis;
- 3)** to aid in structural remodeling.

To elucidate whether the MSC could contribute to each of these three functions, we analyzed long term (21-31 day) tumor conditioned MSC. *In vitro* we saw an increase in growth factor secretion of IL-6, TGF- β and VEGF in response to SCM. The LT-

MSC showed an increase in pericyte markers including α -SMA and the myofibroblast marker desmin. Immunohistochemical staining for desmin and α -SMA have been correlated with disease-free survival and each individually show a reduced recurrence-free survival compared to tumors with little or no positive staining (163). Increased expression of Tn-c and TSP1 in LT-MSC are remodeling proteins indicative of vascular sprouting modulation (164). Lastly, two proteins involved in active wound repair are FAP and FSP, both of which are increased in the LT-MSC. FAP and FSP are up regulated in activated fibroblasts in granulation tissue of healing wounds and likewise in tumor stroma. The function FSP has been linked to modulation of invasion through facilitating extra-cellular matrix adhesion and degradation (36, 165). FAP expression in the reactive tumor stroma has been shown to be a positive prognostic marker in invasive ductal carcinoma of the breast (166); however others have proposed to target FAP in order to target tumor stroma specifically (167).

In vivo, we admixed MSC and Skov-3 tumor cells in order to support our *in vitro* findings that MSC are capable of TAF differentiation. Three months following tumor engraftment, we sacrificed the SCID mice and paraffin embedded the tumors for immunohistochemical analysis. Individual staining for each of the aforementioned markers showed a marked difference between admixed tumors and tumors alone. Furthermore, these experiments were conducted in xenograft models of both breast (MDA-231) and pancreatic (Panc-1) tumors to show the potential of the MSC to support tumor growth as TAF in other adenocarcinoma models (25). The markers were not co-stained because of the potential of the MSC to differentiate into a variety of TAF. Unpublished data from our lab suggests that the FAP and FSP markers are likely to co-express and the pericyte or myofibroblast markers like α -SMA and desmin are likely to co-express. Just as the MSC is a heterogeneous population of cells, the population of TAF it gives rise to is also a heterogeneous population (168).

Finally, we looked at the tumor growth potential between our admixed MSC/Skov-3 tumors versus the Skov-3 tumors alone and saw a growth advantage at the later stage (day 65-70) of tumor growth following an initial tumor growth retardation in the admixed tumors. Also, to confirm that the stromal enhancement of tumor growth was specifically from the human MSC and not from murine stromal cells within or xenograft model, we conducted an *in vitro* tumor growth assay to measure the proliferation of the tumor cells in the presence of human and murine MSC and fibroblasts. Our results confirmed that the human MSC offered a significant growth advantage that could not be afforded by the murine cells. The proliferation potential offered by the human MSC to the Skov-3 ovarian tumor cells was confirmed to be MSC secreted IL-6. Our lab had previously shown the significance of MSC secreted EGF on the proliferation of estrogen receptor positive breast cancer cells (169, 170) using this same method.

It is important to note the differences between the stromal support offered by the MSC as they differentiate into TAF under various TCM, be it ovarian or breast tumors media. We showed the similarity between stromal markers expressed in xenograft ovarian, breast and pancreatic tumor models. However, we did not attempt to define potential differences in expression pattern or expression level that may result from variations between tumor models. The heterogeneity of the TAF is important to the global participation potential in many wounded environments from ovarian carcinomas to gastrointestinal stromal tumors to sarcomas. TAF have a biological impact on tumor progression through their ability to be matrix-modulating through synthesis or degradation (activated fibroblast), contractile (myofibroblast), angiogenic supportive (pericyte) and sustenance (growth factors) providing cells (171).

4.3 Regulating CD44 expression on MSC impedes differentiation into TAF

After establishing the importance of CD44 to the tumor tropic migratory capacity of MSC, we sought to investigate the role of CD44 in the trans-differentiation potential of MSC into TAF. We used our stable CD44 knockdown cell line of human MSC to

analyze their capacity to support angiogenesis *in vitro*. shCD44MSC were unable to support tube formation compared to naïve or shNeg MSC control cells. MSC express pro-angiogenic growth factors that can induce HUVEC tube formation *in vitro* including VEGF A, VEGF C (172), EGF (173), IL-8 (174) and OPN (175). When we compared the growth factor gene expression in tumor conditioned shCD44MSC versus shNeg MSC controls, we observed a decrease in expression of VEGF C, EGF and IL-8. Interestingly, this gene expression change could be rectified by over expression of Twist in the shCD44MSC. Twist expression within endothelial cells is known to be important for the tube formation (157), herein we provide evidence that ectopic Twist expression can enhance the growth factor secretion profiles of shCD44MSC but we have not yet provided evidence that ectopic expression of Twist in shCD44MSC can fully rescue the tube formation capability of the MSC.

After observing growth factor expression differences between shCD44MSC and control shNeg MSC, we looked at the long term differentiation potential of the shCD44MSC under SCM. The shCD44MSC were deficient in the expression of α -SMA, PDGFR- β , FAP, FSP and TSP1 compared the shNeg MSC. Interestingly, the expression of vimentin was similar between the two when looking at the full length product; however there was a clear difference in the cleavage products. Cleavage of vimentin and other intermediate filament proteins like desmin are important in the cytoskeletal remodeling of cells during injury because they aid in cell fusion and cytoskeletal rearrangement and may elucidate an important deficiency of the shCD44MSC compared to the WT counterpart (176, 177).

To further elucidate the role of CD44 expression on MSC we utilized a transgenic CD44 knockout mouse. The murine CD44KO MSC also showed a decreased migratory propensity *in vitro*, and showed a decrease in Twist, FAP and a slight decrease in α -SMA and FSP expression. One interesting similarity between the murine CD44KO MSC and the human shCD44MSC was the expression of PDGFR- β which was reduced, but also appeared in a single band as opposed to the double

band pattern seen in naïve MSC. CD44 and PDGFR β have been shown to form a complex in which hyaluronan activated CD44 inhibited PDGFR β tyrosine kinase activity in dermal fibroblasts (178). This interaction suggests an important cross talk that takes place between CD44 and other cell surface receptors on the MSC that is not yet elucidated.

The last set of experiments conducted were a series of *in vivo* tumor models to study the role of CD44 deficient MSC or stromal cells in the tumor microenvironment. First, EO771 murine breast tumors developed SC in either CD44KO mice or in their WT counterpart (a transgenic tdTomato labeled mouse). Daily caliper measurements revealed a growth advantage in the WT mice compared to the CD44KO mice. Furthermore, the CD44KO mice had a significant survival advantage compared to the WT mice on day 30, when all mice were sacrificed due to tumor burden. Upon immunohistochemical analysis, tumors from WT mice had more dense tumors by H&E staining compared to tumors in the CD44KO mice. Of note, EO771 tumors are rapidly growing tumor with large regions of tumoral hemorrhaging that make overall analysis between stromal regions of the tumor difficult to analyze because of the large amount of Eosin stained red blood cells that mask the stained stromal cells. In the stroma-rich gastrointestinal stromal tumors, the CD44 cleavage activity positively correlated both with mitotic index and negatively correlated with disease free survival (179). These correlations support both the growth advantage and the survival advantage of the CD44KO mice in our breast cancer model.

The next *in vivo* experiment was conducted in SCID mice using a 4T1 murine breast cancer model with and without 1:1 ratio of admixed CD44KO MSC or WT MSC. Analysis of tumor sections revealed that CD44KO MSC admixed tumors had lower expression of α -SMA, FAP, FSP and CD31 staining compared to WT MSC admixed tumors. These data were consistent with the decrease in TAF marker expression on *in vitro* tumor conditioned CD44KOMSC.

When tumor size was evaluated in CD44KO MSC admixed 4T1 tumors versus WT MSC admixed 4T1 tumors versus 4T1 tumors, tumors were engrafted contralateral in the inguinal fat of the mice. The admixed tumors were placed opposite to the 4T1 tumors alone. In group 1, the CD44KO MSC admixed tumors were significantly smaller than its contralateral 4T1 tumor. There was not a significant difference between WT MSC admixed tumors and the respective contralateral 4T1 tumors. These data are reminiscent of the possibility of systemic instigation facilitating or competing with the growth of the opposing tumor. This idea has been previously reported in the growth potential of secondary and/or metastatic lesions occurring from OPN over-expression (180). We looked at human levels of OPN in shCD44MSC and there was a decrease in expression level between shNeg MSC, however, under SCM, the difference was ablated. Future studies will address the murine expressed growth factors systemically or individually in the MSC and the 4T1. Lastly, there was a significant discrepancy in F4/80+ macrophage infiltration between the CD44KO MSC admixed tumors and the WT admixed tumors and the 4T1 tumors alone. This discrepancy may explain the tumor size differences if the tumor infiltrating macrophages are tumor supportive and secrete pro-growth and pro-angiogenic factors including VEGF, bFGF, TNF α , MMPs, IL-6 and IL-8 (181-183).

Our final *in vivo* experiment utilized an allogeneic bone marrow transplantation to investigate the CD44KO bone marrow contribution to the tumor microenvironment. Consistent with our previous experiments, the tumor stroma derived from the CD44KO bone marrow was less than from the WT Red bone marrow, however no statistical significance was reached. Unlike the aforementioned studies, the tumor stroma contribution from the GFP+ local host tissues could be distinguished from the transplanted β -gal+ CD44KO bone marrow or the RFP+ Red bone marrow.

The incorporation of FAP+, FSP+, α -SMA+ and CD31+ components within the tumor microenvironment were analyzed by two separate methods. The first method provided a quantitative analysis of host (GFP+) stromal cells versus bone marrow

derived stromal cells (RFP+ or β -gal+) that co-stained with FAP+, FSP+, α -SMA or CD31 within the tumor. These data suggest that the bone marrow contribution to the tumor microenvironment is less than 1%. Additionally, we observed CD44KO bone marrow derived cells provide less FAP+ and FSP+ stromal components compared to WT Red (RFP+) bone marrow derived cells. Reports in the literature suggest that bone marrow derived cells found within the tumor microenvironment greatly vary and are dependent on tumor stage (184-186).

Using co-staining as our method of analysis, we observed a greater infiltration of TAF-stromal cells originating from the GFP+ host as opposed to RFP+ or CD44KO+ bone marrow in both the WT control Red BMT mice and the CD44KO BMT mice. In this model, there was a greater presence of host (GFP+) derived FSP+ cells within the tumors in CD44KO BMT mice compared to WT Red BMT mice. This finding was contradictory to our previous experiment showing that overall FSP expression was decreased in CD44KO admixed tumors. This contradiction may be due to the non-physiological ratio of admixed tumor:MSC ratio that has often been a source of discrepancy within the field (8, 187). Furthermore, the EO771 murine breast model utilized for the syngenic BMT experiments in immunocompetent mice differs from the previous 4T1 tumor admixing model in the immunocompromised mouse experiments and may be a source of discrepancy between the two results.

The second method of analysis measured only the overall incorporation of FAP+, FSP+, α -SMA+ or CD31+ within the tumor regardless of the origin. Under these parameters, the tumors grown in the CD44KO BMT had less overall incorporation of all four markers as compared to tumors in the WT Red BMT control mice. These findings were in agreement with our previous results in the xenograft 4T1 tumor model.

In our model, we propose that the recruitment of CD44KO bone marrow derived stroma to the tumor microenvironment is diminished compared to recruitment of WT bone marrow derived stroma. We quantify the tumor stroma components by FAP+

and FSP+ markers associated with pathological disease and by α -SMA+ and CD31+ markers associated with neo-angiogenesis. We provide evidence that CD44 expression is significant to the bone marrow derived stromal cell population that contributes to the tumor microenvironment. Several studies have established CD44 as a modulator of invasiveness, chemoprotection and stemness in the context of cancer cells (99, 124, 188). Other investigators have shown the significance of CD44 expression in leukocyte populations. Khan and colleagues showed that CD44 expression is important for leukocyte emigration, but not for subsequent migration within the tissues during chronic inflammation (189). And, Rajasagi and colleagues have shown the importance of CD44 in the repopulation of the T cell population within the thymus following myeloablation/bone marrow reconstitution (190). Ultimately, our tumor stroma markers account for a fraction of the potential differences within the CD44KO bone marrow stromal cells. There are several other markers including chemokines (191), growth factors such as TGF- β (150) and proteases that are potentially altered by the deficiency in CD44 signaling in the integration of tumor stroma.

When tumors recruit the stromal elements of the microenvironment such as the vascular and (myo) fibroblastic components, the majority of the cells are of local origin derived from host tissue as opposed to bone marrow derived cells. However, when the demand for stroma exceeds the local environment's capacity to deliver, the stroma will be systemically recruited from the bone marrow. If the bone marrow stroma is CD44 deficient, the incorporation of the bone marrow contributed tumor stroma will be negligible. However, the local WT derived stromal cells can supersede the CD44 deficient stroma in order to maintain a stroma-rich tumor microenvironment.

5.0 References

- 1. American Cancer Society 2009. Cancer facts & figures 2009.**
- 2. Hanahan, D. and R.A. Weinberg 2000. The hallmarks of cancer. Cell. 100, 57-70.**
- 3. Kidd, S., E. Spaeth, A. Klopp, M. Andreeff, B. Hall and F.C. Marini 2008. The (in) auspicious role of mesenchymal stromal cells in cancer: Be it friend or foe. Cytotherapy. 10, 657-667.**
- 4. Radisky, E. S. and D.C. Radisky 2007. Stromal induction of breast cancer: Inflammation and invasion. Rev. Endocr. Metab. Disord. 8, 279-287.**
- 5. Bauer, M., G. Su, C. Casper, R. He, W. Rehrauer and A. Friedl 2010. Heterogeneity of gene expression in stromal fibroblasts of human breast carcinomas and normal breast. Oncogene. 29, 1732-1740.**
- 6. Gonda, T. A., A. Varro, T.C. Wang and B. Tycko 2010. Molecular biology of cancer-associated fibroblasts: Can these cells be targeted in anti-cancer therapy? Semin. Cell Dev. Biol. 21, 2-10.**
- 7. Udagawa, T., M. Puder, M. Wood, B.C. Schaefer and R.J. D'Amato 2006. Analysis of tumor-associated stromal cells using SCID GFP transgenic mice: Contribution of local and bone marrow-derived host cells. FASEB J. 20, 95-102.**
- 8. Karnoub, A. E., A.B. Dash, A.P. Vo, A. Sullivan, M.W. Brooks, G.W. Bell, A.L. Richardson, K. Polyak, R. Tubo and R.A. Weinberg 2007. Mesenchymal stem cells within tumour stroma promote breast cancer metastasis. Nature. 449, 557-563.**

9. Studeny, M., F.C. Marini, R.E. Champlin, C. Zompetta, I.J. Fidler and M. Andreeff 2002. Bone marrow-derived mesenchymal stem cells as vehicles for interferon-beta delivery into tumors. *Cancer Res.* 62, 3603-3608.
10. Bababeygy, S. R., S.H. Cheshier, L.C. Hou, D.M. Higgins, I.L. Weissman and V.C. Tse 2008. Hematopoietic stem cell-derived pericytic cells in brain tumor angio-architecture. *Stem Cells Dev.* 17, 11-18.
11. Reddy, K., Z. Zhou, K. Schadler, S.F. Jia and E.S. Kleinerman 2008. Bone marrow subsets differentiate into endothelial cells and pericytes contributing to ewing's tumor vessels. *Mol. Cancer. Res.* 6, 929-936.
12. Gothert, J. R., S.E. Gustin, J.A. van Eekelen, U. Schmidt, M.A. Hall, S.M. Jane, A.R. Green, B. Gottgens, D.J. Izon and C.G. Begley 2004. Genetically tagging endothelial cells in vivo: Bone marrow-derived cells do not contribute to tumor endothelium. *Blood.* 104, 1769-1777.
13. Li, H., X. Fan, R.C. Kovi, Y. Jo, B. Moquin, R. Konz, C. Stoicov, E. Kurt-Jones, S.R. Grossman, S. Lyle, A.B. Rogers, M. Montrose and J. Houghton 2007. Spontaneous expression of embryonic factors and p53 point mutations in aged mesenchymal stem cells: A model of age-related tumorigenesis in mice. *Cancer Res.* 67, 10889-10898.
14. Guest, I., Z. Ilic, M. Jun, D. Grant, G. Glinsky and S. Sell 2010. Direct and indirect contribution of bone marrow-derived cells to cancer. *Int. J. Cancer.* 126, 2308-2318.
15. Raman, D., P.J. Baugher, Y.M. Thu and A. Richmond 2007. Role of chemokines in tumor growth. *Cancer Lett.* 256, 137-165.
16. Aggarwal, S. and M.F. Pittenger 2005. Human mesenchymal stem cells modulate allogeneic immune cell responses. *Blood.* 105, 1815-1822.

17. Balkwill, F. and A. Mantovani 2001. Inflammation and cancer: Back to virchow? *Lancet*. 357, 539-545.
18. Crowther, M., N.J. Brown, E.T. Bishop and C.E. Lewis 2001. Microenvironmental influence on macrophage regulation of angiogenesis in wounds and malignant tumors. *J. Leukocyte Biol.* 70, 478-490.
19. El-Shinawi, M., S.F. Abdelwahab, M. Sobhy, M.A. Nouh, B.F. Sloane and M.M. Mohamed 2010. Capturing and characterizing immune cells from breast tumor microenvironment: An innovative surgical approach. *Ann. Surg. Oncol.*, 1-8.
20. Allavena, P., A. Sica, G. Solinas, C. Porta and A. Mantovani 2008. The inflammatory micro-environment in tumor progression: The role of tumor-associated macrophages. *Crit. Rev. Oncol. Hematol.* 66, 1-9.
21. Bunt, S. K., L. Yang, P. Sinha, V.K. Clements, J. Leips and S. Ostrand-Rosenberg 2007. Reduced inflammation in the tumor microenvironment delays the accumulation of myeloid-derived suppressor cells and limits tumor progression. *Cancer Res.* 67, 10019-10026.
22. Hinz, B., S.H. Phan, V.J. Thannickal, A. Galli, M.-. Bochaton-Piallat and G. Gabbiani 2007. The myofibroblast: One function, multiple origins. *Am. J. Pathol.* 170, 1807-1816.
23. Nozawa, H., C. Chiu and D. Hanahan 2006. Infiltrating neutrophils mediate the initial angiogenic switch in a mouse model of multistage carcinogenesis. *Proc. Natl. Acad. Sci. U. S. A.* 103, 12493-12498.
24. Zumsteg, A. and G. Christofori 2009. Corrupt policemen: Inflammatory cells promote tumor angiogenesis. *Curr. Opin. Oncol.* 21, 60-70.
25. Spaeth, E. L., J.L. Dembinski, A.K. Sasser, K. Watson, A. Klopp, B. Hall, M. Andreeff and F. Marini 2009. Mesenchymal stem cell transition to tumor-

associated fibroblasts contributes to fibrovascular network expansion and tumor progression. PLoS ONE. 4, e4992.

- 26. Bhowmick, N. A., E.G. Neilson and H.L. Moses 2004. Stromal fibroblasts in cancer initiation and progression. Nature. 432, 332-337.**
- 27. Desmouliere, A., M. Redard, I. Darby and G. Gabbiani 1995. Apoptosis mediates the decrease in cellularity during the transition between granulation tissue and scar. Am. J. Pathol. 146, 56-66.**
- 28. Sugimoto, H., T.M. Mundel, M.W. Kieran and R. Kalluri 2006. Identification of fibroblast heterogeneity in the tumor microenvironment. Cancer. Biol. Ther. 5, 1640-1646.**
- 29. Rettig, W. J., S.L. Su, S.R. Fortunato, M.J. Scanlan, B.K. Raj, P. Garin-Chesa, J.H. Healey and L.J. Old 1994. Fibroblast activation protein: Purification, epitope mapping and induction by growth factors. Int. J. Cancer. 58, 385-392.**
- 30. Scanlan, M. J., B.K. Raj, B. Calvo, P. Garin-Chesa, M.P. Sanz-Moncasi, J.H. Healey, L.J. Old and W.J. Rettig 1994. Molecular cloning of fibroblast activation protein alpha, a member of the serine protease family selectively expressed in stromal fibroblasts of epithelial cancers. Proc. Natl. Acad. Sci. U. S. A. 91, 5657-5661.**
- 31. Bauer, S., M.C. Jendro, A. Wadle, S. Kleber, F. Stenner, R. Dinser, A. Reich, E. Faccin, S. Godde, H. Dinges, U. Muller-Ladner and C. Renner 2006. Fibroblast activation protein is expressed by rheumatoid myofibroblast-like synoviocytes. Arthritis Res. Ther. 8, R171.**
- 32. Koperek, O., C. Scheuba, C. Puri, P. Birner, C. Haslinger, W. Rettig, B. Niederle, K. Kaserer and P. Garin Chesa 2007. Molecular characterization**

of the desmoplastic tumor stroma in medullary thyroid carcinoma. *Int. J. Oncol.* 31, 59-67.

33. Welt, S., C.R. Divgi, A.M. Scott, P. Garin-Chesa, R.D. Finn, M. Graham, E.A. Carswell, A. Cohen, S.M. Larson and L.J. Old 1994. Antibody targeting in metastatic colon cancer: A phase I study of monoclonal antibody F19 against a cell-surface protein of reactive tumor stromal fibroblasts. *J. Clin. Oncol.* 12, 1193-1203.
34. Liao, D., Y. Luo, D. Markowitz, R. Xiang and R.A. Reisfeld 2009. Cancer associated fibroblasts promote tumor growth and metastasis by modulating the tumor immune microenvironment in a 4T1 murine breast cancer model. *PLoS ONE.* 4.
35. Helfman, D. M., E.J. Kim, E. Lukanidin and M. Grigorian 2005. The metastasis associated protein S100A4: Role in tumour progression and metastasis. *Br. J. Cancer.* 92, 1955-1958.
36. Grum-Schwensen, B., J. Klingelhöfer, M. Grigorian, K. Almholt, B.S. Nielsen, E. Lukanidin and N. Ambartsumian 2010. Lung metastasis fails in MMTV-PyMT oncomice lacking S100A4 due to a T-cell deficiency in primary tumors. *Cancer Res.* 70, 936-947.
37. Schneider, M., J.L. Hansen and S.P. Sheikh 2008. S100A4: A common mediator of epithelial-mesenchymal transition, fibrosis and regeneration in diseases? *J. Mol. Med.* 86, 507-522.
38. Zhang, H. -. and S.H. Phan 1999. Inhibition of myofibroblast apoptosis by transforming growth factor β_1 . *Am. J. Resp. Cell Mol. Biol.* 21, 658-665.
39. Hawinkels, L. J., H.W. Verspaget, J.J. van der Reijden, J.M. van der Zon, J.H. Verheijen, D.W. Hommes, C.B. Lamers and C.F. Sier 2009. Active

TGF-beta1 correlates with myofibroblasts and malignancy in the colorectal adenoma-carcinoma sequence. Cancer. Sci. 100, 663-670.

- 40. Fidler, I. J., S. Yano, R.D. Zhang, T. Fujimaki and C.D. Bucana 2002. The seed and soil hypothesis: Vascularisation and brain metastases. Lancet Oncol. 3, 53-57.**
- 41. Carpini, J. D., A.K. Karam and L. Montgomery 2010. Vascular endothelial growth factor and its relationship to the prognosis and treatment of breast, ovarian, and cervical cancer. Angiogenesis. 13, 43-58.**
- 42. Bose, D., F. Meric-Bernstam, W. Hofstetter, D.A. Reardon, K.T. Flaherty and L.M. Ellis 2010. Vascular endothelial growth factor targeted therapy in the perioperative setting: Implications for patient care. Lancet Oncol. 11, 373-382.**
- 43. Gao, D., D. Nolan, K. McDonnell, L. Vahdat, R. Benezra, N. Altorki and V. Mittal 2009. Bone marrow-derived endothelial progenitor cells contribute to the angiogenic switch in tumor growth and metastatic progression. Biochim. Biophys. Acta.**
- 44. Calzi, S. L., M.B. Neu, L.C. Shaw, J.L. Kielczewski, N.I. Moldovan and M.B. Grant 2010. EPCs and pathological angiogenesis: When good cells go bad. Microvasc. Res. 79, 207-216.**
- 45. Dome, B., J. Timar, A. Ladanyi, S. Paku, F. Renyi-Vamos, W. Klepetko, G. Lang, P. Dome, K. Bogos and J. Tovari 2009. Circulating endothelial cells, bone marrow-derived endothelial progenitor cells and proangiogenic hematopoietic cells in cancer: From biology to therapy. Crit. Rev. Oncol. Hematol. 69, 108-124.**
- 46. Papetti, M. and I.M. Herman 2002. Mechanisms of normal and tumor-derived angiogenesis. Am. J. Physiol. Cell Physiol. 282.**

47. Pietras, K., K. Rubin, T. Sjöblom, E. Buchdunger, M. Sjöquist, C.-. Heldin and A. Östman 2002. Inhibition of PDGF receptor signaling in tumor stroma enhances antitumor effect of chemotherapy. *Cancer Res.* 62, 5476-5484.
48. Crawford, Y., I. Kasman, L. Yu, C. Zhong, X. Wu, Z. Modrusan, J. Kaminker and N. Ferrara 2009. PDGF-C mediates the angiogenic and tumorigenic properties of fibroblasts associated with tumors refractory to anti-VEGF treatment. *Cancer Cell.* 15, 21-34.
49. Muguruma, Y., T. Yahata, H. Miyatake, T. Sato, T. Uno, J. Itoh, S. Kato, M. Ito, T. Hotta and K. Ando 2006. Reconstitution of the functional human hematopoietic microenvironment derived from human mesenchymal stem cells in the murine bone marrow compartment. *Blood.* 107, 1878-1887.
50. Hall, A. P. 2006. Review of the pericyte during angiogenesis and its role in cancer and diabetic retinopathy. *Toxicol. Pathol.* 34, 763-775.
51. Phinney, D. G. and D.J. Prockop 2007. Concise review: Mesenchymal stem/multipotent stromal cells: The state of transdifferentiation and modes of tissue repair - current views. *Stem Cells.* 25, 2896-2902.
52. Reger, R. L., A. H. Tucker and M. R. Wolfe 2008. Differentiation and characterization of human MSCs. 93-107.
53. Martin, P. and S.J. Leibovich 2005. Inflammatory cells during wound repair: The good, the bad and the ugly. *Trends Cell Biol.* 15, 599-607.
54. Castro-Malaspina, H., W. Ebell and S. Wang 1984. Human bone marrow fibroblast colony-forming units (CFU-F). *Prog. Clin. Biol. Res.* 154, 209-236.

55. da Silva Meirelles, L., P.C. Chagastelles and N.B. Nardi 2006. Mesenchymal stem cells reside in virtually all post-natal organs and tissues. *J. Cell. Sci.* 119, 2204-2213.
56. Gronthos, S., M. Mankani, J. Brahimi, P.G. Robey and S. Shi 2000. Postnatal human dental pulp stem cells (DPSCs) in vitro and in vivo. *Proc. Natl. Acad. Sci. U. S. A.* 97, 13625-13630.
57. Zuk, P. A., M. Zhu, H. Mizuno, J. Huang, J.W. Futrell, A.J. Katz, P. Benhaim, H.P. Lorenz and M.H. Hedrick 2001. Multilineage cells from human adipose tissue: Implications for cell-based therapies. *Tissue Eng.* 7, 211-228.
58. Erices, A., P. Conget and J.J. Minguell 2000. Mesenchymal progenitor cells in human umbilical cord blood. *Br. J. Haematol.* 109, 235-242.
59. Williams, J. T., S.S. Southerland, J. Souza, A.F. Calcutt and R.G. Cartledge 1999. Cells isolated from adult human skeletal muscle capable of differentiating into multiple mesodermal phenotypes. *Am. Surg.* 65, 22-26.
60. Spaeth, E., A. Klopp, J. Dembinski, M. Andreeff and F. Marini 2008. Inflammation and tumor microenvironments: Defining the migratory itinerary of mesenchymal stem cells. *Gene Ther.*
61. Mahmood, A., D. Lu, M. Lu and M. Chopp 2003. Treatment of traumatic brain injury in adult rats with intravenous administration of human bone marrow stromal cells. *Neurosurgery.* 53, 697-702; discussion 702-3.
62. Wu, G. D., J.A. Nolta, Y.S. Jin, M.L. Barr, H. Yu, V.A. Starnes and D.V. Cramer 2003. Migration of mesenchymal stem cells to heart allografts during chronic rejection. *Transplantation.* 75, 679-685.

63. Chen, J., Y. Li, L. Wang, Z. Zhang, D. Lu, M. Lu and M. Chopp 2001. Therapeutic benefit of intravenous administration of bone marrow stromal cells after cerebral ischemia in rats. *Stroke*. 32, 1005-1011.
64. Barbash, I. M., P. Chouraqui, J. Baron, M.S. Feinberg, S. Etzion, A. Tessone, L. Miller, E. Guetta, D. Zipori, L.H. Kedes, R.A. Kloner and J. Leor 2003. Systemic delivery of bone marrow-derived mesenchymal stem cells to the infarcted myocardium: Feasibility, cell migration, and body distribution. *Circulation*. 108, 863-868.
65. Ortiz, L. A., F. Gambelli, C. McBride, D. Gaupp, M. Baddoo, N. Kaminski and D.G. Phinney 2003. Mesenchymal stem cell engraftment in lung is enhanced in response to bleomycin exposure and ameliorates its fibrotic effects. *Proc. Natl. Acad. Sci. U. S. A.* 100, 8407-8411.
66. Kidd, S., E. Spaeth, J.L. Dembinski, M. Dietrich, K. Watson, A. Klopp, L. Battula, M. Weil, M. Andreeff and F.C. Marini 2009. Direct evidence of mesenchymal stem cell tropism for tumor and wounding microenvironments using in vivo bioluminescence imaging. *Stem Cells*.
67. Dvorak, H. F. 1986. Tumors: Wounds that do not heal. similarities between tumor stroma generation and wound healing. *N. Engl. J. Med.* 315, 1650-1659.
68. Gao, H., W. Priebe, J. Glod and D. Banerjee 2009. Activation of signal transducers and activators of transcription 3 and focal adhesion kinase by stromal cell-derived factor 1 is required for migration of human mesenchymal stem cells in response to tumor cell-conditioned medium. *Stem Cells*. 27, 857-865.
69. Ringe, J., S. Strassburg, K. Neumann, M. Endres, M. Notter, G.-. Burmester, C. Kaps and M. Sittinger 2007. Towards in situ tissue repair: Human mesenchymal stem cells express chemokine receptors CXCR1,

CXCR2 and CCR2, and migrate upon stimulation with CXCL8 but not CCL2. J. Cell. Biochem. 101, 135-146.

- 70. Dwyer, R. M., S.M. Potter-Beirne, K.A. Harrington, A.J. Lowery, E. Hennessy, J.M. Murphy, F.P. Barry, T. O'Brien and M.J. Kerin 2007. Monocyte chemotactic protein-1 secreted by primary breast tumors stimulates migration of mesenchymal stem cells. Clin. Cancer Res. 13, 5020-5027.**
- 71. Ries, C., V. Egea, M. Karow, H. Kolb, M. Jochum and P. Neth 2007. MMP-2, MT1-MMP, and TIMP-2 are essential for the invasive capacity of human mesenchymal stem cells: Differential regulation by inflammatory cytokines. Blood.**
- 72. Lopez Ponte, A., E. Marais, N. Gallay, A. Langonne, B. Delorme, O. Herault, P. Charbord and J. Domenech 2007. The in vitro migration capacity of human bone marrow mesenchymal stem cells: Comparison of chemokine and growth factor chemotactic activities. Stem Cells.**
- 73. Li, Y., X. Yu, S. Lin, X. Li, S. Zhang and Y.H. Song 2007. Insulin-like growth factor 1 enhances the migratory capacity of mesenchymal stem cells. Biochem. Biophys. Res. Commun. 356, 780-784.**
- 74. Thibault, M. M., C.D. Hoemann and M.D. Buschmann 2007. Fibronectin, vitronectin, and collagen I induce chemotaxis and haptotaxis of human and rabbit mesenchymal stem cells in a standardized transmembrane assay. Stem Cells Dev. 16, 489-502.**
- 75. Tomchuck, S. L., K.J. Zwezdaryk, S.B. Coffelt, R.S. Waterman, E.S. Danka and A.B. Scandurro 2007. Toll-like receptors on human mesenchymal stem cells drive their migration and immunomodulating responses. Stem Cells.**

76. Klopp, A. H., E.L. Spaeth, J.L. Dembinski, W.A. Woodward, A. Munshi, R.E. Meyn, J.D. Cox, M. Andreeff and F.C. Marini 2007. Tumor irradiation increases the recruitment of circulating mesenchymal stem cells into the tumor microenvironment. *Cancer Res.* 67, 11687-11695.
77. Kim, D. -, J.H. Kim, J. Kwon Lee, S.J. Choi, J.-. Kim, S.-. Jeun, W. Oh, Y.S. Yang and J.W. Chang 2009. Overexpression of CXC chemokine receptors is required for the superior glioma-tracking property of umbilical cord blood-derived mesenchymal stem cells. *Stem Cells Dev.* 18, 511-519.
78. Xu, F., J. Shi, B. Yu, W. Ni, X. Wu and Z. Gu 2010. Chemokines mediate mesenchymal stem cell migration toward gliomas in vitro. *Oncol. Rep.* 23, 1561-1567.
79. Tondreau, T., N. Meuleman, B. Stamatopoulos, C. De Bruyn, A. Delforge, M. Dejeneffe, P. Martiat, D. Bron and L. Lagneaux 2009. In vitro study of matrix metalloproteinase/tissue inhibitor of metalloproteinase production by mesenchymal stromal cells in response to inflammatory cytokines: The role of their migration in injured tissues. *Cytotherapy.* 11, 559-569.
80. Maestroni, G. J., E. Hertens and P. Galli 1999. Factor(s) from nonmacrophage bone marrow stromal cells inhibit lewis lung carcinoma and B16 melanoma growth in mice. *Cell Mol. Life Sci.* 55, 663-667.
81. Ohlsson, L. B., L. Varas, C. Kjellman, K. Edvardsen and M. Lindvall 2003. Mesenchymal progenitor cell-mediated inhibition of tumor growth in vivo and in vitro in gelatin matrix. *Exp. Mol. Pathol.* 75, 248-255.
82. Nakamura, K., Y. Ito, Y. Kawano, K. Kurozumi, M. Kobune, H. Tsuda, A. Bizen, O. Honmou, Y. Niitsu and H. Hamada 2004. Antitumor effect of genetically engineered mesenchymal stem cells in a rat glioma model. *Gene Ther.* 11, 1155-1164.

83. Khakoo, A. Y., S. Pati, S.A. Anderson, W. Reid, M.F. Elshal, I.I. Rovira, A.T. Nguyen, D. Malide, C.A. Combs, G. Hall, J. Zhang, M. Raffeld, T.B. Rogers, W. Stetler-Stevenson, J.A. Frank, M. Reitz and T. Finkel 2006. Human mesenchymal stem cells exert potent antitumorigenic effects in a model of kaposi's sarcoma. *J. Exp. Med.* 203, 1235-1247.
84. Djouad, F., P. Plence, C. Bony, P. Tropel, F. Apparailly, J. Sany, D. Noel and C. Jorgensen 2003. Immunosuppressive effect of mesenchymal stem cells favors tumor growth in allogeneic animals. *Blood.* 102, 3837-3844.
85. Yu, J. M., E.S. Jun, Y.C. Bae and J.S. Jung 2008. Mesenchymal stem cells derived from human adipose tissues favor tumor cell growth in vivo. *Stem Cells Dev.* 17, 463-473.
86. Zhu, W., W. Xu, R. Jiang, H. Qian, M. Chen, J. Hu, W. Cao, C. Han and Y. Chen 2006. Mesenchymal stem cells derived from bone marrow favor tumor cell growth in vivo. *Exp. Mol. Pathol.* 80, 267-274.
87. Houghton, J., C. Stoicov, S. Nomura, A.B. Rogers, J. Carlson, H. Li, X. Cai, J.G. Fox, J.R. Goldenring and T.C. Wang 2004. Gastric cancer originating from bone marrow-derived cells. *Science.* 306, 1568-1571.
88. Schäfer, M. and S. Werner 2008. Cancer as an overhealing wound: An old hypothesis revisited. *Nat. Rev. Mol. Cell Biol.* 9, 628-638.
89. Soria, G. and A. Ben-Baruch The inflammatory chemokines CCL2 and CCL5 in breast cancer. *Cancer Lett.*
90. Tabatabai, G., B. Frank, R. Möhle, M. Weller and W. Wick 2006. Irradiation and hypoxia promote homing of haematopoietic progenitor cells towards gliomas by TGF- β -dependent HIF-1 α -mediated induction of CXCL12. *Brain.* 129, 2426-2435.

91. Kidd, S., L. Caldwell, M. Dietrich, I. Samudio, E.L. Spaeth, K. Watson, Y. Shi, J. Abbruzzese, M. Konopleva, M. Andreeff and F.C. Marini 2010. Mesenchymal stromal cells alone or expressing interferon-beta suppress pancreatic tumors in vivo, an effect countered by anti-inflammatory treatment. *Cytotherapy*.
92. Koyama, H., N. Kobayashi, M. Harada, M. Takeoka, Y. Kawai, K. Sano, M. Fujimori, J. Amano, T. Ohhashi, R. Kannagi, K. Kimata, S. Taniguchi and N. Itano 2008. Significance of tumor-associated stroma in promotion of intratumoral lymphangiogenesis: Pivotal role of a hyaluronan-rich tumor microenvironment. *Am. J. Pathol.* 172, 179-193.
93. Ponta, H., L. Sherman and P.A. Herrlich 2003. CD44: From adhesion molecules to signalling regulators. *Nat. Rev. Mol. Cell Biol.* 4, 33-45.
94. Screaton, G. R., M.V. Bell, D.G. Jackson, F.B. Cornelis, U. Gerth and J.I. Bell 1992. Genomic structure of DNA encoding the lymphocyte homing receptor CD44 reveals at least 12 alternatively spliced exons. *Proc. Natl. Acad. Sci. U. S. A.* 89, 12160-12164.
95. Yonemura, S., M. Hirao, Y. Doi, N. Takahashi, T. Kondo, S. Tsukita and S. Tsukita 1998. Ezrin/radixin/moesin (ERM) proteins bind to a positively charged amino acid cluster in the juxta-membrane cytoplasmic domain of CD44, CD43, and ICAM-2. *J. Cell Biol.* 140, 885-895.
96. Legg, J. W., C.A. Lewis, M. Parsons, T. Ng and C.M. Isacke 2002. A novel PKC-regulated mechanism controls CD44-ezrin association and directional cell motility. *Nature Cell Biol.* 4, 399-407.
97. Bourguignon, L. Y. W., H. Zhu, L. Shao, D. Zhu and Y.-. Chen 1999. Rho-kinase (ROK) promotes CD44^{v3,8-10}-ankyrin interaction and tumor cell migration in metastatic breast cancer cells. *Cell Motil. Cytoskeleton.* 43, 269-287.

98. Lee, J. -, M.-. Wang and J.-. Chen 2009. Acetylation and activation of STAT3 mediated by nuclear translocation of CD44. *J. Cell Biol.* 185, 949-957.
99. Bourguignon, L. Y. W., W. Xia and G. Wong 2009. Hyaluronan-mediated CD44 interaction with p300 and SIRT1 regulates β -catenin signaling and NF κ B-specific transcription activity leading to MDR1 and bcl-xL gene expression and chemoresistance in breast tumor cells. *J. Biol. Chem.* ; *J. Biol. Chem.* 284, 2657-2671.
100. Klingbeil, P., R. Marhaba, T. Jung, R. Kirmse, T. Ludwig and M. Zöller 2009. CD44 variant isoforms promote metastasis formation by a tumor cell-matrix cross-talk that supports adhesion and apoptosis resistance. *Mol. Cancer Res.* 7, 168-179.
101. Pályi-Krekk, Z., M. Barok, J. Isola, M. Tammi, J. Szöllosi and P. Nagy 2007. Hyaluronan-induced masking of ErbB2 and CD44-enhanced trastuzumab internalisation in trastuzumab resistant breast cancer. *Eur. J. Cancer.* 43, 2423-2433.
102. Fujita, Y., M. Kitagawa, S. Nakamura, K. Azuma, G. Ishii, M. Higashi, H. Kishi, T. Hiwasa, K. Koda, N. Nakajima and K. Harigaya 2002. CD44 signaling through focal adhesion kinase and its anti-apoptotic effect. *FEBS Lett.* ; *FEBS Lett.* 528, 101-108.
103. Ek-Rylander, B. and G. Andersson 2010. Osteoclast migration on phosphorylated osteopontin is regulated by endogenous tartrate-resistant acid phosphatase. *Exp. Cell Res.* 316, 443-451.
104. Raheja, L. F., D.C. Genetos and C.E. Yellowley 2008. Hypoxic osteocytes recruit human MSCs through an OPN/CD44-mediated pathway. *Biochem. Biophys. Res. Commun.* 366, 1061-1066.

105. Tuck, A. B., B.E. Elliott, C. Hota, E. Tremblay and A.F. Chambers 2000. Osteopontin-induced, integrin-dependent migration of human mammary epithelial cells involves activation of the hepatocyte growth factor receptor (met). *Journal of Cellular Biochemistry*. 78, 465.
106. Koh, A., A.P.B. Da Silva, A.K. Bansal, M. Bansal, C. Sun, H. Lee, M. Glogauer, J. Sodek and R. Zohar 2007. Role of osteopontin in neutrophil function. *Immunology*. 122, 466-475.
107. Laird, D. J., U.H. von Andrian and A.J. Wagers 2008. Stem cell trafficking in tissue development, growth, and disease. *Cell*. 132, 612-630.
108. Sonabend, A. M., I.V. Ulasov, M.A. Tyler, A.A. Rivera, J.M. Mathis and M.S. Lesniak 2008. Mesenchymal stem cells effectively deliver an oncolytic adenovirus to intracranial glioma. *Stem Cells*. 26, 831-841.
109. Kanehira, M., H. Xin, K. Hoshino, M. Maemondo, H. Mizuguchi, T. Hayakawa, K. Matsumoto, T. Nakamura, T. Nukiwa and Y. Saijo 2007. Targeted delivery of NK4 to multiple lung tumors by bone marrow-derived mesenchymal stem cells. *Cancer Gene Ther*. 14, 894-903.
110. Kyriakou, C. A., K.L. Yong, R. Benjamin, A. Pizzey, A. Dogan, N. Singh, A.M. Davidoff and A.C. Nathwani 2006. Human mesenchymal stem cells (hMSCs) expressing truncated soluble vascular endothelial growth factor receptor (tsFlk-1) following lentiviral-mediated gene transfer inhibit growth of burkitt's lymphoma in a murine model. *J. Gene Med*. 8, 253-264.
111. Sonabend, A. M., I.V. Ulasov, M.A. Tyler, A.A. Rivera, J.M. Mathis and M.S. Lesniak 2008. Mesenchymal stem cells effectively deliver an oncolytic adenovirus to intracranial glioma. *Stem Cells*.

112. Binger, T., S. Stich, K. Andreas, C. Kaps, O. Sezer, M. Notter, M. Sittinger and J. Ringe 2009. Migration potential and gene expression profile of human mesenchymal stem cells induced by CCL25. *Exp. Cell Res.*
113. Dauer, D. J., B. Ferraro, L. Song, B. Yu, L. Mora, R. Buettner, S. Enkemann, R. Jove and E.B. Haura 2005. Stat3 regulates genes common to both wound healing and cancer. *Oncogene.* 24, 3397-3408.
114. Wang, L., Y. Li, X. Chen, J. Chen, S.C. Gautam, Y. Xu and M. Chopp 2002. MCP-1, MIP-1, IL-8 and ischemic cerebral tissue enhance human bone marrow stromal cell migration in interface culture. *Hematology.* 7, 113-117.
115. Hata, N., N. Shinojima, J. Gumin, R. Yong, F. Marini, M. Andreeff and F.F. Lang 2010. Platelet-derived growth factor BB mediates the tropism of human mesenchymal stem cells for malignant gliomas. *Neurosurgery.* 66, 144-156.
116. Andl, C. D., T. Mizushima, K. Oyama, M. Bowser, H. Nakagawa and A.K. Rustgi 2004. EGFR-induced cell migration is mediated predominantly by the JAK-STAT pathway in primary esophageal keratinocytes. *Am. J. Physiol. Gastrointest. Liver Physiol.* 287.
117. Price, J. T., T. Tiganis, A. Agarwal, D. Djakiew and E.W. Thompson 1999. Epidermal growth factor promotes MDA-MB-231 breast cancer cell migration through a phosphatidylinositol 3'-kinase and phospholipase C-dependent mechanism. *Cancer Res.* 59, 5475-5478.
118. Denhardt, D. T., M. Noda, A.W. O'Regan, D. Pavlin and J.S. Berman 2001. Osteopontin as a means to cope with environmental insults: Regulation of inflammation, tissue remodeling, and cell survival. *J. Clin. Invest.* 107, 1055-1061.

119. Jiang, D., J. Liang and P.W. Noble 2007. Hyaluronan in tissue injury and repair. *Annu. Rev. Cell Dev. Biol.* 23, 435-461.
120. Coffelt, S. B., F.C. Marini, K. Watson, K.J. Zvezdaryk, J.L. Dembinski, H.L. Lamarca, S.L. Tomchuck, K.H. Zu Bentrup, E.S. Danko, S.L. Henkle and A.B. Scandurro 2009. The pro-inflammatory peptide LL-37 promotes ovarian tumor progression through recruitment of multipotent mesenchymal stromal cells. *Proc. Natl. Acad. Sci. U. S. A.*
121. Ghatak, S., S. Misra and B.P. Toole 2005. Hyaluronan constitutively regulates ErbB2 phosphorylation and signaling complex formation in carcinoma cells. *J. Biol. Chem.* 280, 8875-8883.
122. Misra, S., B.P. Toole and S. Ghatak 2006. Hyaluronan constitutively regulates activation of multiple receptor tyrosine kinases in epithelial and carcinoma cells. *J. Biol. Chem.* 281, 34936-34941.
123. Shi, X., L. Leng, T. Wang, W. Wang, X. Du, J. Li, C. McDonald, Z. Chen, J.W. Murphy, E. Lolis, P. Noble, W. Knudson and R. Bucala 2006. CD44 is the signaling component of the macrophage migration inhibitory factor-CD74 receptor complex. *Immunity.* 25, 595-606.
124. Ghatak, S., V.C. Hascall, R.R. Markwald and S. Misra 2010. Stromal hyaluronan interaction with epithelial CD44 variants promotes prostate cancer invasiveness by augmenting expression and function of hepatocyte growth factor and androgen receptor. *J. Biol. Chem.* 285, 19821-19832.
125. Cheng, G. Z., J. Chan, Q. Wang, W. Zhang, C.D. Sun and L.-. Wang 2007. Twist transcriptionally up-regulates AKT2 in breast cancer cells leading to increased migration, invasion, and resistance to paclitaxel. *Cancer Res.* ; *Cancer Res.* 67, 1979-1987.

126. Cheng, G. Z., W. Zhang, M. Sun, Q. Wang, D. Coppola, M. Mansour, L. Xu, C. Costanzo, J.Q. Cheng and L.-. Wang 2008. Twist is transcriptionally induced by activation of STAT3 and mediates STAT3 oncogenic function. *J. Biol. Chem.* 283, 14665-14673.
127. Debidda, M., L. Wang, H. Zang, V. Poli and Y. Zheng 2005. A role of STAT3 in rho GTPase-regulated cell migration and proliferation. *J. Biol. Chem.* 280, 17275-17285.
128. Thisse, B., M.E. Messal and F. Perrin-Schmitt 1987. The twist gene: Isolation of a drosophila zygote gene necessary for the establishment of dorsoventral pattern. *Nucleic Acids Res.* 15, 3439-3453.
129. Chen, Z. -. and R.R. Behringer 1995. Twist is required in head mesenchyme for cranial neural tube morphogenesis. *Genes Dev.* 9, 686-699.
130. Yang, J., S.A. Mani, J.L. Donaher, S. Ramaswamy, R.A. Itzykson, C. Come, P. Savagner, I. Gitelman, A. Richardson and R.A. Weinberg 2004. Twist, a master regulator of morphogenesis, plays an essential role in tumor metastasis. *Cell*; *Cell.* 117, 927-939.
131. Brouard, N., A. Chapel, D. Thierry, P. Charbord and B. Peault 2000. Transplantation of gene-modified human bone marrow stromal cells into mouse-human bone chimeras. *J. Hematother. Stem Cell Res.* 9, 175-181.
132. Sato, H., N. Kuwashima, T. Sakaida, M. Hatano, J.E. Dusak, W.K. Fellows-Mayle, G.D. Papworth, S.C. Watkins, A. Gambotto, I.F. Pollack and H. Okada 2005. Epidermal growth factor receptor-transfected bone marrow stromal cells exhibit enhanced migratory response and therapeutic potential against murine brain tumors. *Cancer Gene Ther.* 12, 757-768.

133. Li, A. L., C. Li, Y.G. Feng, G.H. Yuan, G.M. Wang, J. Hao, X. Gao and S.S. Xie 2005. Antileukemic effect of interleukin-7-transduced bone marrow stromal cells in mice following allogeneic T-cell-depleted bone marrow transplantation. *Transplant. Proc.* 37, 2297-2299.
134. Chen, X., X. Lin, J. Zhao, W. Shi, H. Zhang, Y. Wang, B. Kan, L. Du, B. Wang, Y. Wei, Y. Liu and X. Zhao 2008. A tumor-selective biotherapy with prolonged impact on established metastases based on cytokine gene-engineered MSCs. *Mol. Ther.* 16, 749-756.
135. Kim, S. M., J.Y. Lim, S.I. Park, C.H. Jeong, J.H. Oh, M. Jeong, W. Oh, S.H. Park, Y.C. Sung and S.S. Jeun 2008. Gene therapy using TRAIL-secreting human umbilical cord blood-derived mesenchymal stem cells against intracranial glioma. *Cancer Res.* 68, 9614-9623.
136. Fritz, V., D. Noel, C. Bouquet, P. Opolon, R. Voide, F. Apparailly, P. Louis-Pence, C. Bouffi, H. Drissi, C. Xie, M. Perricaudet, R. Muller, E. Schwarz and C. Jorgensen 2008. Antitumoral activity and osteogenic potential of mesenchymal stem cells expressing the urokinase-type plasminogen antagonist amino-terminal fragment in a murine model of osteolytic tumor. *Stem Cells.* 26, 2981-2990.
137. Kyriakou, C. A., K.L. Yong, R. Benjamin, A. Pizzey, A. Dogan, N. Singh, A.M. Davidoff and A.C. Nathwani 2006. Human mesenchymal stem cells (hMSCs) expressing truncated soluble vascular endothelial growth factor receptor (tsFlk-1) following lentiviral-mediated gene transfer inhibit growth of burkitt's lymphoma in a murine model. *J. Gene Med.* 8, 253-264.
138. Kucerova, L., M. Matuskova, A. Pastorakova, S. Tyciakova, J. Jakubikova, R. Bohovic, V. Altanero and C. Altaner 2008. Cytosine deaminase expressing human mesenchymal stem cells mediated tumour regression in melanoma bearing mice. *J. Gene Med.* 10, 1071-1082.

139. Kucerova, L., V. Altanerova, M. Matuskova, S. Tyciakova and C. Altaner 2007. Adipose tissue-derived human mesenchymal stem cells mediated prodrug cancer gene therapy. *Cancer Res.* 67, 6304-6313.
140. Matuskova, M., K. Hlubinova, A. Pastorakova, L. Hunakova, V. Altanerova, C. Altaner and L. Kucerova 2010. HSV-tk expressing mesenchymal stem cells exert bystander effect on human glioblastoma cells. *Cancer Lett.* 290, 58-67.
141. Cheng, Z., L. Ou, X. Zhou, F. Li, X. Jia, Y. Zhang, X. Liu, Y. Li, C.A. Ward, L.G. Melo and D. Kong 2008. Targeted migration of mesenchymal stem cells modified with CXCR4 gene to infarcted myocardium improves cardiac performance. *Mol. Ther.* 16, 571-579.
142. Short, B. J., N. Brouard and P.J. Simmons 2009. Prospective isolation of mesenchymal stem cells from mouse compact bone. *Methods Mol. Biol.* 482, 259-268.
143. Yotnda, P., C. Zompeta, H.E. Heslop, M. Andreeff, M.K. Brenner and F. Marini 2004. Comparison of the efficiency of transduction of leukemic cells by fiber-modified adenoviruses. *Hum. Gene Ther.* 15, 1229-1242.
144. Sordi, V., M.L. Malosio, F. Marchesi, A. Mercalli, R. Melzi, T. Giordano, N. Belmonte, G. Ferrari, B.E. Leone, F. Bertuzzi, G. Zerbini, P. Allavena, E. Bonifacio and L. Piemonti 2005. Bone marrow mesenchymal stem cells express a restricted set of functionally active chemokine receptors capable of promoting migration to pancreatic islets. *Blood.* 106, 419-427.
145. Studeny, M., F.C. Marini, J.L. Dembinski, C. Zompetta, M. Cabreira-Hansen, B.N. Bekele, R.E. Champlin and M. Andreeff 2004. Mesenchymal stem cells: Potential precursors for tumor stroma and targeted-delivery vehicles for anticancer agents. *J. Natl. Cancer Inst.* 96, 1593-1603.

146. Yu, Q., B.P. Toole and I. Stamenkovic 1997. Induction of apoptosis of metastatic mammary carcinoma cells *invivo* by disruption of tumor cell surface CD44 function. *J. Exp. Med.* 186, 1985-1996.
147. Zeng, C., B.P. Toole, S.D. Kinney, J.-. Kuo and I. Stamenkovic 1998. Inhibition of tumor growth *in vivo* by hyaluronan oligomers. *Int. J. Cancer.* 77, 396-401.
148. Weber, G. F., G.S. Lett and N.C. Haubein 2010. Osteopontin is a marker for cancer aggressiveness and patient survival. *Br. J. Cancer.* 103, 861-869.
149. Wang, X., L. Chao, G. Ma, L. Chen, B. Tian, Y. Zang and J. Sun 2008. Increased expression of osteopontin in patients with triple-negative breast cancer. *Eur. J. Clin. Invest.* 38, 438-446.
150. Acharya, P. S., S. Majumdar, M. Jacob, J. Hayden, P. Mrass, W. Weninger, R.K. Assoian and E. Pure 2008. Fibroblast migration is mediated by CD44-dependent TGF beta activation. *J. Cell. Sci.* 121, 1393-1402.
151. Nagano, O., D. Murakami, D. Hartmann, B. De Strooper, P. Saftig, T. Iwatsubo, M. Nakajima, M. Shinohara and H. Saya 2004. Cell-matrix interaction via CD44 is independently regulated by different metalloproteinases activated in response to extracellular Ca^{2+} influx and PKC activation. *J. Cell Biol.* 165, 893-902.
152. Okamoto, I., Y. Kawano, D. Murakami, T. Sasayama, N. Araki, T. Miki, A.J. Wong and H. Saya 2001. Proteolytic release of CD44 intracellular domain and its role in the CD44 signaling pathway. *J. Cell Biol.* 155, 755-762.
153. Okamoto, I., Y. Kawano, H. Tsuiki, J.-. Sasaki, M. Nakao, M. Matsumoto, M. Suga, M. Ando, M. Nakajima and H. Saya 1999. CD44 cleavage induced

by a membrane-associated metalloprotease plays a critical role in tumor cell migration. *Oncogene*. 18, 1435-1446.

154. Nagano, O. and H. Saya 2004. Mechanism and biological significance of CD44 cleavage. *Cancer Sci*. 95, 930-935.
155. Matsuo, N., H. Shiraha, T. Fujikawa, N. Takaoka, N. Ueda, S. Tanaka, S. Nishina, Y. Nakanishi, M. Uemura, A. Takaki, S. Nakamura, Y. Kobayashi, K. Nouse, T. Yagi and K. Yamamoto 2009. Twist expression promotes migration and invasion in hepatocellular carcinoma. *BMC Cancer*. 9, 240.
156. Qin, L., Z. Liu, H. Chen and J. Xu 2009. The steroid receptor coactivator-1 regulates twist expression and promotes breast cancer metastasis. *Cancer Res*. 69, 3819-3827.
157. Hu, L., J.M. Roth, P. Brooks, S. Ibrahim and S. Karpatkin 2008. Twist is required for thrombin-induced tumor angiogenesis and growth. *Cancer Res*. ; *Cancer Res*. 68, 4296-4302.
158. Ren, C., S. Kumar, D. Chanda, L. Kallman, J. Chen, J.D. Mountz and S. Ponnazhagan 2008. Cancer gene therapy using mesenchymal stem cells expressing interferon-beta in a mouse prostate cancer lung metastasis model. *Gene Ther*. 15, 1446-1453.
159. Dembinski, J. L., E.L. Spaeth, J. Fueyo, C. Gomez-Manzano, M. Studeny, M. Andreeff and F.C. Marini 2010. Reduction of nontarget infection and systemic toxicity by targeted delivery of conditionally replicating viruses transported in mesenchymal stem cells. *Cancer Gene Ther*. 17, 289-297.
160. Mishra, P. J., P.J. Mishra, R. Humeniuk, D.J. Medina, G. Alexe, J.P. Mesirov, S. Ganesan, J.W. Glod and D. Banerjee 2008. Carcinoma-associated fibroblast-like differentiation of human mesenchymal stem cells. *Cancer Res*. 68, 4331-4339.

161. Dong, J., J. Grunstein, M. Tejada, F. Peale, G. Frantz, W.C. Liang, W. Bai, L. Yu, J. Kowalski, X. Liang, G. Fuh, H.P. Gerber and N. Ferrara 2004. VEGF-null cells require PDGFR alpha signaling-mediated stromal fibroblast recruitment for tumorigenesis. *EMBO J.* 23, 2800-2810.
162. Jodele, S., C.F. Chanttrain, L. Blavier, C. Lutzko, G.M. Crooks, H. Shimada, L.M. Coussens and Y.A. Declerck 2005. The contribution of bone marrow-derived cells to the tumor vasculature in neuroblastoma is matrix metalloproteinase-9 dependent. *Cancer Res.* 65, 3200-3208.
163. Ayala, G., J.A. Tuxhorn, T.M. Wheeler, A. Frolov, P.T. Scardino, M. Ohori, M. Wheeler, J. Spitler and D.R. Rowley 2003. Reactive stroma as a predictor of biochemical-free recurrence in prostate cancer. *Clin. Cancer Res.* 9, 4792-4801.
164. Canfield, A. E. and A.M. Schor 1995. Evidence that tenascin and thrombospondin-1 modulate sprouting of endothelial cells. *J. Cell. Sci.* 108, 797-809.
165. Kwak, J. M., H.J. Lee, S.H. Kim, H.K. Kim, Y.J. Mok, Y.T. Park, J.S. Choi and H.Y. Moon 2010. Expression of protein S100A4 is a predictor of recurrence in colorectal cancer. *World J. Gastroenterol.* 16, 3897-3904.
166. Foote, J. A., R.B. Harris, A.R. Giuliano, D.J. Roe, T.E. Moon, B. Cartmel and D.S. Alberts 2001. Stromal expression of fibroblast activation protein/seprase, a cell membrane serine proteinase and gelatinase, is associated with longer survival in patients with invasive ductal carcinoma of breast. *Int. J. Cancer.* 95, 67-72.
167. Lee, J., M. Fassnacht, S. Nair, D. Boczkowski and E. Gilboa 2005. Tumor immunotherapy targeting fibroblast activation protein, a product expressed in tumor-associated fibroblasts. *Cancer Res.* 65, 11156-11163.

168. Kunz-Schughart, L. A. and R. Knuechel 2002. Tumor-associated fibroblasts (part I): Active stromal participants in tumor development and progression? *Histol. Histopathol.* 17, 599-621.
169. Sasser, A. K., B.L. Mundy, K.M. Smith, A.W. Studebaker, A.E. Axel, A.M. Haidet, S.A. Fernandez and B.M. Hall 2007. Human bone marrow stromal cells enhance breast cancer cell growth rates in a cell line-dependent manner when evaluated in 3D tumor environments. *Cancer Lett.* 254, 255-264.
170. Sasser, A. K., N.J. Sullivan, A.W. Studebaker, L.F. Hendey, A.E. Axel and B.M. Hall 2007. Interleukin-6 is a potent growth factor for ER- α -positive human breast cancer. *FASEB J.* 21, 3763-3770.
171. Hall, B., M. Andreeff and F. Marini 2007. The participation of mesenchymal stem cells in tumor stroma formation and their application as targeted-gene delivery vehicles. *Handb. Exp. Pharmacol.* (180), 263-283.
172. Lin, C. -, C.-. Chen, M.-. Huang, S.-. Lee, C.-. Lin, C.-. Chang and H. Lee 2008. Lysophosphatidic acid upregulates vascular endothelial growth factor-C and tube formation in human endothelial cells through LPA_{1/3}, COX-2, and NF- κ B activation- and EGFR transactivation-dependent mechanisms. *Cell. Signal.* 20, 1804-1814.
173. Mehta, V. B. and G.E. Besner 2007. HB-EGF promotes angiogenesis in endothelial cells via PI3-kinase and MAPK signaling pathways. *Growth Factors.* 25, 253-263.
174. Li, A., S. Dubey, M.L. Varney, B.J. Dave and R.K. Singh 2003. IL-8 directly enhanced endothelial cell survival, proliferation, and matrix metalloproteinases production and regulated angiogenesis. *J. Immunol.* 170, 3369-3376.

175. Dai, J., L. Peng, K. Fan, H. Wang, R. Wei, G. Ji, J. Cai, B. Lu, B. Li, D. Zhang, Y. Kang, M. Tan, W. Qian and Y. Guo 2009. Osteopontin induces angiogenesis through activation of PI3K/AKT and ERK1/2 in endothelial cells. *Oncogene*. 28, 3412-3422.
176. Elamrani, N., J.J. Brustis, N. Dourdin, D. Balcerzak, S. Poussard, P. Cottin and A. Ducastaing 1995. Desmin degradation and Ca^{2+} -dependent proteolysis during myoblast fusion. *Biol. Cell*. 85, 177-183.
177. Nelson, W. J. and P. Traub 1983. Proteolysis of vimentin and desmin by the Ca^{2+} -activated proteinase specific for these intermediate filament proteins. *Mol. Cell. Biol.* 3, 1146-1156.
178. Li, L., C.-. Heldin and P. Heldin 2006. Inhibition of platelet-derived growth factor-BB-induced receptor activation and fibroblast migration by hyaluronan activation of CD44. *J. Biol. Chem.* 281, 26512-26519.
179. Hsu, K. -, H.-. Tsai, P.-. Lin, Y.-. Hsu, Y.-. Shan and P.-. Lu 2010. Clinical implication and mitotic effect of CD44 cleavage in relation to osteopontin/CD44 interaction and dysregulated cell cycle protein in gastrointestinal stromal tumor. *Ann. Surg. Oncol.* 17, 2199-2212.
180. McAllister, S. S., A.M. Gifford, A.L. Greiner, S.P. Kelleher, M.P. Saelzler, T.A. Ince, F. Reinhardt, L.N. Harris, B.L. Hylander, E.A. Repasky and R.A. Weinberg 2008. Systemic endocrine instigation of indolent tumor growth requires osteopontin. *Cell; Cell*. 133, 994-1005.
181. Lewis, C. E. and J.W. Pollard 2006. Distinct role of macrophages in different tumor microenvironments. *Cancer Res.* 66, 605-612.
182. Luo, Y., H. Zhou, J. Krueger, C. Kaplan, S.-. Lee, C. Dolman, D. Markowitz, W. Wu, C. Liu, R.A. Reisfeld and R. Xiang 2006. Targeting tumor-

associated macrophages as a novel strategy against breast cancer. J. Clin. Invest. 116, 2132-2141.

- 183. Duff, M. D., J. Mestre, S. Maddali, Z.P. Yan, P. Stapleton and J.M. Daly 2007. Analysis of gene expression in the tumor-associated macrophage. J. Surg. Res. 142, 119-128.**
- 184. Direkze, N. C., K. Hodivala-Dilke, R. Jeffery, T. Hunt, R. Poulson, D. Oukrif, M.R. Alison and N.A. Wright 2004. Bone marrow contribution to tumor-associated myofibroblasts and fibroblasts. Cancer Res. 64, 8492-8495.**
- 185. Ishii, G., T. Sangai, T. Ito, T. Hasebe, Y. Endoh, H. Sasaki, K. Harigaya and A. Ochiai 2005. In vivo and in vitro characterization of human fibroblasts recruited selectively into human cancer stroma. Int. J. Cancer. 117, 212-220.**
- 186. Roni, V., W. Habeler, A. Parenti, S. Indraccolo, E. Gola, V. Tosello, R. Cortivo, G. Abatangelo, L. Chieco-Bianchi and A. Amadori 2003. Recruitment of human umbilical vein endothelial cells and human primary fibroblasts into experimental tumors growing in SCID mice. Exp. Cell Res. 287, 28-38.**
- 187. Muehlberg, F. L., Y.H. Song, A. Krohn, S.P. Pinilla, L.H. Droll, X. Leng, M. Seidensticker, J. Ricke, A.M. Altman, E. Devarajan, W. Liu, R.B. Arlinghaus and E.U. Alt 2009. Tissue-resident stem cells promote breast cancer growth and metastasis. Carcinogenesis. 30, 589-597.**
- 188. Donnenberg, V. S., A.D. Donnenberg, L. Zimmerlin, R.J. Landreneau, R. Bhargava, R.A. Wetzel, P. Basse and A.M. Brufsky 2010. Localization of CD44 and CD90 positive cells to the invasive front of breast tumors. Cytometry Part B Clin. Cytometry. 78, 287-301.**

189. Khan, A. I., M. Steven, Kerfoot, B. Heit, L. Liu, G. Andonegui, B. Ruffell, P. Johnson and P. Kubes 2004. Role of CD44 and hyaluronan in neutrophil recruitment. *J. Immunol.* 173, 7594-7601.
190. Rajasagi, M., M. Vitacolonna, B. Benjak, R. Marhaba and M. Zöller 2009. CD44 promotes progenitor homing into the thymus and T cell maturation. *J. Leukoc. Biol. ; J. Leukocyte Biol.* 85, 251-261.
191. Van Der Windt, G. J. W., C. Van 't Veer, S. Florquin and T. Van Der Poll 2010. CD44 deficiency is associated with enhanced escherichia coli-induced proinflammatory cytokine and chemokine release by peritoneal macrophages. *Infect. Immun.* 78, 115-124.

6.0 Vita

Erika Leigh Spaeth was born in Dallas, Texas on July 9, 1983, the Daughter of Mary Shepard Spaeth and Alan Colin Spaeth. After completing work at Choate Rosemary Hall, Wallingford, Connecticut in 2001, she entered the University of Connecticut in Storrs, Connecticut. She received the degree of Bachelor of Science with a major in molecular and cell biology from UCONN in May, 2005. For the next year, she worked as a research scientist at Quattromed Ltd in Tartu, Estonia. In September of 2006, she entered The University of Texas Health Science Center at Houston Graduate School of Biomedical Sciences.

Permanent address:

2350 Bagby St

Houston, TX 77006

Articles/book chapters published as GSBS graduate student 2006-2010

1. Klopp AH, Gupta A, **Spaeth E**, et al. Dissecting a Discrepancy in the Literature Do Mesenchymal Stem Cells Support or Suppress Tumor Growth. *Stem Cells*. 2010. In press
2. Klopp AH, Lacerda L, Gupta A, Debeb BG, Solley T, Li L, **Spaeth E**. et al. 2010 Mesenchymal Stem Cells Promote Mammosphere Formation and Decrease E-Cadherin in Normal and Malignant Breast Cells. *PLoS ONE* 5(8): e12180. doi:10.1371/journal.pone.0012180
3. Dembinski JL, **Spaeth EL**, Fueyo J et al. Reduction of nontarget infection and systemic toxicity by targeted delivery of conditionally replicating viruses transported in mesenchymal stem cells. *Cancer Gene Ther*. 2010 Apr;17(4):289-97
4. Kidd S, **Spaeth E**, Dembinski JL et al. Direct Evidence of Mesenchymal Stem Cell Tropism for Tumor and Wounding Microenvironments Using In Vivo Bioluminescence Imaging. [Stem Cells](#). 2009 Jul 30.
5. **Spaeth EL**, Dembinski JL, Sasser AK et al. Mesenchymal stem cell transition to tumor-associated fibroblasts contributes to fibrovascular network expansion and tumor progression. [PLoS One](#). 2009;4(4):e4992. Epub 2009 Apr 7
6. Kidd S, **Spaeth E**, Klopp A, et al. The (in) auspicious role of mesenchymal stromal cells in cancer: be it friend or foe. [Cytotherapy](#). 2008;10(7):657-67
7. **Spaeth E**, Klopp A, Dembinski J, Andreeff M, Marini F. Inflammation and tumor microenvironments: defining the migratory itinerary of mesenchymal stem cells. [Gene Ther](#). 2008 May;15(10):730-8. Epub 2008 Apr 10

8. Klopp AH, **Spaeth EL**, Dembinski JL et al. Tumor irradiation increases the recruitment of circulating mesenchymal stem cells into the tumor microenvironment. [Cancer Res.](#) 2007 Dec 15;67(24):11687-95
9. **Spaeth EL**, Kidd S, Marini FC. (2011) Inflammation Induced Mobilization of Mesenchymal Stem Cells. In Kolonin M & Simmons P, *Stem Cell Mobilization: Methods and Protocols*. New York, USA: Humana Press. *In preparation*
10. **Spaeth EL** & Marini FC. (2010) Dissecting Mesenchymal Stem Cell Movement: Migration Assays for Tracing and Deducing Cell Migration. In Filippi M-D & Geiger H (Eds.), *Methods in Molecular Biology: Stem Cell Migration Methods and Protocols*. New York, USA: Humana Press. *In Press*
11. Marini FC, Studeny M, Dembinski JL, Watson KL, Kidd S, **Spaeth E**. (2010) Mesenchymal Stem/Stromal Cells as Cellular Vehicles for Tumor Targeting. Roth J, *Gene-based Therapies for Cancer*. New York, USA: Springer.